REDUCING ENERGY WASTE IN CENTRIFUGAL PUMP SYSTEMS THROUGH THE IMPLEMENTATION OF BEP OPTIMIZED PRESSURE AND FLOW CONTROL

A Dissertation

presented to

the Faculty of the Engineering School

at the University of Missouri-Columbia

In Partial Fulfillment

of the Requirements for the Degree

Doctor of Philosophy

of Mechanical Engineering

---

by

SHANE CORLMAN

Dr. A. Sherif El-Gizawy, Dissertation Supervisor

DECEMBER 2015

The undersigned, have examined the dissertation entitled

REDUCING ENERGY WASTE IN CENTRIFUGAL PUMP SYSTEMS THROUGH THE IMPLEMENTATION OF BEP OPTIMIZED PRESSURE AND FLOW CONTROL

presented by Shane Corlman,

a candidate for the degree of doctor of philosophy of mechanical engineering,

and hereby certify that, in their opinion, it is worthy of acceptance.

Professor A. Sherif El-Gizawy

Professor Noah Manring

Professor Roger Fales

Professor Steven Borgelt

Professor Yuwen Zhang

To Julia.

ACKNOWLEDGEMENTS

I would like to thank Dr. A. Sherif El-Gizawy for his guidance and support through this entire process.

TABLE OF CONTENTS

LIST OF FIGURES

LIST OF TABLES

LIST OF VARIABLES

N - *Rotational Speed (RPM)*

P_T - *Total Dynamic Pressure (psi; Pa)*

P_p - *Pressure Added by Pump (psi; Pa)*

Q - *Volumetric Flowrate (GPM; m^3/s)*

E - *emf; Electromotive Force (V)*

V - *Voltage (V)*

I - *Electrical Current (A)*

N_S - *Specific Speed (unitless)*

P_s - *Static Pressure (psi, Pa)*

P_d - *Discharge Pressure (psi; Pa)*

H_s - *Static Head (ft; m)*

P_v - *Velocity Pressure (psi; Pa)*

H_v - *Velocity Head (ft; m)*

P_l - *Pressure Losses; viscous (psi; Pa)*

H_l - *Head Losses; viscous (ft; m)*

ρ - *Density (lbm/gal; kg/m^3)*

h - *Elevation Head (ft; m)*

f - *Friction Factor (unitless)*

K - *Loss Coefficient (unitless)*

v - *Velocity (ft/min; m/s)*

η - *Efficiency (unitless)*

A - *Area (ft^2; m^2)*

D - *Diameter (in; m^2)*

Re - *Reynolds Number (unitless)*

LIST OF ABBREVIATIONS

CFD - Computational Fluid Dynamics

VSP - Variable Speed Pump

VFD - Variable Frequency Drive

BEP - Best Efficiency Point

CV - Control Valve

BHP - Brake Horsepower

PD - Positive Displacement

PPH - Pounds per Hour

TBEP - True Best Efficiency Point

MIMO - Multiple Input, Multiple Output

FFT - Fast Fourier Transform

PSD - Power Spectral Density

DFT - Discrete Fourier Transform

ABSTRACT

There currently exists a gap in the technology surrounding centrifugal pumps. When looking at modern literature regarding the application of centrifugal pump systems, the existing methods for control are throttle and speed control. Herein is described a new method, one which uses both throttle and speed control simultaneously to allow for the ability to precisely regulate pressure and flow for an entire system. Variable speed pumping, when combined with a control valve allows for control techniques which have the goal of optimizing the efficiency of the pump instead of just controlling flowrate. Developing a variable speed characterization and finding the best efficiency curve of a pump gives all the necessary tools to create a "dual controller" to operate a pump in the region of greatest reliability, always.

Experiments show that neither fixed speed operation nor variable speed operation without a control valve can accurately maintain operation at the best efficiency point of the pump. Therefore, a novel control system using both a variable speed pump and a control valve is proposed to replace individual throttle and speed control. The proposed system, when used with the best efficiency curve as the operational target, maintains the best efficiency point for any flow requirement within the applicable range of the pump. Additionally, experiments have shown that energy savings from the proposed control scheme can exceed 60%—a savings which no fixed speed system can match. Dual control with a variable speed drive and control valve can reduce energy consumption and increase pump life and reliability when compared to throttle control or speed control alone by reducing the amount of time that the pump is operating away from its best efficiency point. Similarly, it provides the tools needed to produce any performance that an operator desires, whatever the application may be.

1 INTRODUCTION

1.1 Research Basis

According to a 2000 study, between 15-20% of the energy consumed by motors across secondary and tertiary sectors in the European Union (EU) is consumed by pumps (Institute of Systems and Robotics – University of Coimbra, 2000). In a follow-up 2001 study addressing the need for improving energy efficiency in pumps (using 1996 EU data), centrifugal pumps in particular were estimated to consume 117 TWh per annum, which equated to 73% of the energy consumed by all pumps (and about 10% of all electrical energy consumed by industry and commerce). In fact, over the life of a pump, approximately 85% of the cost of a pump is from electricity (Energy Technology Support Unit, 2001). Considering centrifugal pumps in particular, there are many avenues that lead to increased pump efficiency, and some are explored much more heavily than others.

Impeller and volute design, often with the aid of commercial Computational Fluid Dynamics (CFD) software, is a popular topic for geometric optimization. Economic impact analysis of pump selection and regularly scheduled maintenance has also been evaluated and shows that existing systems can be improved at a net financial gain to the user. Unfortunately, very little work has been done to research and develop intelligent and dynamic system control to maintain peak performance in real-time.

The use of Variable Frequency Drives (VFDs) allows for expanding the useful region of a pump, or Best Efficiency Point (BEP), by changing its operating speed. In general, a pump can move more fluid at higher head, while remaining at its BEP, if its speed is increased; inversely, a pump can move less fluid at lower head, while remaining at its BEP, if its speed is decreased. The

effect is that centrifugal pumps can be operated far outside of their normal operation zones without great risk to reliability or loss of efficiency simply by varying the pump speed. Designers of pumps and pumping systems know and understand this principle but do not always take advantage of its implications due to the additional design overhead.

In some cases, simply varying the speed of a pump is not sufficient to dynamically maintain performance at the BEP; as discussed below in Chapter 5. Since a centrifugal pump is governed by its pressure-flow curve, both pressure and flow must come together at the BEP. Consider the example of an engine whose power output is regulated by the mass flowrate of fuel; the system represents a static pressure change with any other system losses resulting from viscous friction. In theory, the flowrate to the engine can be regulated simply by adjusting the pump speed to deliver more or less fuel according to the affinity laws. The affinity laws state that flow changes proportionally to impeller speed and head changes proportionally to the square of speed; however, this alone does not imply that the pump will be operating either efficiently or reliably. In order to assure operation at the BEP, one must also have control over the dynamic characteristics of the system.

The system being analyzed (see Figure 1-1), which is also the inspiration for this discussion, is the fuel pumping system used in aircraft. Currently, aircraft fuel pumps are operated under ‘dead-head’ conditions where the pump is kept running at maximum capacity and flowrate is controlled by a throttling valve which is actuated by input from the pilot. In addition to the Control Valve (CV), the fuel may be routed through a system of heat exchangers—which serve a dual purpose of cooling electronic components and heating the fuel to an optimum temperature before entering the combustion chamber of the engines—which combine to create the major and

minor flow losses seen in the system curve. This scenario may also have a static pressure component since fuel chambers may be pressurized and extreme elevation changes may affect static pressure at the engines. The objective of the pump is a desired flowrate, but, like most fluid systems, pressure also plays an important role in the operation of the system.

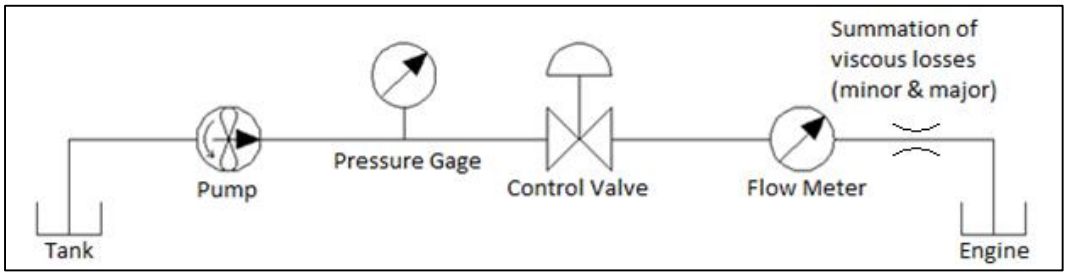

Figure 1-1. Diagram of flow setup with pump, CV, and sensors.

The proposed system combines traditional throttle control with modern speed control to achieve a more intelligent system which is capable of maintaining the BEP of the pump across a wide range of flowrates. There may not be a substantial increase in hydraulic efficiency, but raw power usage could drop considerably. According to the affinity laws, the brake horsepower (BHP) required by the pump is proportional to the cube of the speed (Equation 4-7); so a 50% decrease in speed can reduce energy consumption by 87.5%. (Affinity Laws are discussed in more detail in section 4.1.) If the pumps in aircraft are designed for peak operation—which is during takeoff—and the rest of the time there is a much lower flow requirement, then there is a great potential for raw energy savings. This savings could be of substantial benefit to aircraft since energy is limited to onboard fuel capacity.

This idea however is not limited to fuel systems or even just aircraft. Energy savings is important across all sectors and centrifugal pumps can be found in a great number of applications. All that is required for the control system to work is an understanding of pump and system

dynamics; which is true for any engineering application. The idea is not simply that efficiency will be increased or that energy will be saved, but that the entire system can be continuously optimized real-time and save energy while simultaneously increasing the life and reliability of the pump. These savings go beyond those that will be discussed in the following section by using a multivariable approach which optimizes BEP instead of pressure or flowrate alone.

1.2 Literature Review

Centrifugal pumps have been an integral part of industrial processes and machinery for decades. As a result, a substantial amount of work has been done to improve the performance, cost, life, and reliability of these devices. The following discussion covers some of the work that has been done to improve the overall implementation of centrifugal pump systems up to the writing of this dissertation: 2015.

1.2.1. Analytical Analysis

A novel method for analytically determining pump power efficiency is developed to assist in design and highlight which components affect overall efficiency. Total efficiency is broken into hydraulic, bulk, and mechanical efficiencies. Hydraulic efficiency has the largest impact and is affected by viscous losses between the eye and the tip of the impeller. The theoretical maximum hydraulic efficiency is found to be <0.9 and increases with decreasing diameter ratio. Bulk efficiency is the difference between total flow and leakage flow and is not thoroughly explored since it is highly implementation dependent, but is generally found to be in the range of 0.96-0.98. Mechanical efficiency is affected by friction between mechanical components and comes from a general equation for friction energy loss. In the end, the speed coefficient can have up to a 3%

effect on efficiency and doubling impeller diameter can change efficiency by 1-2% (Aleksandrov & Klimovskii, 2012).

1.2.2. Numerical Analysis

Some work has been done using numerical methods to intelligently improve the geometry of pump components. Evolutionary algorithms implemented in MATLAB using pressure and flow models to predict impeller performance have been able to optimize the shape of the vane and shroud (Kim, Choi, Husain, & Kim, 2010). Unfortunately, since the mechanical design techniques for these parts has already matured quite thoroughly, the authors were only able to improve the base design by <1% in terms of hydraulic efficiency.

Although the design of impellers is fairly matured, new methods are still being developed to model fluid flow across the impeller vanes to automatically generate 3D models. A method developed specifically for multistage centrifugal pumps uses a parametric solver to generate impeller geometry (Zhang, Shi, & Lu, 2012). The system is said to improve design accuracy and efficiency; however, no empirical data is given nor any analysis performed to support the claim.

Pressure and vibration data from a centrifugal pump operating under unsteady flow were measured and compared to a numerical model. Analysis of vibration and pressure fluctuations showed peaks at harmonics associated with the rotational frequency of the motor and the blade pass frequency of the impeller. Experimentally, vibration data showed magnitude increases with pump speed in general, but that natural frequencies amplified the effect in a narrow region. By contrast, vibration near the tongue tends to decrease with increasing pump speed which is indicative of increased efficiency as the pump moves towards its BEP. A CFD model of the pump

under similar conditions showed comparable results for efficiency, but pressure values were not accurate. This was assumed to be the result of the CFD model not being able to include the backside impeller blades due to mesh complexity. It is concluded that pressure and vibration data can be used to determine pump efficiency if the efficiency curve is known; also, that operation away from the BEP is less detrimental at lower pump speeds (Mele, Guzzomi, & Pan, 2014).

1.2.3. Economic Analysis

Many papers focus on the lowest hanging fruit for performance improvement: pump selection. By simply analyzing pump systems in larger industries such as desalination or chemical processing, several authors have found ways to reduce energy and maintenance costs over the course of years by investing in properly sized pumps and performing regular maintenance.

One such paper looked at the operation of centrifugal pumps in a seaside brine pump plant. They posited that operating pumps at or near 100% capacity is optimal for both pumps and driver motors. The authors evaluated the energy consumption and output capacity of the pumps and calculated the operation efficiency of each pump. Pumps that were operating far below nameplate efficiency were recommended for replacement and low efficiency motors and pumps were recommended to be replaced with comparable high efficiency, reliable models. In addition, recommendation was given for operating pumps below sea level to eliminate the presence of cavitation which was found to cause significant wear on pumps. An investment in new capital equipment increased the efficiency of pumps by 10-30%; and due energy cost reduction the payback periods were calculated to be between 14-70 months depending on the level of improvement and pump cost (Kaya, Yagmur, Yigit, Kilic, Eren, & Celik, 2008).

Another article supports the idea that pump selection is important for ensuring reliable pump operation; this paper does not go into detail about the fiscal implications: it only focuses on a methodology for proper component selection. According to the author the first thing to do is identify the process requirements including fluid properties, process capacity, and any head to overcome. The second part is to have a system in place for ensuring that the NPSHa is always greater than the NPSHr by either controlling the static head of the system or reducing friction losses between the source and the pump. Sometimes it may be more economical to use multiple pumps in parallel instead of a single pump, this selection will determine pump capacity. The calculations for power consumption are the product of total dynamic head and flowrate, this is necessary to select a driver and appropriate power source. The method for sealing a pump is driven primarily by the risk associated with leakage: a dangerous fluid requires a higher level of seal and may result in increased process cost. Finally, if variable flow requirements exist or may exist in the future, the pump may be installed with an undersized impeller to allow for increased capacity later on; alternatively, a VSD can be implemented, but may not be recommended with some pumps. Most likely flow control will be achieved using an on/off level controller attached to a control valve and may also include a recirculation line to keep the pump capacity from falling below the manufacturer stated minimum allowable value. If fluid temperature rises an undesirable amount, a heat exchanger may also be implemented, but this is typically only a risk when operating close to shut-off head (Fernandez, Pyzdrowski, Schiller, & Smith, 2002).

One author evaluates the cost benefit of using speed control in place of throttle control for centrifugal pumps. The power consumed by a pump decreases with the speed at a rate much faster than the pump efficiency. In addition, by not using a throttle valve, the air supply that operates the control valve may also be removed leading to decreased implementation costs and overall

complexity. The analysis is made to be very general, but in order to do an economic analysis of the economic benefit, the pump performance, system requirements, time component of operation, implementation differences between throttle and speed control, and investment criteria must be known (Morton, 1975).

Here the use of variable speed pumping was economically evaluated for desalination plant brine blowdown service. The author noted that for pumps with high specific speed, that pump efficiency decreases undesirably when moving away from the design point. The author suggests improving efficiency and reducing energy consumption by using a VFD in place of a throttle valve for MSF level control. The author predicts that the relatively small increase in cost for implementing a variable speed system will quickly be recouped in energy costs due to improved process design (Garibotti, 2008).

Another author performed an economic study to analyze the potential energy savings and payback period from improving process design in relation to pumps for the chemical process industry. The authors suggest that implanting a variable capacity pump is the first step for systems that operate at variable levels instead of using bypass valves and piping. The next step is to replace pipes and fittings with more properly designed layouts to reduce friction losses. Finally, pumps should be checked for appropriate sizing and motors should be replaced if they are regularly operating below 60%. Inspection and maintenance should also be performed regularly on motor and pump systems to increase life and reduce soft-costs associated with process failures and unexpected maintenance. Although no cost predictions are made due to the general nature of the recommendations, they suggest methods for payback periods based on reduced energy

consumption, increased motor and pump reliability, and reduced maintenance costs (Tutterow, Doolin, & Paul, 1996).

1.2.4. General Pump/System Analysis

Another article supports the idea that pump selection is important for ensuring reliable pump operation; this paper does not go into detail about the fiscal implications: it only focuses on a methodology for proper component selection. According to the author the first thing to do is identify the process requirements including fluid properties, process capacity, and any head to overcome. The second part is to have a system in place for ensuring that the NPSHa is always greater than the NPSHr by either controlling the static head of the system or reducing friction losses between the source and the pump. Sometimes it may be more economical to use multiple pumps in parallel instead of a single pump, this selection will determine pump capacity. The calculations for power consumption are the product of total dynamic head and flowrate, this is necessary to select a driver and appropriate power source. The method for sealing a pump is driven primarily by the risk associated with leakage: a dangerous fluid requires a higher level of seal and may result in increased process cost. Finally, if variable flow requirements exist or may exist in the future, the pump may be installed with an undersized impeller to allow for increased capacity later on; alternatively, a VSD can be implemented, but may not be recommended with some pumps. Most likely flow control will be achieved using an on/off level controller attached to a control valve and may also include a recirculation line to keep the pump capacity from falling below the manufacturer stated minimum allowable value. If fluid temperature rises an undesirable amount, a heat exchanger may also be implemented, but this is typically only a risk when operating close to shut-off head (Fernandez, Pyzdrowski, Schiller, & Smith, 2002).

Methods for determining performance correction factors are compared for a small pump with a specific speed <50 min^{-1}. The correction factors predict how a pump will change in head, flow, and efficiency performance as the Reynolds number of the flow changes. To simulate large changes in Re the pump is operated with three different fluids of varying viscosity and data is collected to determine the pump curve, power, and efficiency for each fluid. The three methods being compared are the European KSB, American ANSI/HI, and the semi-empirical power losses analysis method proposed by Gülich. By comparing test data to the three methods the authors found that in most cases the semi-empirical method gave the best results, even when the other two methods were in close agreement with one another. However, the author did find that for low Re, the power losses method deviated from empirical data for efficiency correction factor, but not as dramatically as the other two methods. All three methods show similarly well performing results for head and flowrate correction factors. The author recommends a new formula for calculating efficiency correction factors for pumps with specific speeds between 20-50 min^{-1} (Ladouani & Nemdili, 2013).

In 2008, Chinese industry consumed 74% of the nation's total energy consumption and 30% of that power was used by blowers, pumps, and air compressors. The average efficiency of pumps and air compressors was 30-40%. The authors evaluate the effect on energy efficiency when using multiple pumps in parallel to reduce energy consumption. Focus is placed on using pumps of differing capacities to see if effectiveness changes when similar pumps are not available to be paralleled. The result is that using two different pumps will reduce efficiency more as the flow ratio between the pumps increases. Reductions of 20% are found with ratios of < 1.6 and reductions of >30% are found for pumping ratios >2 (Wen, Zhang, & Wang, 2010).

1.2.5. Variable Speed Operation

HVAC systems that incorporate centrifugal pumps can take advantage of variable speed drives to reduce energy consumption during off-peak hours. Since most systems only utilize peak flow at certain hours, the rest of the time the same output can be achieved with less energy by using parallel pumps or reducing the speed of a single pump. The overall efficiency is reduced by slowing a pump, but the energy reduction that goes down with the cube of speed more than makes up for the difference. Installation of a variable speed or primary/secondary configuration can sometimes have a payback period of less than 12 months making the choice very economical (Taber, 2011).

Another author has done work to develop an equation for approximating the efficiency of a pump while its speed is varied from the designed speed and capacity. Traditionally, the affinity laws are used to approximate energy consumption changes with changes in pump speed, but these rather simple equations do not take into consideration systems with static pressure. Start by assuming that head and efficiency are quadratic functions of flowrate, Q, and that efficiency has a maximum value at the designed pump capacity, Q_D. A static pressure component is simply added to the head approximation to compensate for the extra dynamics in the solution. To make the solution nondimensional, the flowrate and head are taken as ratios of the designed values and are found to have a linear relationship to efficiency on a log-log scale. An approximation with eight unknowns which can be calculated computationally using experimental or manufacturer provided data was developed. The author concludes by suggesting that, with the rising popularity of VSDs, pump manufacturers start publishing this data with their pumps to help engineers with application and improve pump prediction for implementation (Chantasiriwan, 2013).

When using the Affinity Laws to predict energy savings it is easy to assume that reducing pump speed by 50% will reduce flowrate by 50% and energy output by 87.5%, but do not assume that using two parallel pumps will move the same fluid at 25% of the energy cost of a single pump. The Affinity Laws make no attempt to predict energy efficiency changes with speed: only changes in pump output are predicted. Part of the energy savings comes from the reduction in viscous losses which are proportional to the square of the fluid velocity; however, any changes in elevation or static pressure will not benefit from reduced flowrate (Ford, 2011).

Martins and Lima apply a VFD to an existing AC motor driven centrifugal pump in an attempt to increase the pump life characteristics. Methods for measuring predicted life performance are vibration amplitude (lower-the-better) and specific energy (lower-the-better). The study found that using a VFD to reduce the pump speed is conjunction with a throttle valve reduced the two above values and theoretically should increase overall reliability and MTBF; in fact, the pumps lasted more than 24 months with the new system when the previous MTBF was 12 months. The control system used was very basic consisting of Boolean logic that turns a valve in a 10 degree range and then changes the pump speed once the valve reaches its limit. This method reduces pump power consumption and vibration by reducing the speed of the pump dramatically with the BEP as a target. However, this system does not have a control system which uses the BEP as a reference and is a tune-up type of implementation where the system is setup initially and then left to run near the BEP for years on end. The title claims an automatic tune-up, but the actual implementation is fairly unintelligent since it does not monitor the system over time or adjust its parameters based on system changes (Martins & Lima, 2008).

A 15 hp variable speed motor is operated using a PWM variable speed drive to determine the effect of inputs on overall system efficiency. Three independent variables were tested, VSD switching frequency, pump speed, and pump load (expressed as % of rated torque). The authors found that the largest impact on efficiency was motor torque, especially as load fell below 50% of the motor rating. The second largest impact was the result of switching frequency which reduced the efficiency of the VSD as frequency increased; however, the author noted that it may still be desirable to increase switching speed to avoid natural frequencies or undesirable audible noise. The last variable, the motor speed, was shown to result in a decrease in efficiency as speed decreased, but it was the smallest effect of all three. The author then equated motor performance to predicted motor/pump performance using the affinity laws. The author supposed that since pressure is proportional to the square of pump speed, such that at 50% speed pressure will be approximately 25%, by reducing motor speed for a pump will reduce the loading on the pump significantly. The author already showed that motor torque was the largest contributor to overall efficiency at torque loads below 50% and predicted that changes in speed at low load would result in significant changes in motor efficiency: efficiency would be reduced with decreasing speed (Gao, McInerny, & Kavanaugh, 2001).

The authors evaluate the potential energy savings of using a VFD for proportional pressure control in a water supply pump. Water loss is often an issue for energy loss in water supply systems and therefore pressure control is often implemented to provide flow at the lowest pressure to reduce the effect of losses. Throttle control and variable speed control are both investigated for this application. The throttle control, which is more common, results in higher pressure and higher water loss during operation when compared to variable speed pressure control. Also, since power is a product of flow and pressure, the higher pressure solution uses more energy even when

neglecting water loss. A method called proportional pressure control, where pressure is allowed increase with flowrate such that static pressure at the end of the pipe is constant, is the shown to result in the lowest energy consumption and water loss. The authors perform a cost analysis of each solution along with a few other methods (which are ultimately ineffective) to show that using a VFD with proportional pressure control results in the lowest annual maintenance costs (Halkijevic, Vukovic, & Vouk, 2013).

The author seeks to dispel fears surrounding the use of VFD technology and variable speed pumps. VFD technology has continued to mature over the years and has decreased in cost while simultaneously increasing in reliability to the point that fixed-speed systems cannot always be considered cheaper to implement. Although design considerations for VFDs are different from fixed-speed systems, all that is needed is an understanding of those issues to make implementation feasible. In general, the potential for energy savings and increased reliability outweigh any of the risks associated with using VFDs in modern systems (Pemberton, 2005).

1.3 Summary

There has been quite a substantial amount of work done towards improving the performance, life, and costs associated with the operation of centrifugal pumps. These pumps have been around for many decades and have penetrated all sectors with a myriad of applications and styles. As a result, the work surrounding centrifugal pumps has been thoroughly exhaustive when it comes to improving key performance characteristics. In order to bring something truly innovative to the field, new concepts and ways of looking at the way pumps perform is needed. This paper attempts to do this by implementing pump and system controls in a manner that has widely been ignored. This paper details the advantages of such a system.

2 BACKGROUND

Centrifugal pumps are used across all sectors in a wide variety of applications. Other pumps, such as positive displacement (PD) pumps, are equally as prominent, but are typically reserved for high-pressure, low-flowrate scenarios, whereas centrifugal pumps are usually used for low-pressure, high-flow applications. The governing equations for centrifugal pumps are based on the First Law of Thermodynamics, which is also known as the Law of Conservation of Energy. A centrifugal pump is a device that adds energy to fluid by accelerating it. This energy is then converted into pressure and flow based on the characteristics of the pump and system. At the relatively low pressures experienced by centrifugal pumps, the pumped fluid can be considered incompressible; additionally, the small temperature change is assumed to have negligible effect on fluid density, so the fluid is considered to be a constant density, ρ.

Researchers have conducted studies on the optimization of impeller blades for centrifugal pumps. Designs for impellers can vary greatly and affect the performance and style of the pump. Impeller geometry determines the type of centrifugal pump between radial/mixed/axial flow and shape optimization gives some performance and efficiency improvements. This field of research benefits greatly from commercial CFD software where designs can be simulated and adjusted without the need for manufacturing test samples. Although the field continues to be very popular among researchers, the relative gain from changing impeller geometry is only substantial in the case of specialty pumps and applications.

Another common method of improving pump performance is by increasing the engineering effort put into system analysis and pump selection. This approach is primarily one of economic analysis since the work does not change how individual pumps perform but attempts to make the

best selections for pumps, motors, valves, and fittings to assure optimum performance when they come together to form a whole system. In addition to part selection, wear analysis and scheduled preventative maintenance are also employed to keep efficiency and performance high over time. These methods are capable of returning good results, but there is virtually no change in pumping technology and many hours of effort must go into analyzing each target system individually in order to make optimal part selections. A true engineering solution should be easily adaptable to a wide range of applications with minimal effort once the initial work is completed. The use of VFDs makes an important step in this direction.

With the increasing availability of VFDs, many researchers have turned their efforts to create variable speed pumping systems which promise substantial energy savings according to the affinity laws. The affinity laws show that the power output by a centrifugal pump is proportional to the cube of its speed (Equation 4-7); however, the affinity laws say nothing about the effect on pump efficiency. Therefore, one might assume that reducing a pump speed by 50% will reduce its energy consumption by 87.5%; however, it only reduces energy output by that amount. If reducing the speed of the pump moves the pump a substantial distance from its BEP, there may be a considerable loss in efficiency making the consumed energy much higher than anticipated. For this reason, speed control alone is only a partial solution in terms of pump optimization. In order to achieve reliable energy savings and optimal performance, the pump must be kept operating as close as possible to its BEP. The best way to achieve these results is through a combination of system dynamics with pump speed and pump selection to achieve a network capable of robust, reliable and efficient performance.

Martins and Lima proposed a control system to increase the reliability (see Figure 2-1) of centrifugal pump systems through the use of VFDs and CVs used in compliment with one another. They proposed that one could adjust the speed of the pump and the pressure drop across the CV to cause the pump to remain within its BEP while maintaining its operational capacity. Their results showed that this type of control system is not only possible, but improves a great number of aspects including vibration, power usage, efficiency, heat generation, and overall pump wear. This method of pump and system control is the basis for the research addressed in this proposal and promises much more significant gains than can be realized by any other individual method of optimization.

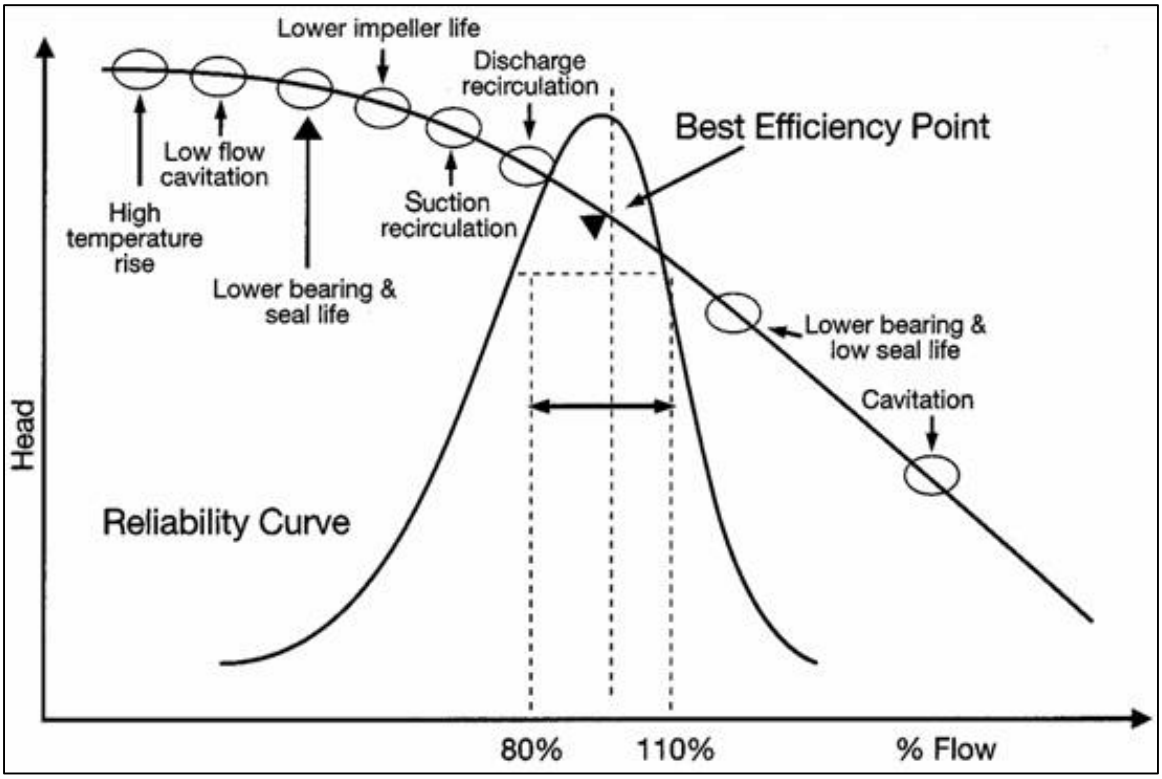

Figure 2-1. Operational range of centrifugal pump via Barringer & Associates, Inc. (2004).

The work done by Martins and Lima brings to light the importance of a control valve for operating a pump at or near its BEP, but they did not make it their goal to continuously minimize deviation from the BEP only to reduce deviation while providing the target flow. They label their

work as a “tune-up” since it does not continually optimize both pump speed and valve position. Their system allows for restricted operation under the conventional method (CV position), but switches to speed control when the valve opens or closes beyond a certain amount (e.g. 45-55% open). In order to improve upon this theory, the system proposed herein will operate by varying both the speed and CV to minimize deviation from the BEP while providing the desired flowrate.

3 GOALS

The goal of this study is to create a control system for running centrifugal pumps. The control system objective will be simply to maintain close adherence to the reference input for flowrate and head. The way the controller achieves this objective, however, will involve metering both the pump speed (N) and the control valve position to reach the desired flowrate while keeping the pump operating at its best efficiency point (BEP), based on head. In order to achieve this goal, the efficiency and pressure-flow curve of the pump needs to be studied. Figure 5-1 shows the combined motor and pump efficiency across the pressure-flow curve at several speeds; the peak of each curve is selected as the BEP for that particular speed. Figure 5-2 shows the pump pressure-flow curve with the resulting BEP curve in black. According to Figure 5-2, the study pump can only operate at approximately 10 – 20 GPM while remaining reasonably close to the BEP. The high end of the speed is limited by the peak power of the motor and the low end of the speed is limited by the shutoff voltage of the "black box" motor controller. In application, the control system response will have differing performance requirements for each output. Flowrate should reach the desired value very quickly and maintain small steady-state error. However, the system itself can take longer to reach the target performance with respect to the BEP. In an ideal world, the perfect system would achieve all requirements instantly and maintain infinitesimal error at all times; however, realistic requirements are selected to be reasonably able to achieve. This means that the system can be allowed to function outside of its BEP for short amounts of time as the system converges to an optimal setting, so long as the necessary flowrate is always maintained. As far as pump life is considered, appreciable wear takes time on the order of hours so convergence on the order of seconds should be reasonable assuming that the output requirement changes are relatively infrequent (minutes to hours).

In addition to developing the desired control system, the performance of said system will be evaluated and compared to each of the two prevailing control techniques: throttle control and speed control. Several metrics will be used to compare performance such as peak power, total energy consumption, flowrate and pressure error, and overall efficiency.

Finally, the control system will be implemented in a physical system as a proof-of-concept. The results will be compared to those from the simulation as a measure of goodness for the numerical model. Based on the results, a summary of the methodology will show how to reproduce these results with any hydrodynamic pump system. Due to the nature of the proposed control system, there should be virtually no limitation to its applicability in these types of systems even if BEP is not the target for optimization.

4 INVESTIGATIVE APPROACH

The investigative approach covers the methods used in this work to analyze the physical principles surrounding the key subjects. The analytical portion starts by using basic physical principles and relating them to the problem being discussed. These principles, which are commonly presented in the form of equations, lay the groundwork for further analysis by showing the expected interactions between different system components. The experimental (or empirical) approach goes a step further by looking at these relationships in action. The physical principles are observed through actual experimentation to simultaneously validate the analytical assumptions and provide essential data for further analysis using numerical methods and simulations.

4.1 Analytical

The analytical nature of centrifugal pumps are regulated by the First Law of Thermodynamics or The Law of Conservation of Energy; in a closed loop system, the energy dissipated within the loop must equal the energy added by the pump. From this basis we can take the expanded Bernoulli's equation, which includes viscous losses, and create the first step to analyzing centrifugal pumps. Equation 4-1 below shows the most common form of Bernoulli's equation.

Equation 4-1 $$P_1 + \frac{1}{2}\rho v_1^2 + \rho g h_1 + P_l = P_2 + \frac{1}{2}\rho v_2^2 + \rho g h_2$$

In engineering applications, the standard form of the equation is often manipulated into a more useful form; the head form is shown in Equation 4-2. Additionally, to better represent the system

being analyzed, P_1 and P_2 will be replaced by P_s (static pressure or Net Positive Suction Head available—NPSHa) and P_d (discharge pressure), respectively.

Equation 4-2

$$\frac{P_s}{\rho g} + \frac{v_1^2}{2g} + h_1 + \frac{P_l}{\rho g} = \frac{P_d}{\rho g} + \frac{v_2^2}{2g} + h_2$$

The equations above can be further rearranged and simplified based on some assumptions. First, the change in elevation is negligible, making $h_1 \approx h_2$; second, the bulk of the fluid in the tank is not moving, so $v_1 \approx 0$. Finally, P_l can be represented as a multiple of dynamic head, where K is a coefficient representing the sum of all dynamic components in the system.

Equation 4-3

$$\frac{P_d - P_s}{\rho g} = K\frac{v^2}{2g}$$

Equation 4-3 can be considered the pump equation where $P_p - P_s$ is the pressure added by the pump, P_p, and *v* is the velocity of the fluid leaving the pump. From Equation 4-3 the most important laws governing centrifugal pumps can be derived: the Affinity Laws.

Consider the rotating impeller of a centrifugal pump as shown in Figure 4-1. As the rotational speed, N, of the impeller changes, the fluid velocity, *v*, changes in a directly proportional manner. Since volumetric flowrate is the product of fluid velocity and the cross-sectional area of the region that the fluid is flowing through, flowrate, *Q*, is also directly proportional to speed. This gives the first Affinity Law, Equation 4-5.

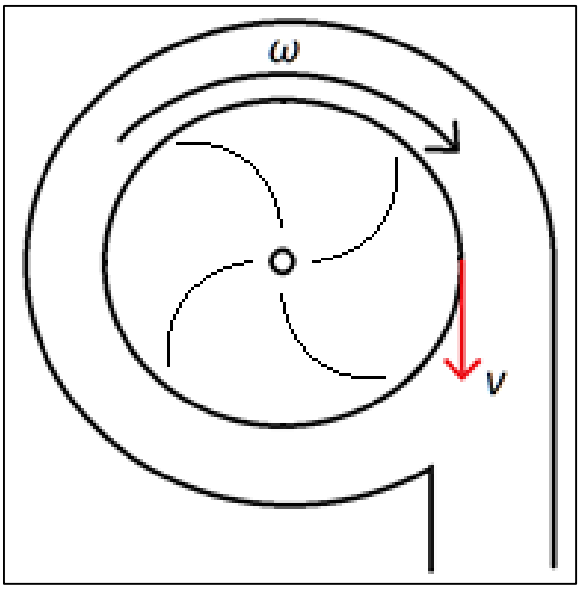

Figure 4-1. Diagram of a pump impeller.

Looking at Equation 4-3, the pressure rise across the pump is proportional to the square of the fluid velocity; therefore, the pressure added to the system by the pump is also proportional to the square of the rotational speed. This gives the second Affinity Law, Equation 4-6.

Equation 4-4 $$Hydraulic\ Power = P_T Q$$

Equation 4-4 shows how to calculate the hydraulic power delivered by any pump. It has already been shown that the flowrate of a pump is proportional to the impeller speed and that the pressure rise is proportional to the square of the impeller speed; since the hydraulic power is the product of pressure rise and flowrate, then hydraulic power is proportional to the cube of the impeller speed. This gives the third and final Affinity Law, Equation 4-7.

Equation 4-5 $$\frac{Q_1}{Q_2} = \frac{N_1}{N_2}$$

Equation 4-6 $$\frac{\Delta P_1}{\Delta P_2} = \left(\frac{N_1}{N_2}\right)^2$$

Equation 4-7

$$\frac{Power_1}{Power_2} = \left(\frac{N_1}{N_2}\right)^3$$

These Affinity Laws govern the analytical nature of centrifugal pumps and can be used to determine how its characteristics will change as impeller speed changes. From Equation 4-7, halving speed will reduce power output by 87.5%; this concept is the prime reasoning behind the use of variable-speed centrifugal pumps.

4.2 Experimental

The test fixture has gone through a few revisions originating from the original proposal from Boeing (Figure 4-2). The proposal originally called for a 15,000 – 20,000 PPH (pound per hour) mass flow pump powered by a 400 Hz, 115 VAC power source. Although one is not shown, a primary line should connect the study tank to the drain tank to allow for simulation of fuel being consumed during flight. The original design includes two motor operated valves for flow control; one solenoid valve is also included to allow for the simulation of rapid changes in flow demand (i.e. rapid increase in fuel demand during takeoff). Sensors for temperature, pressure, and flowrate are also included to monitor power conversion into fluid flow and heat. For simplicity, the system is not pressurized and vents are included to ensure that the study and drain tanks have equal static pressure. Boeing intended for the proposed design to be reproduced verbatim and they expected a revised design based on the knowledge, experience, and practical capabilities of the research team.

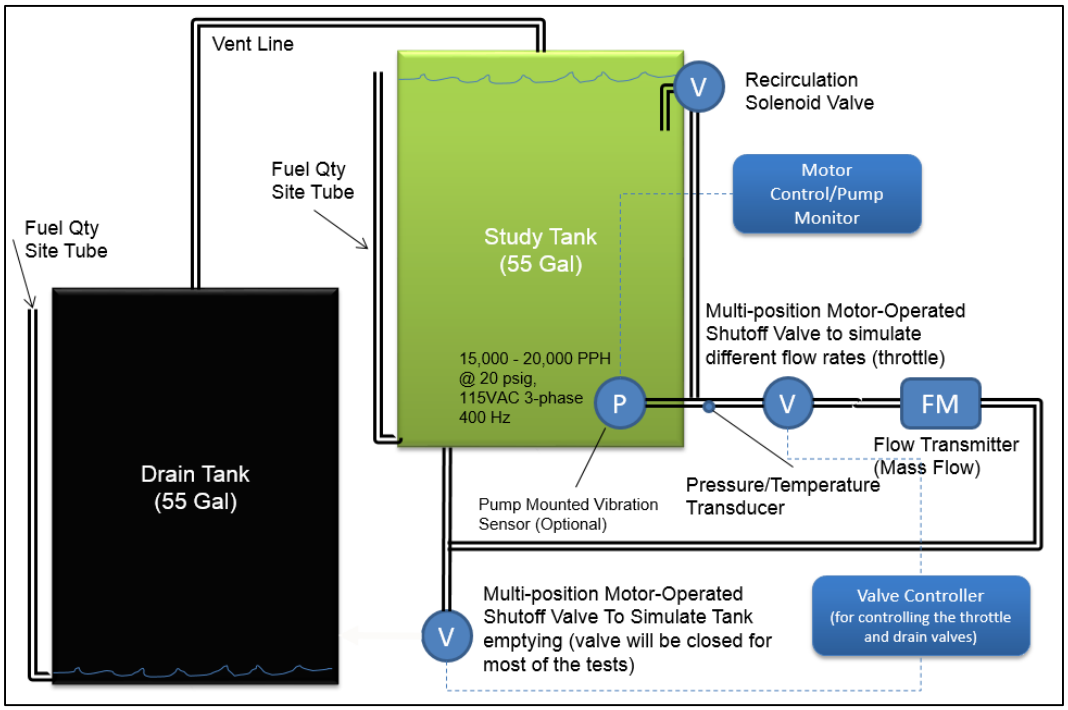

Figure 4-2. System configuration as proposed by Boeing.

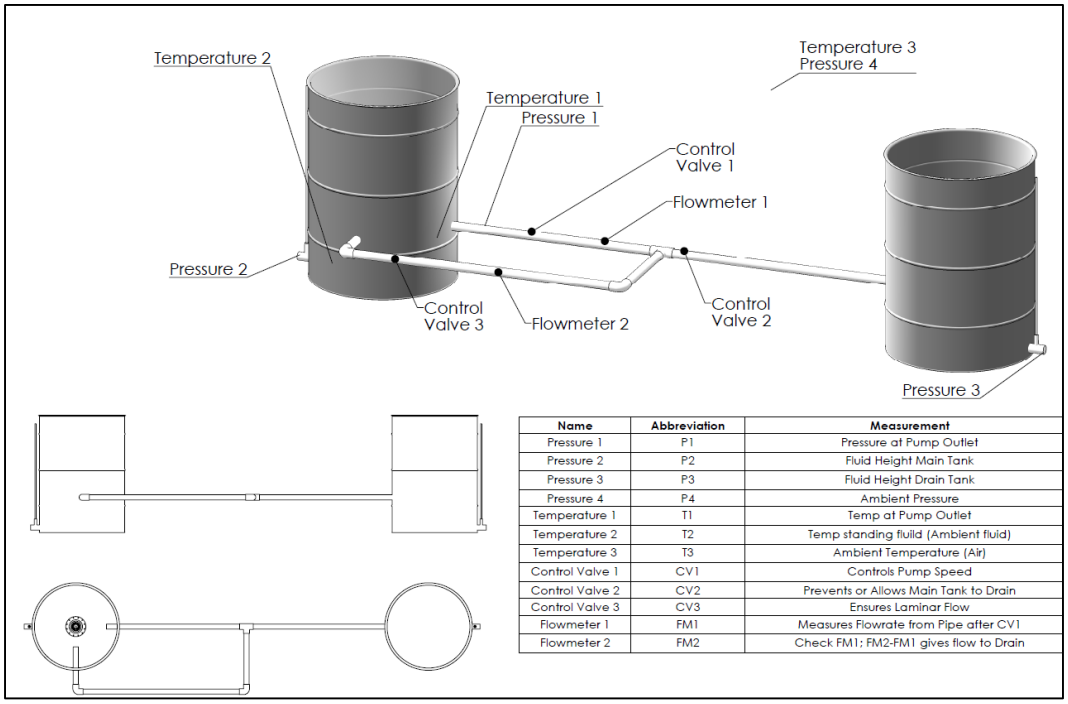

Name	Abbreviation	Measurement
Pressure 1	P1	Pressure at Pump Outlet
Pressure 2	P2	Fluid Height Main Tank
Pressure 3	P3	Fluid Height Drain Tank
Pressure 4	P4	Ambient Pressure
Temperature 1	T1	Temp at Pump Outlet
Temperature 2	T2	Temp standing fluild (Ambient fluid)
Temperature 3	T3	Ambient Temperature (Air)
Control Valve 1	CV1	Controls Pump Speed
Control Valve 2	CV2	Prevents or Allows Main Tank to Drain
Control Valve 3	CV3	Ensures Laminar Flow
Flowmeter 1	FM1	Measures Flowrate from Pipe after CV1
Flowmeter 2	FM2	Check FM1; FM2-FM1 gives flow to Drain

Figure 4-3. Revised system as proposed by Mizzou research team.

The first version of the revised system is shown in Figure 4-3. The system includes two flow meters, primary flow and return flow; three control valves, one for throttling and one each for controlling return and drain flowrates; three temperature transducers, one inlet, one outlet, and one ambient sensor; and four pressure transducers, two for measuring the fluid height in each tank, one for measuring discharge pressure of the pump, and one for ambient pressure. Unfortunately, high implementation cost of the proposed revisions forced the elimination of one of the flow sensors (return) and two of the control valves which were replaced with hand operated versions. This led to the second proposed system which became the first implemented configuration. The final design incorporated additional sensors to increase data acquisition capability (Figure 4-4).

The implemented system mostly follows the system shown in Figure 4-3, but with the changes listed above. However, one important additional change that occurred was the substitution of a smaller 12,000 PPH pump for the proposed 20,000 PPH pump. This change was made due to the fact that the intended pump would not be available for testing in a reasonable time—at least 9 months later than expected. The change in pump capacity called for a reduction in pipe diameter to keep fluid velocity high enough to measure flowrate. The current design also updated the means of controlling the pump; where the original pump would need a 2 to 3 hp AC variable frequency drive (VFD), the new pump was powered by DC voltage with power peaking at about 1 hp. The new pump also includes a variable speed driver internally so that varying input voltage from 14 to 32 VDC automatically varies the pump speed from approximately 6,000 to 12,000 RPM. This particular centrifugal pump is a canister pump design, meaning that the motor and impeller is enclosed in an aluminum canister which is fitted into the side of a tank. Figure 4-6, Figure 4-5 and Figure 4-7 illustrate the pump structural design. The primary advantage of this design allows for removal and service of the motor and pump without needing to empty the service tank.

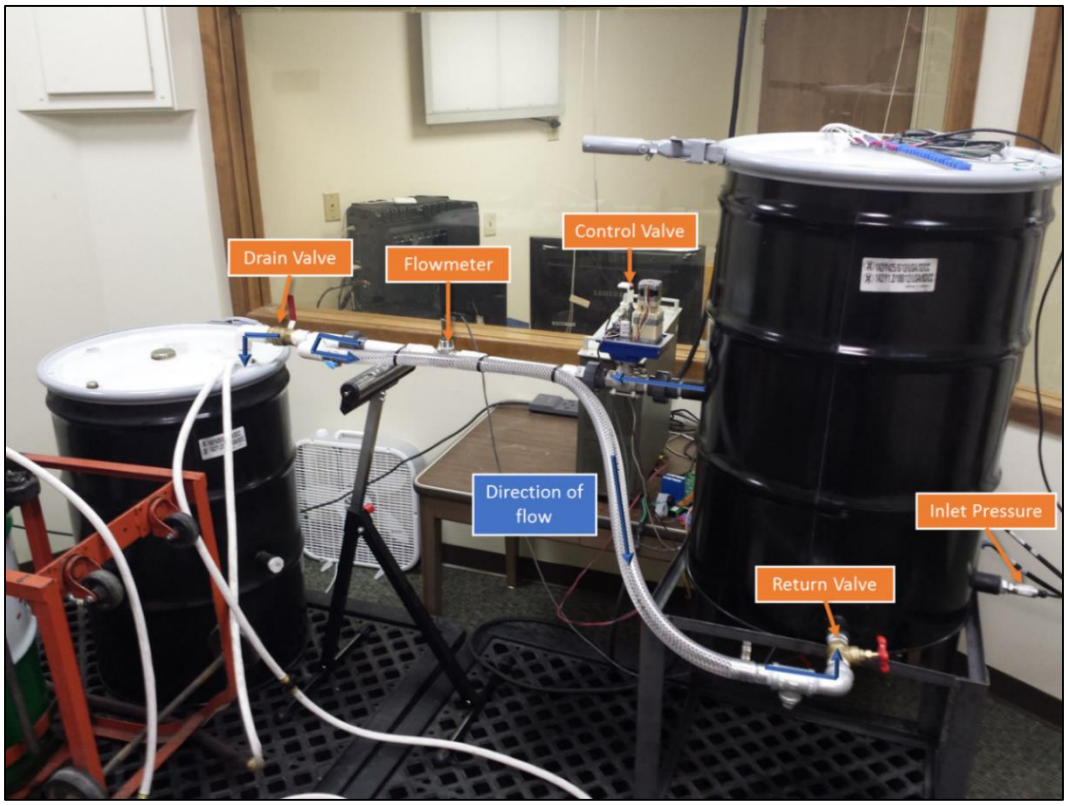

Figure 4-4. Final design.

Figure 4-5. Canister attached to study tank.

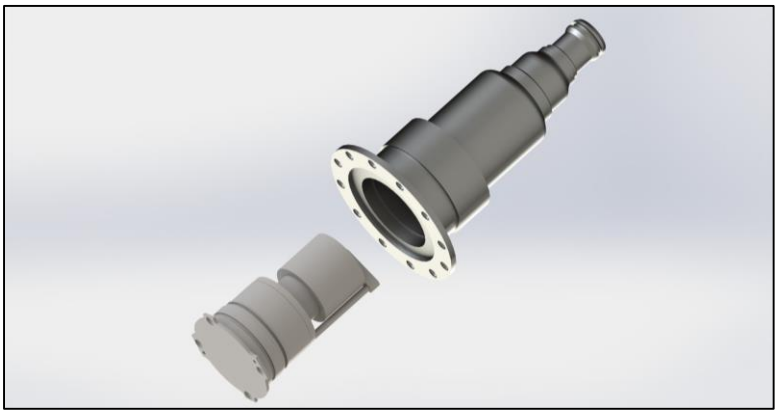

Figure 4-6. Pump and canister.

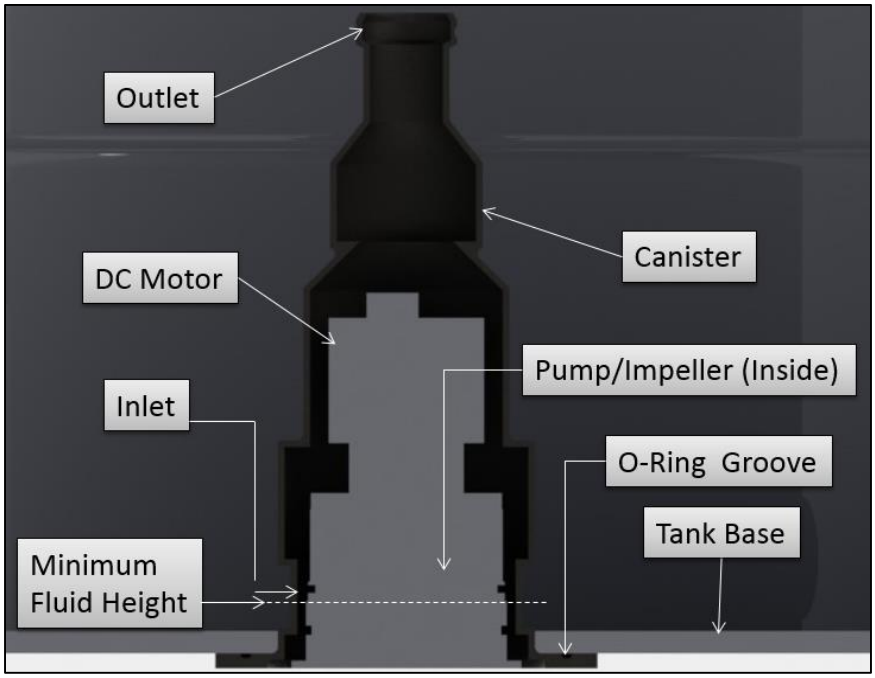

Figure 4-7. Detailed view of the pump and canister as installed.

5 PUMP/SYSTEM ANALYSIS

In order to make a control system for any given pump, the pump pressure-flow curve must be known. In the case of this study, instead of taking one curve and extrapolating based on the affinity laws, the pump is physically tested across all speeds and flowrates to obtain a full analysis. There is a second advantage to manually testing the pump at all speeds; the combined efficiency of the pump and electric motor can be precisely measured for all speeds and flowrates. This is essential for the type of control that is being developed here, which is efficiency optimization.

The system used to analyze the pump and test the control system is shown in Figure 1-1. The system used to evaluate the pump characteristics is the same as the one that will be used to evaluate its performance once the control system is applied. The system appears simple, and in essence it is, but the equipment being used to measure and control the system is highly sophisticated and allows for complete automation. Full factorial simulation can be easily achieved through National Instruments LabVIEW since everything about the system can be simultaneously controlled and measured remotely.

Figure 5-1 shows the results of the measured efficiency. Efficiency, η, is measured by taking the ratio of input electrical power to output hydraulic power resulting in the equation

$$\eta = \frac{P_T Q}{EI} * 0.435$$

Equation 5-1

$$0.435 = \left[\frac{\left(1\,\frac{lbf}{in^2}\right)\left(1\,\frac{gal}{min}\right)}{(1\,V)(1\,A)}\right] * \frac{(1\,V)(1\,A)}{1\,W} * \frac{231\,in^3}{1\,gal} * \frac{1\,min}{60\,s} * \frac{1\,ft}{12\,in} * \frac{1\,hp}{550\,\frac{ft-lbf}{s}} * \frac{746\,W}{1\,hp}$$

where the factor 0.435 is used for unit conversion. All values are measured by transducers whose calibration details can be found in Appendix A. The efficiency curves in Figure 5-1 have a peculiar tendency. One would expect for the efficiency curve to be translated to the left or right as speed is

decreased or increased, respectively, according to the affinity laws; in reality, the curves also move downwards with decreasing speed. This tendency occurs because the efficiency is not purely that of the pump, but of the motor-pump combination. Electric motors are typically only capable of achieving their optimal efficiency when being operated at or near full power; as the motor is slowed, its efficiency lowers accordingly. This means that a larger portion of the energy is being converted into heat and vibrations; however, the lower total energy means that the slight decrease in efficiency is acceptable. Table 5-1 illustrates how this concept works. Even though the efficiency between the highest and lowest speed drops by roughly 5%, the input power (and wasted power) also drops by a factor of 5—substantially outweighing the relatively small losses in efficiency. It is important to remember that not all work done by a pump is "useful work"; for example, pumping through a recirculation circuit uses energy while providing nothing useful to the system as a whole, no matter how high the pump efficiency may be.

Table 5-1. Wasted power based on total power.

N	Total Power In (W)	η	Wasted Power (W)
6000	120.1	0.2544	89.5
7000	180.3	0.2746	130.8
8000	260.5	0.2892	185.1
9000	360.0	0.2991	252.3
10,000	485.8	0.3060	337.2
11,000	630.1	0.3088	435.6

By combining the efficiency curves with the pressure-flow curves of the pump, the region of optimal performance can be defined; Figure 5-2 shows the result of these characterization experiments. The BEP alone (as it is traditionally defined) is not able to determine the ideal pump conditions for a given flowrate. The traditional Best Efficiency Point (BEP) only shows the best

operating point for a given speed (Figure 5-2, shown as black triangles); this would pertain to the peak of any constant speed curve as shown in Figure 5-1. The True BEP (hereafter referred to as the TBEP) is actually a minimization problem where the system should move along the TBEP line (Figure 5-2, black dotted line) in the direction of decreasing energy to the lowest point that still satisfies the flowrate requirement. With the pressure-flow curves and the TBEP curve for the pump properly defined, a control system can be developed to operate the pump at its optimal conditions.

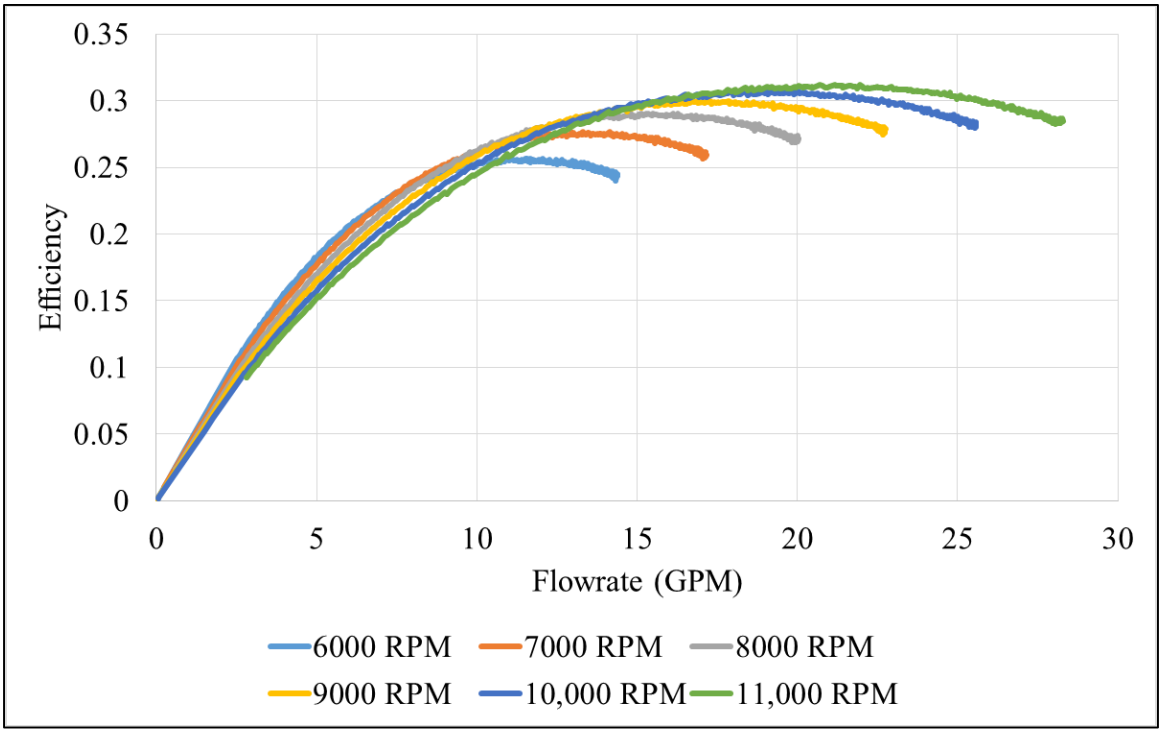

Figure 5-1. Combined motor and pump efficiency.

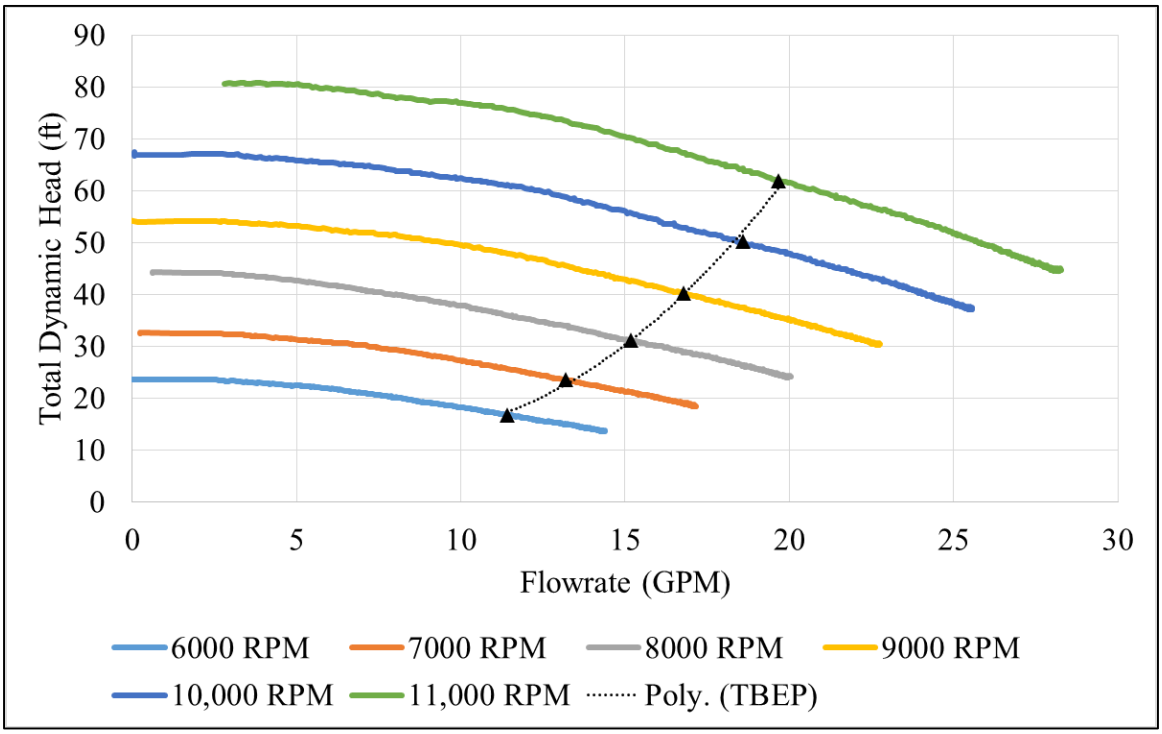

Figure 5-2. Pressure-flow curve for study pump.

6 CONTROL SYSTEM DEVELOPMENT

6.1 System Configuration

A block diagram for the dynamic system is shown in Figure 6-1. The system uses flowrate as a reference input which is passed through the True Best Efficiency Point (TBEP) equation to determine the optimal pressure for the required flowrate. Two controllers—working in parallel—are used to move the system towards the desired flowrate and ideal pressure. The flow controller, K_1, adjusts the voltage to the pump motor and is able to rapidly change the flowrate being delivered to the pump. The pressure controller, K_2, gradually adjusts the position of the control valve (CV) to change the pressure drop through the system. Each controller has to continually adjust to compensate for any changes made by the other controller, but the highly dampened nature of the CV being used keeps the system from oscillating unnecessarily.

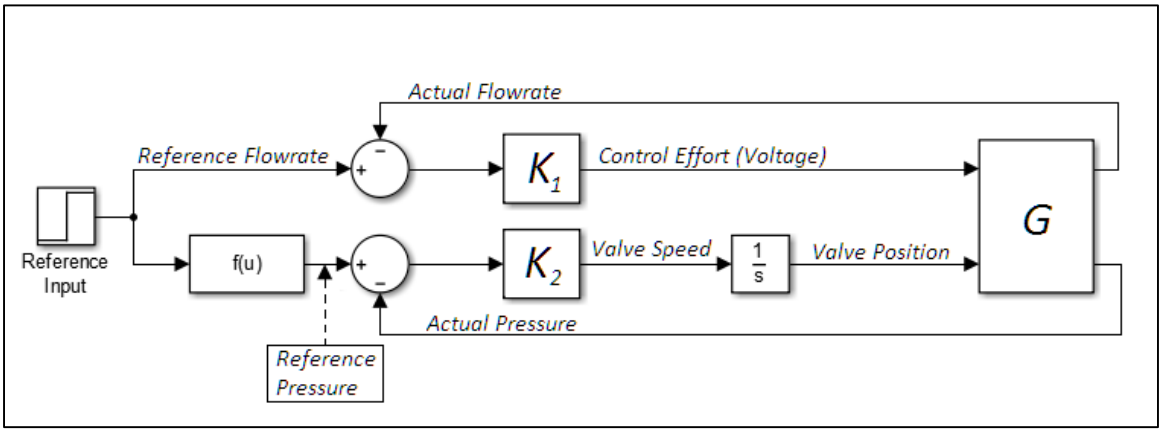

Figure 6-1. System block diagram.

6.2 Flow Dynamics

6.2.1. Head Analysis

A centrifugal pump operates by adding kinetic energy to a fluid. That fluid is then tangentially ejected from the pump, and the kinetic energy is converted to flow and pressure based on the configuration of the system it is entering. For example, pumping directly into an open tank will result in most of the energy becoming kinetic with a high flow and almost no static pressure; conversely, pumping into a closed line will result in all of the energy going towards increasing the static pressure of the fluid (also known as dead-head or dead-heading of the pump). However, both of the above situations can potentially cause damage forcing operation outside of the conditional design of the pump.

Head is the term used to define the total amount of energy added to fluid by a pump and is given units of length. A relationship exists between head and the resulting flowrate by considering the ways that energy is consumed. If a pump is moving fluid between two sealed tanks, there will be an amount of energy added to (or removed from) the fluid in the form of static pressure. Any change in elevation will also add or consume potential energy. When including friction, additional energy is consumed by major and minor losses associated primarily with system geometry. Major losses are a result of friction in flow over any distance and minor losses result from any sudden changes in flow such as orifices, changes in pipe diameter, or changes in flow direction (tees, elbows, wyes, etc.) In general the totality of these factors are combined to represent the Total Dynamic Head (TDH) of the system for a given flowrate, Q. The TDH represents everything working against the pump, and under steady-state conditions the TDH is equal to the head added to the fluid by the pump, ΔH. The following assumes that leakage is negligible.

Equation 6-1 $$\Delta H = \frac{P_2 - P_1}{\rho g} + \frac{v^2}{2g} + (h_2 - h_1) + f\frac{l}{D}\frac{v^2}{2g} + K\frac{v^2}{2g}$$

In the above equation (Munson, Okiishi, Young, & Huebsch, 2009), the subscripts 1 and 2 represent upstream and downstream of the pump respectively. *P* is the static pressure of the fluid source or drain, ρ is the density of the fluid being pumped, *g* is the rate of acceleration due to gravity, *h* represents the height of the source or drain relative to a common datum, *f* is the Darcy-Weisbach friction factor (sometimes referred to simply as friction factor), *l* is the total length of pipe that the fluid flows through, *D* is the pipe diameter, and *K* is the summation of minor losses throughout the entire length of fluid travel.

The friction factor is the most difficult to predict since it changes based on the Reynolds Number (Re) and has points of extreme non-linearity for Re between ~2300-4000. For the following derivation, the flow is assumed to always be laminar (Re < 2300). From (Munson, Okiishi, Young, & Huebsch, 2009):

Equation 6-2 $$f = \frac{64}{Re}$$

Equation 6-3 $$Re = \frac{vD}{\nu}$$

Equation 6-4 $$v = \frac{Q}{A}$$

Equation 6-5 $$A = \frac{\pi D^2}{4}$$

Substituting the above into Equation 6-1.

Equation 6-6 $$\Delta H = \frac{P_2 - P_1}{\rho g} + (h_2 - h_1) + \left(1 + \frac{16\pi l\nu}{Q} + K\right)\frac{8Q^2}{g(\pi D^2)^2}$$

Simplifying.

Equation 6-7 $$\Delta H - \frac{P_2 - P_1}{\rho g} - (h_2 - h_1) = \frac{8(1+K)}{g(\pi D^2)^2}\left[Q^2 + \frac{16\pi l\nu}{1+K}Q\right]$$

Completing the square and solving for Q.

Equation 6-8 $$Q = \sqrt{\frac{g(\pi D^2)^2}{8(1+K)}\left[\Delta H - \frac{P_2 - P_1}{\rho g} - (h_2 - h_1)\right] + \left(\frac{8\pi l\nu}{1+K}\right)^2} - \frac{8\pi l\nu}{1+K}$$

Equation 6-8 is the equation which governs flowrate for any system with ΔH to motivate that flow assuming an incompressible fluid and no leakage. For the study system, fluid is pumped through a closed loop making no relative change in static pressure or elevation so Equation 6-8 can be further simplified to

Equation 6-9 $$Q = \sqrt{\frac{g(\pi D^2)^2}{8(1+K)}\Delta H + \left(\frac{8\pi l\nu}{1+K}\right)^2} - \frac{8\pi l\nu}{1+K}$$

Equation 6-9 has only two unknowns, the minor loss coefficient, K, and the head added by the pump, ΔH. Both K and ΔH can vary greatly based on a number of factors so they are best defined through experimentation.

6.2.2. Energy Analysis

Another common way to look at dynamic systems to create an energy balance. According to the First Law of Thermodynamics, energy cannot be created or destroyed: only converted from

one form to another. By looking at the power that is being added to the system—the hydraulic power—another prediction can be made for the systems operational state.

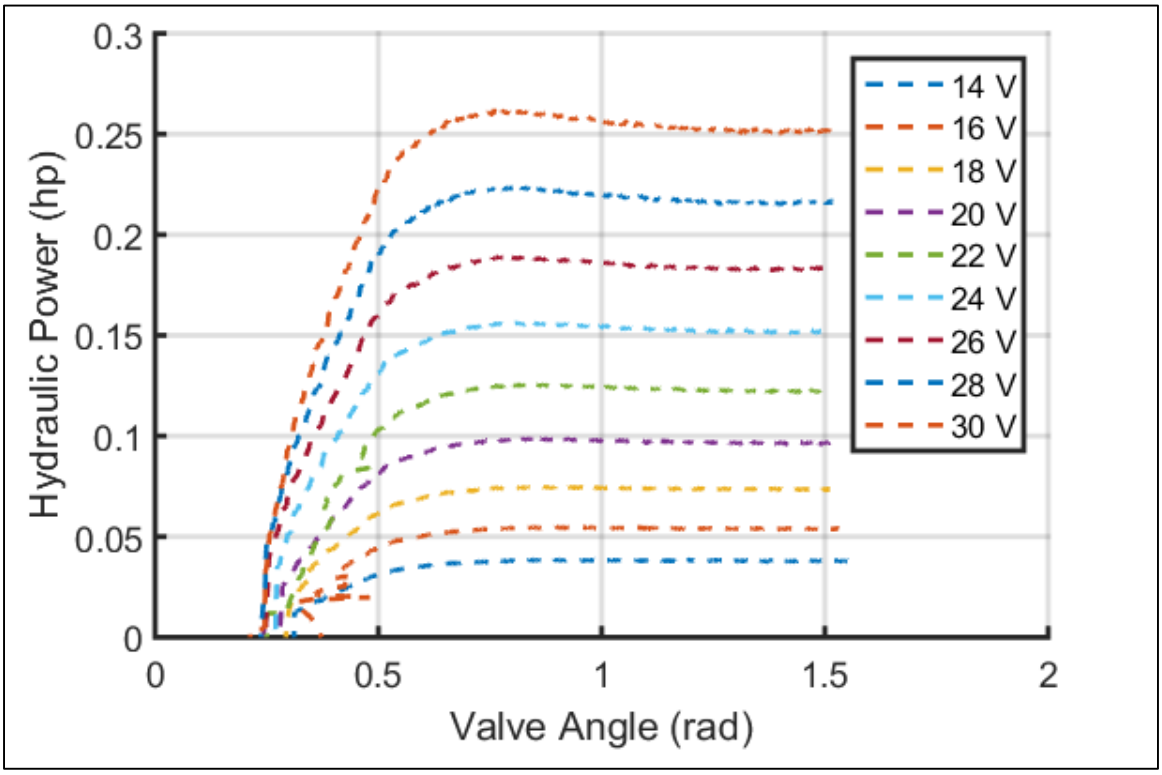

Figure 6-2. Hydraulic power generated by the pump.

Equation 4-4 shows how hydraulic power is calculated as the product of pressure and flowrate at a point in the system just at the outlet of the pump. There exist some minor losses before the fluid reaches this point, but since fluid cannot be used to do work until it leaves the pump, those losses are considered characteristic of the pump hydraulic efficiency. If the hydraulic power is divided by the density of the fluid and the acceleration of gravity (both of which are constants), the pressure can be represented in head form. This allows Equation 6-6 to be substituted in and slightly simplified to get

Equation 6-10 $$\frac{Power}{\rho g} = \left(\frac{P_2 - P_1}{\rho g} + (h_2 - h_1)\right) Q + \frac{128 l \nu}{g \pi D^4} Q^2 + \frac{(1+K)8}{g(\pi D^2)^2} Q^3$$

The coefficients from Equation 6-10 can be considered, from left to right, as the static, elevation, viscous, and dynamic components. The fact that this equation is a function of the flowrate cubed is no coincidence. This falls back on the Affinity laws where the flowrate scales proportionally with speed and the power scales proportionally with the cube of speed; since speed and flowrate scale proportionally, flowrate can be substituted into the latter relationship to show that power scales with the cube of flowrate as well. However, the Affinity Laws neglect the linear and quadratic components seen here which is why basing analysis solely on these laws can be a false assumption.

Equation 6-11 $$f(\omega) = AQ + BQ^2 + CQ^3$$

In general, Equation 6-10 can be simplified to the form shown in Equation 6-11. So long as the system operates in the flattened region of the power curve shown in Figure 6-2, the hydraulic power can be considered mostly constant for a given impeller speed. According to Figure 6-2, the power begins to fall steeply as the valve closes past approximately 35°, but data acquisition cannot be considered accurate in this region since the flowmeter loses the ability to take reliable measurements (as can be seen by the large spikes in data). On the left hand side of Equation 6-11, the power can be approximated as a function of the voltage being applied to the pump. Even though permanent magnet DC synchronous motors require complex electronics to work, the always-relevant Ohm's Law still applies. Ohm's Law states that voltage is the product of current and resistance; combining that with the fact that electrical power is the product of voltage and current, Equation 6-12 shows the relevant relationship between power and voltage (Nilsson, J. W. & Riedel, S., 2014). Here, the resistance of the pump is considered a constant value since the motor windings behave similar to resistors; although there is an inductive component involved which

makes the impedance of the circuit slightly higher than the DC resistance value. In reality, the electrical power shown in Equation 6-12 will differ from the hydraulic power by some overall efficiency, η, but this will suffice for developing the form of the final approximation.

Equation 6-12 $$Power \propto \frac{V^2}{R}$$

Looking at Equation 6-10 and Equation 6-11, the coefficient *C* is based on the minor loss coefficient, *K*. This means that Equation 6-11 can be expanded slightly to include the effect of the control valve on the system. Making *C* a function of the valve position, θ gives Equation 6-13 where $P_n(\theta)$ is an n^{th} order polynomial of the relationship between the position of the control valve and the minor loss coefficient, *K*; the relationship is very nonlinear, especially as the valve moves further away from its nominal position, so it will be modeled with a relatively high order polynomial to get the largest amount of travel that can accurately be simulated. This makes the flowrate, *Q*, completely defined by the control inputs *V* and θ. Although in reality, the position of the control valve is difficult to control directly without some sort of indexed pivot mechanism, here it is actually controlled by a simple DC motor.

Equation 6-13 $$g(V^2) = AQ + BQ^2 + P_n(\theta) * Q^3$$

Head is already known in general from Equation 6-6, but the form shown in Equation 6-14 simplifies the function and applies the same assumptions that have already been made for the flowrate equation.

Equation 6-14 $$h(V^2) = A + BQ + P_n(\theta)Q^2$$

Efficiency is the final piece of the puzzle. Fortunately, pump efficiency is fairly well understood already. Equation 6-15 shows the general form of pump efficiency. However, this pump is being operated at variable speed and each distinct speed has a distinct design flow that differs from the basic BEP. This is the basis of the TBEP. The design flow will vary with the speed of the pump by some manner that is unique to every pump. This makes the TBEP relation to speed have to be experimentally determined, so it will have a polynomial approximation similar to the minor loss of the ball valve.

Equation 6-15 $$\eta(Q) = \frac{\eta_{BEP}}{Q_{BEP}} Q \left[2 - \frac{Q}{Q_{BEP}}\right]$$

6.3 Controller Design

In the study system there are two PID controllers which are operated in parallel: the flow controller and the pressure controller. The flow controller adjusts the voltage to the pump based on the amount of flow error. This requires an integral controller at a minimum which will continuously increase or decrease the voltage to the desired level. The controller may also contain a proportional gain to slightly speed up the response time, but too large of a proportional gain could be destabilizing. Derivative gain is not used since there is a fair amount of noise in the system which can cause derivative control to have a destabilizing effect. Since there is a predetermined range that the pump can operate in, there is also output coercion which limits the output to the specified range. When including integral control with coercion, it is important to have an anti-windup technique; otherwise, the control effort will attempt to grow infinitely while it is being coerced and it will not be able to respond to new inputs appropriately. In this system the windup is handled by simple clamping whereby the integral portion of the effort is frozen while the output

is saturated. Some controllers may choose to reset the integral gain during saturation, but this could cause undesired output oscillations. Equation 6-16 shows the voltage control effort where $K_{P,V}$ is the proportional gain, $K_{I,V}$ is the integral gain, and e_f is the flowrate error. The more important gain here is the integral gain since it will be doing most of the work, it may even be desirable to use an integral only controller, but for now including a proportional gain will help slightly with response time and overshoot.

Equation 6-16 $$V = K_{P,V} e_f + K_{I,V} \int e_f dt$$

The second plant input is the position of the control valve, but the control effort is actually the turning speed of the valve since it is simpler to physically control. Since the valve speed is integrated to get a position, a proportional controller alone works sufficiently well. There is the possibility of overshoot, but the naturally high damping of the valve due to the large gear reduction and the relatively small inertia makes the risk of overshoot very small. By adding integral control, the risk of overshoot increases and the two controllers each having the possibility to overshoot can make convergence difficult. The valve is said to be heavily damped because it can only turn at a maximum speed of 1/10 RPM. This is a physical restriction on the experimental setup that cannot be avoided, so pressure response times will be very slow. However, this may be good for the controller since there is less competition for convergence between the two controllers. Equation 6-17 shows the head (pressure) controller where $K_{P,\theta}$ is the proportional gain and e_h is the head error.

Equation 6-17 $$\dot{\theta} = K_{P,\theta} e_h$$

6.4 Experiment Based Modelling

6.4.1. Selection of Control Parameters

Commercial software such as MathWork's Simulink, which is included with some MATLAB packages, requires an accurate model of the pump and system to create a control simulation. According to the scientific process, the simplest way to determine how a system operates is to change the independent variables and observe how the dependent variables react. In this system, the two independent variables are the voltage supplied to the motor (pump speed) and the position of the control valve (minor loss coefficient); the dependent variables are the resulting static pressure rise and volumetric flowrate of the fluid as it passes through the pump.

Figure 5-2 shows the result of fixing the pump speed and varying the control valve position; unfortunately, fixing the voltage and fixing the pump speed are not the same thing since the motor experiences a phenomenon known as slip; this phenomenon is amplified as the target speed increases. In fact, the study only shows data up to 11,000 RPM despite the fact that the pump has a max speed closer to 12,000 RPM because even the (highly sophisticated) voltage regulator used to supply the reference voltage has trouble stabilizing that voltage when the motor controller error gets very large. Since the goal here is not to evaluate these particular performance issues, the maximum pump speed is set to 11,000 RPM to avoid unnecessary obfuscation of the actual goals. Fortunately, fixed-speed tests are only truly needed to show pump curves in the traditional context; for the purpose of creating a simulation model, fixed-voltage tests are actually more accurate and much easier to produce.

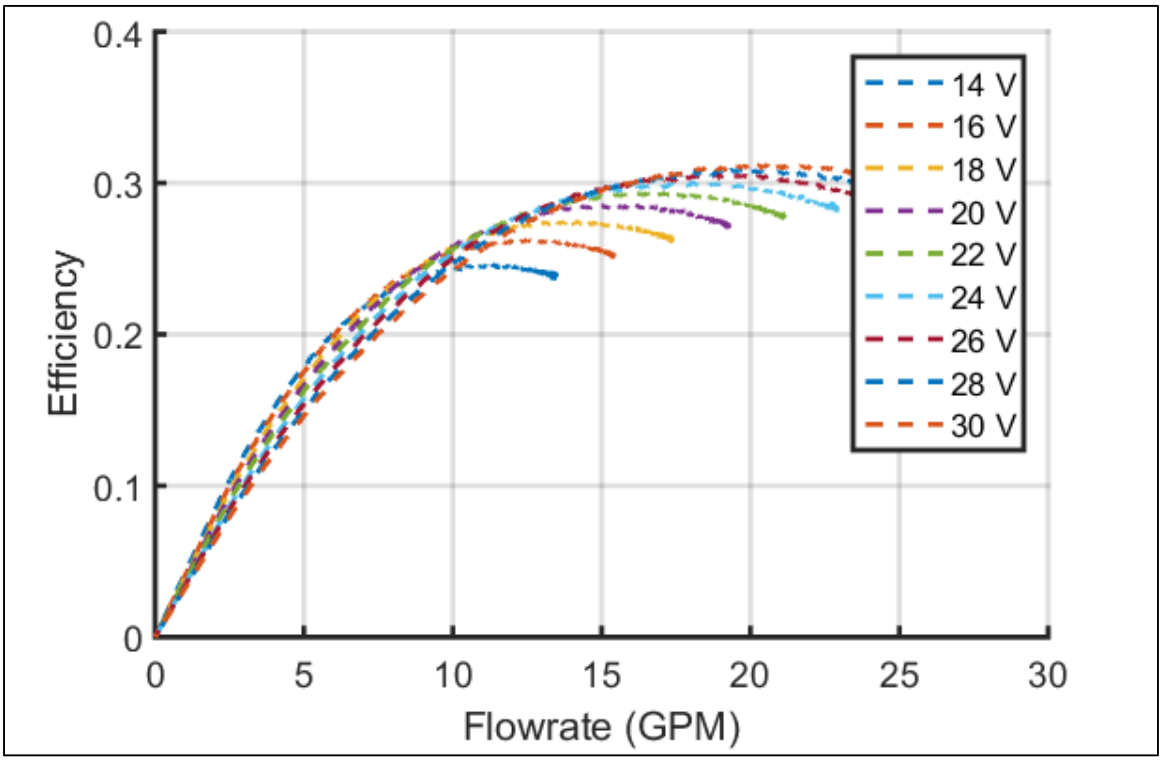

Figure 6-3. Efficiency curves for constant-voltage experiments.

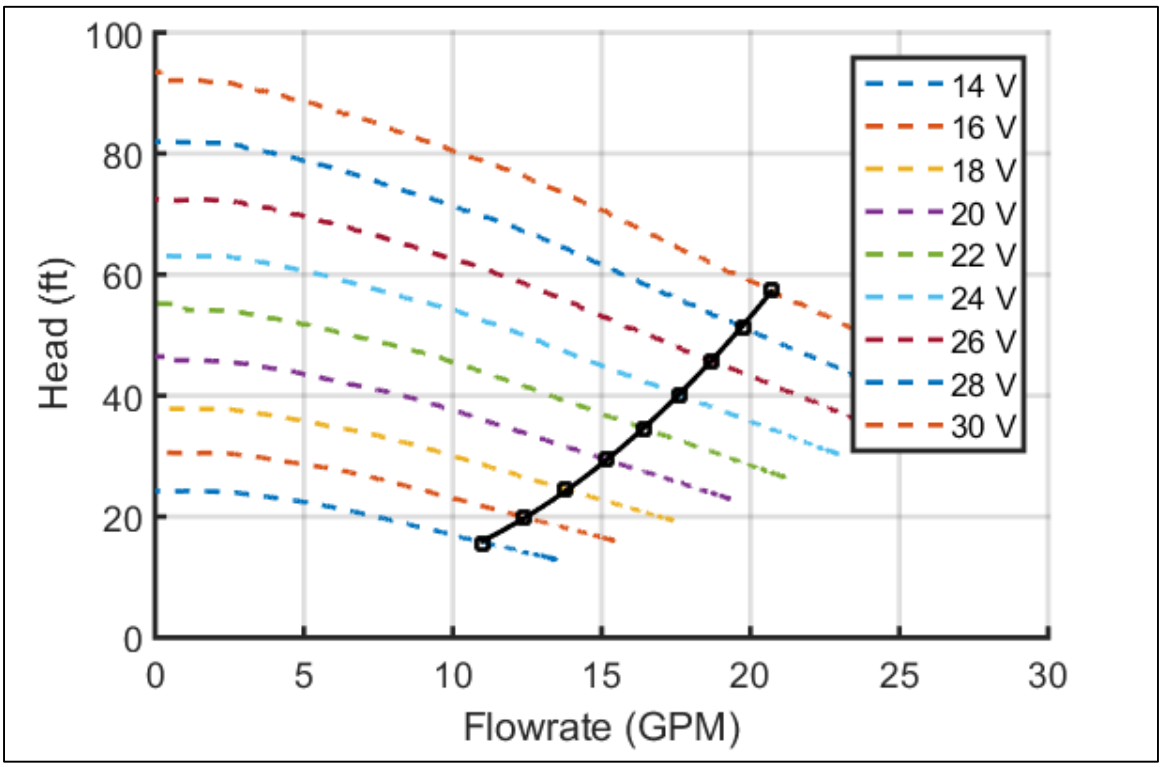

Figure 6-4. Pressure-flow curves for constant-voltage experiments.

Figure 6-3 and Figure 6-4 show the results of the constant-voltage experiments. During these tests, the reference voltage applied to the pump is held constant and the position of the control valve is varied through its entire range. The curves look very similar to the constant speed curves because the two have a strong correlation, but are not directly coupled. However, these minor differences can make a substantial difference when developing a simulation model.

6.4.2. Simulation Modelling

The model for this pump was generated by a method based on multiple regression. In multiple regression (like normal regression analysis) data is fit by a curve that minimizes the error between the fit values and the actual data points. It is important to understand the underlying physical principles behind the data that is being fit so that appropriate dependent and independent variables can be selected and the appropriate function is used to fit the data. Here the relationship between the two independent variables and the data being fit, as well as their relationship with each other are important to consider. A novel method which is shown below uses the collected data to generate a relationship between several values and the two dependent variables, motor voltage and control valve position.

The data shown in Figure 6-5 is collected by fixing the voltage input and varying the position of the valve. Because both of these values are independently applied from external to the system, they are completely independent and have virtually no cross-correlation; this makes the particular fitting technique used here very reliable. It is clear from the data that each curve has a nearly identical shape, but it is scaled by some value proportional to the voltage. In order to make a multivariable fit, a single variable fit is first made for each curve using some arbitrary order and normal regression techniques available in software such as Microsoft Excel or MATLAB.

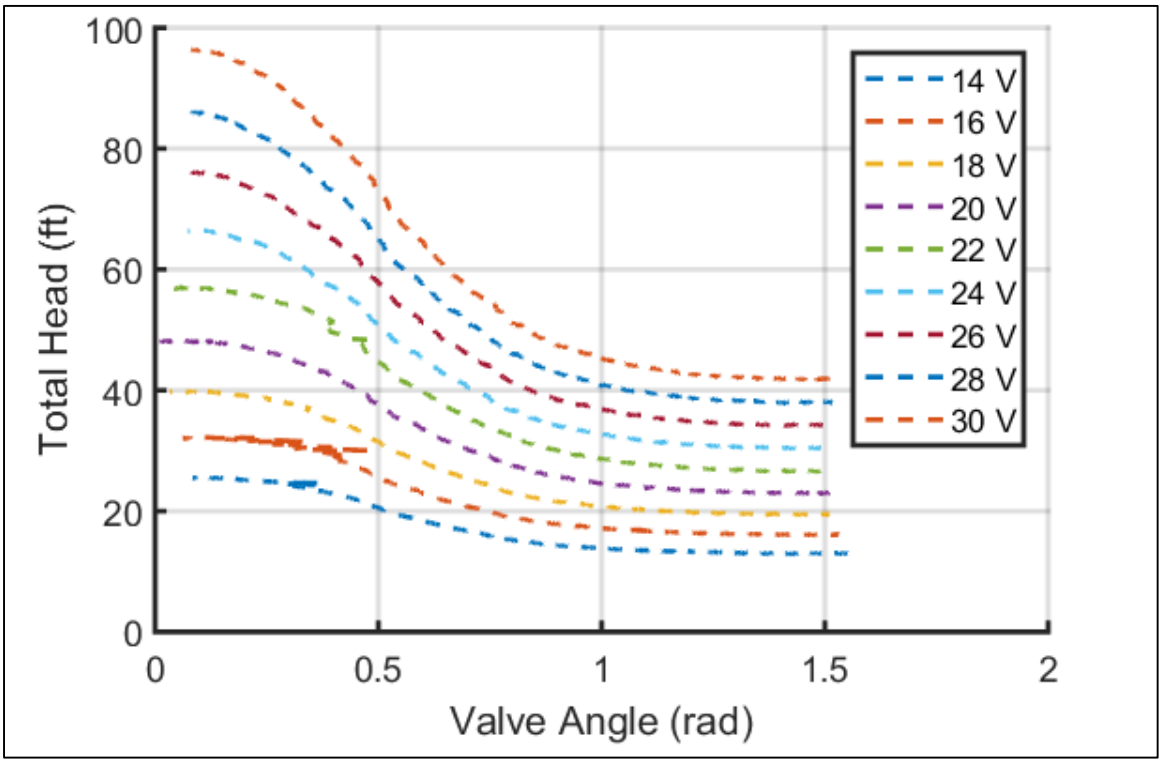

Figure 6-5. Pressure rise across the pump versus valve position for several fixed voltages.

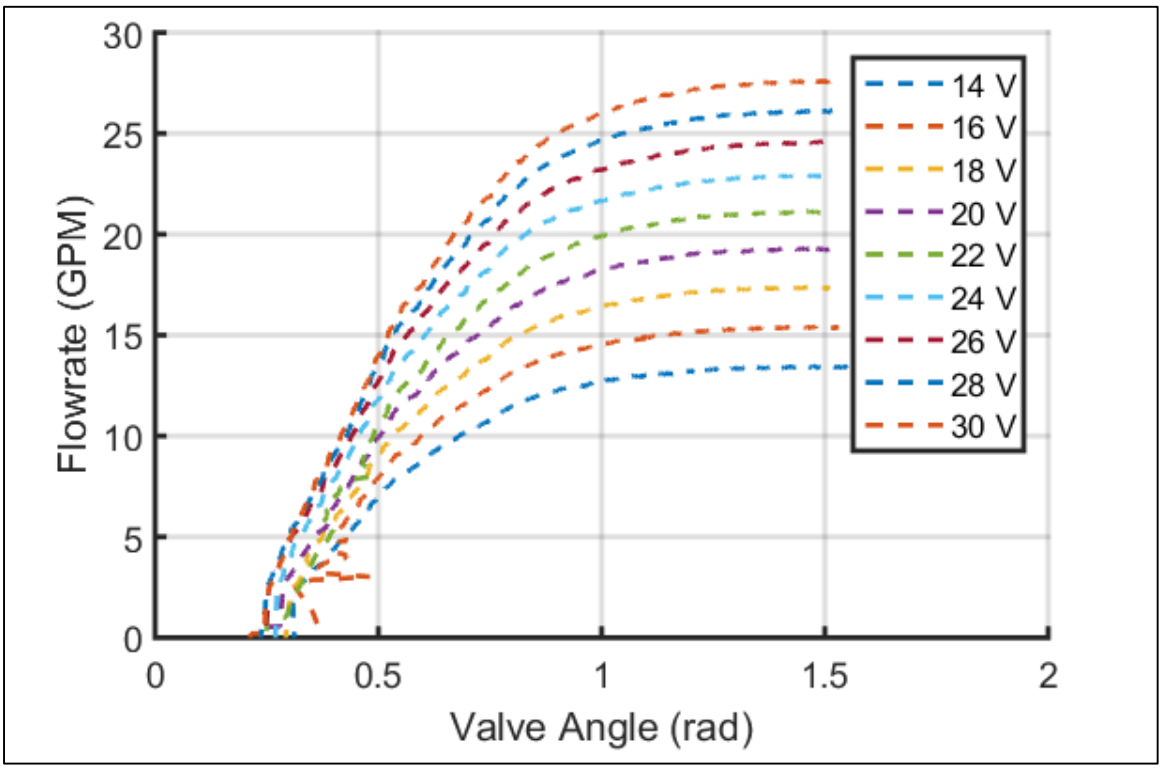

Figure 6-6. Valve position versus flowrate for fixed voltages.

Equation 6-18

$$E = \left(\sum_{i=1}^{m}[y_i - P_n(x_i)]^2\right)$$
$$= \sum_{i=1}^{m} y_i^2 - 2\sum_{j=0}^{n} a_j\left(\sum_{i=1}^{m} y_i x_i^j\right) + \sum_{j=0}^{n}\sum_{k=0}^{n} a_j a_k\left(\sum_{i=1}^{m} x_i^{j+k}\right)$$
$$0 = \frac{\partial E}{\partial a_j} = -2\sum_{i=1}^{m} y_i x_i^j + 2\sum_{k=0}^{n} a_k \sum_{i=1}^{m} x_i^{j+k}$$

Equation 6-18 shows the general form of single variable linear regression (Burden, R. L. & Faires, J. D., 2011). This is applied to each of the constant voltage curves in Figure 6-5 to get a set of related fits. But first, in order to produce a good fit, the data must be truncated to remove regions that are difficult to fit a curve to or where data collection is unreliable. One such limitation occurs when the valve is mostly closed and the actual flowrate drops below the minimum value that the flow sensor is capable of measuring, which is ~5 GPM. Below this fluid velocity there is not enough force acting on the turbine to reliably overcome its mechanical friction. This is seen where the data starts to jump unpredictably in Figure 6-6. On the other end of the spectrum, changes in flow and pressure become very flat past a certain point where the valve is mostly open and small changes in position have very little impact on these dependent variables. In order to combat these conditions, the valve is limited to the range of 30–70° for simulation, the impact of this limitation is minimal since the BEP occurs around 40–50°.

After the set of similar curves are generated, the truly novel approach comes into play to finish creating the relationship. Since the curves are mostly just scaled versions of one another, the voltage variable is used to create a relationship between the coefficients of the first set of fits. That is to say, if each of the initial fits are of the form shown in Equation 6-19, that they can be converted to the single equation form show in Equation 6-20.

Equation 6-19

$$f_1(y) = A_0 + A_1 y + \cdots + A_n y^n$$
$$f_2(y) = B_0 + B_1 y + \cdots + B_n y^n$$
$$\ldots$$

Equation 6-20 $$z(x,y) = P_0(x) + P_1(x)y + \cdots + P_n(x)y^n$$

If each function in Equation 6-19 has the same number of coefficients (which it must for this technique to work), each of those coefficients changes between functions with the motor voltage. By applying Equation 6-18 to all of the coefficients of the same order, a new equation is found that relates them with respect to voltage. This results in a single function with two independent variables for any of the outputs that are desired to be modeled.

To define a goodness-of-fit for this technique, the coefficient of determination (R-squared value) is used to determine if the fit data is aligned with the experimental data: shown in Figure 6-8. Due to the fairly large number of data points, a 4^{th} order fit was used for both the valve position and the voltage. The data that were chosen for fitting are based on the performance criteria that are important for analyzing. First, pressure and flow since these are the variables being controlled for. Power consumption is also modeled since this is one of the most considered aspects of centrifugal pump systems and presents a point of potential improvement beyond that which has been achieved using traditional techniques. And finally, efficiency, due to its integral role in determining the location of the BEP and the effect of operating away from the design point. The results of all of these fits are shown in Figure 6-7.

The quality of the fits in Figure 6-7 are quite good and reflect the measured data very accurately. However, since the goodness-of-fit is not verified, it is important to stress-test the function by attempting to fit data from the same system but which has a different basis. By fixing the valve position and varying the applied voltage, a new set of curves can be generated. The ability of the fits to match this data should prove whether or not the method is reliable enough to use in developing a dynamic model for simulation. The results are shown in the figures below. The fit

appears to be of good quality except at the highest voltage which is 32 V for this experiment. This may be a sign of over fitting the voltage, but the data is still accurate for voltages ≤ 30 V and for the range of valve positions shown here. Since the voltage in the simulation is limited to be between 14–30 V, this model should be sufficiently accurate for generating reliable results. Note that this model is designed using a system with a closed circulation loop and a single pump, systems using multiple pumps may behave differently and require further investigation for control system application.

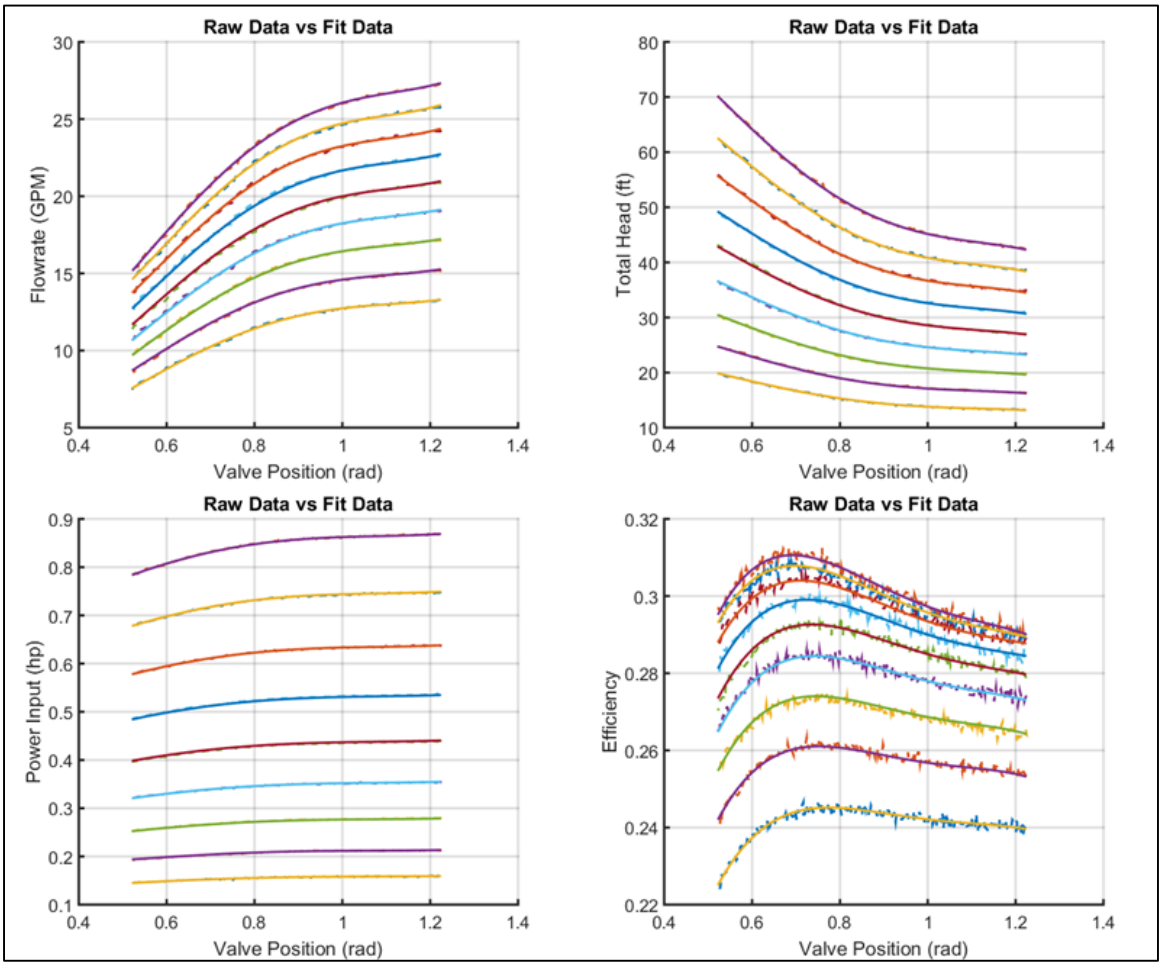

Figure 6-7. Fit data.

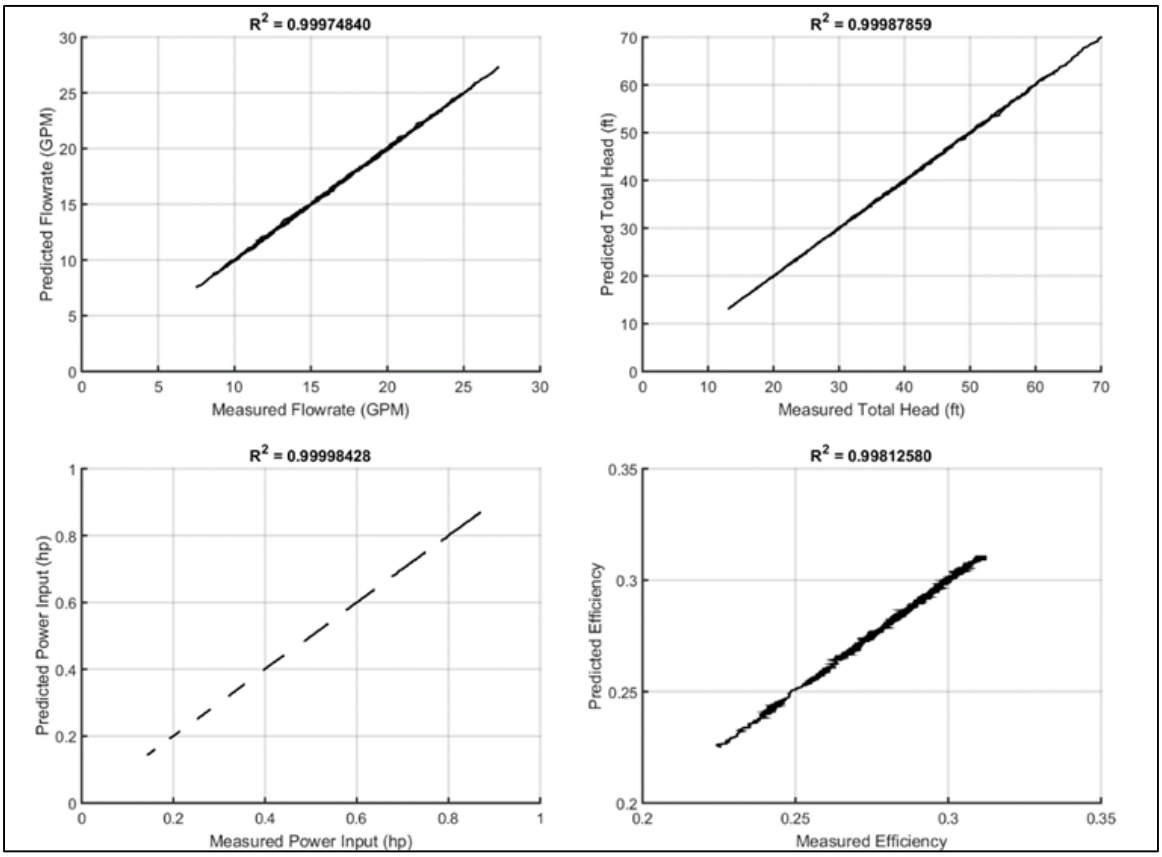

Figure 6-8. Goodness of fit for empirical data.

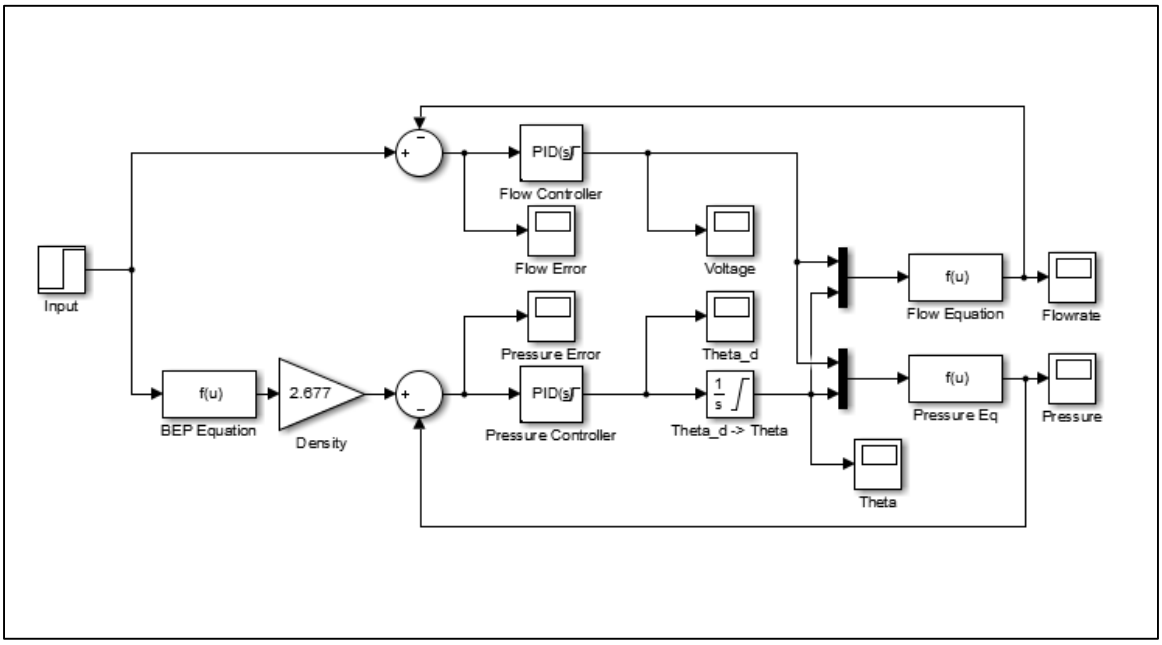

Figure 6-9. Simulink model.

6.4.3. Model Evaluation

The proposed system uses two straightforward PID, controllers which work continuously to reduce the error of the outputs. The flowrate controller outputs a reference voltage to an Agilent HP 6269B laboratory power supply, which is then amplified to a value between 14-32 V to power the pump motor. The pressure controller outputs a frequency in the range of ±1600 Hz to an EasyDriver - Stepper Motor Driver (ROB-12779) which rotates a stepper motor at a speed proportional to that frequency. 1600 Hz corresponds to a rotational speed of 1 rev/s, but the motor is geared approximately 600:1, so the valve takes 150 seconds to travel through its entire range at max speed. Before making a computer simulation, the two PID controllers are programmed with gains manually adjusted by hand; this serves the purpose of showing what sort of values can realistically be expected, as well as outline possible issues that may require more complex modelling.

The relatively slow nature of the pressure response makes the system behave as though it has significant damping, which also contributes to overall stability as both controllers vie to achieve their own output goals. In application, the flowrate can be changed rapidly by increasing or decreasing the reference voltage as necessary; this makes the flowrate error go to zero fairly quickly. At the same time, the valve is either opening (to reduce pressure) or closing (to increase pressure) in an attempt to reduce pressure error. The gradual changes in flow caused by the motion of the valve are easily compensated for by the integral component of the flow controller. Since a solution for the appropriate flowrate and pressure is guaranteed for the applicable range of the TBEP, both controllers will eventually reach a very small error.

The flowrate is capable of reaching its target value and maintaining it with very small error within about a second. However the pressure controller can take several seconds to eliminate pressure error as a result of the slow speed of the valve motor. Figure 6-10 shows the response when the flow is commanded to increase by 50% of its full range. The input change happens at t = 2.2 s and the error reaches about 1% at t = 4.26; the error actually reaches <2% at t = 3.17 s, but then rebounds to about 10% error due to a small amount of integrator wind-up.

The effect of the wind-up can be seen where the flowrate error oscillates discretely. This happens because of a short delay in the flowmeter response; in fact, any change in flow takes about 300 ms to be reflected by the flowmeter output. The result is a destabilizing effect on controlling the flowrate that becomes more pronounced as the integrator coefficient increases. This creates an upper limit for the integrator coefficient and caps the rate at which error can be reduced.

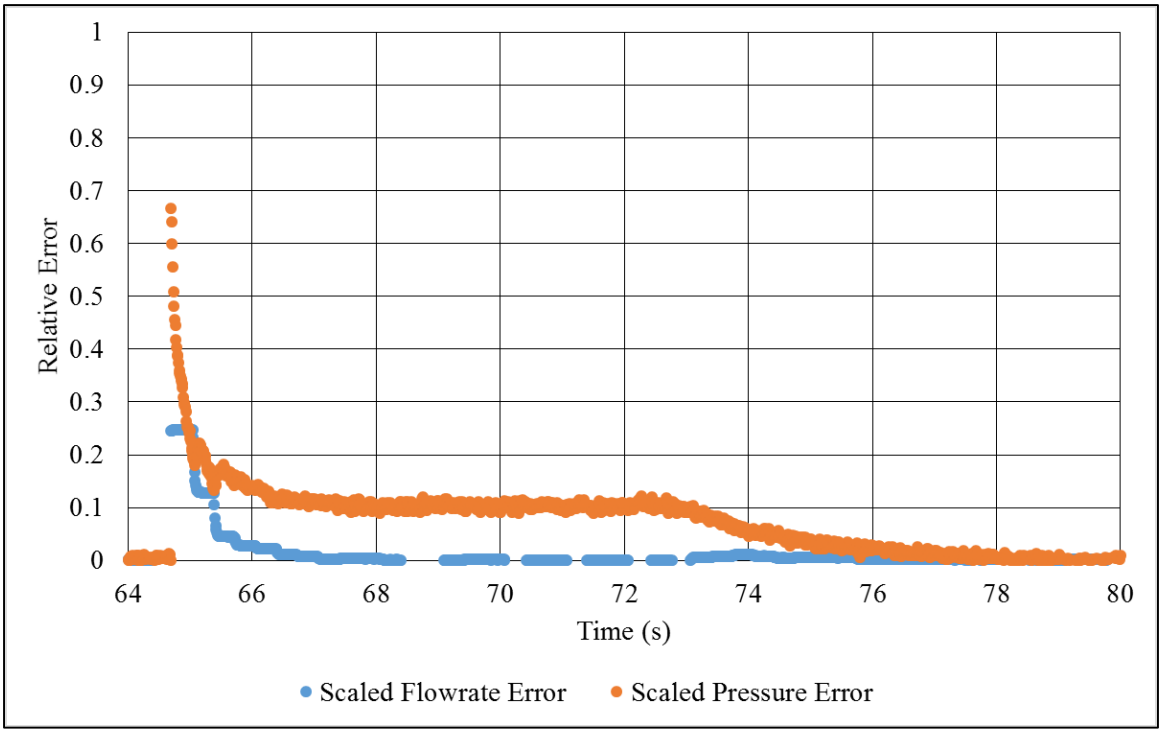

Figure 6-10. Error over time with PID controller. Based on % full scale range.

Again, the model is compared against the test data to see if the results are similar; **Error! R eference source not found.** and Figure 6-11 show the results being compared. As far as models go, **Error! Reference source not found.** shows a very close approximation to what is seen in REF _Ref418459531 \h * MERGEFORMAT Figure 6-11. The primary differences arise as a result of the discrete data collection for flowrate during the experiment, which also causes the controller to respond with an emphasized oscillation. The pressure response in the real system also does not converge completely due to a restriction in the controller where the speed of the valve has a non-zero minimum value; therefore, convergence slows dramatically when error becomes sufficiently small. The primary difference between the two physical sets of data is that Figure 6-10 shows the effect of hysteresis in the valve which significantly extends the time taken for the pressure to converge while Figure 6-11 is intentionally run after taking out the hysteresis so as to mimic the simulation more precisely.

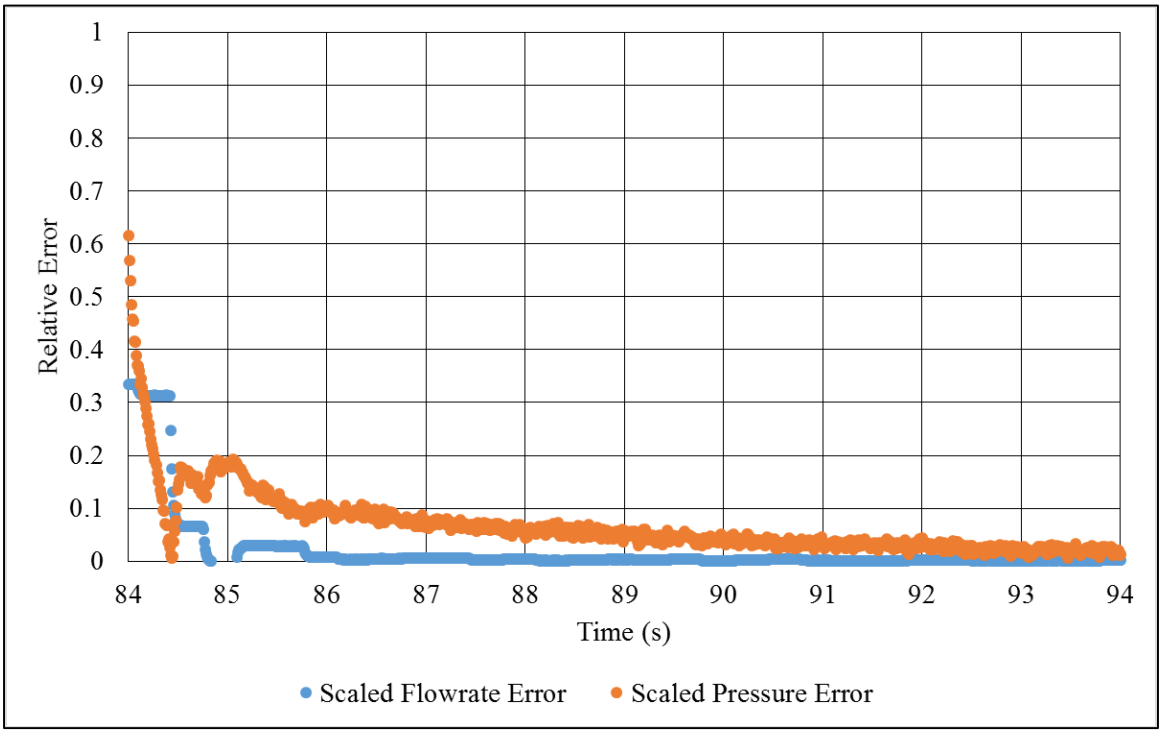

Figure 6-11. Measured step convergence for physical pump system.

7 CONTROL APPLICATIONS

7.1 Control Introduction

Traditionally, control of centrifugal pumping systems has been done through the use of fixed speed pumps and motors with a control valve. This represents the simplest and cheapest method of creating a system that moves fluids between two points. However, with the now dominant presence of electric motors and the Variable Speed Drives (VSDs) that can be used to operate them, variable speed pumps have come into popular use. For some industries, like oil and chemical, pumps are selected to fit a specific system and then operate for their entire life without ever changing capacity; these systems are ideal for the simple approach since there is nothing dynamically changing in the system and the Best Efficiency Point (BEP) will never change from the day the engineer first selects the operating point. For other applications, such as desalination and demand-based fluid transport (like the fuel pump in a vehicle), variable speed pumping starts to differentiate its advantages. A car or plane needs a varying amount of fuel to be delivered to the engines based on the speed and acceleration desired. A desalination plant may need to operate at decreased capacity during off-peak hours or perhaps even increased capacity during certain times of the year. If these demand changes are fairly frequent and last for prolonged periods of time, the effect on the life and reliability of the pump starts to become an active concern with throttle control.

Dual control is the name given to a system that exhibits characteristics of both of the aforementioned control methods. Under dual control, both the speed of the pump and the throttle of the control valve are regulated. Typically, in a variable speed system the control valve is removed to decrease implementation cost to offset the additional cost of the specialized motors and drivers. Under dual control this valve is reintroduced to vastly expand the operational envelope

of the hydraulic system. First, the variable speed pump allows for energy reduction with reduced flow demand as per the Affinity Laws. Second, the control valve allows for dramatically widening the pressure range through which the pump can operate reliably without significant impact to reliability. This makes the concept of a dual control system more powerful than any centrifugal pump control methodology currently in use.

Below, all three control systems are simulated using the data collected from the study pump. The collected data shows how each system performs in a commercial flight fuel pump scenario. As of now, Boeing uses throttle control to operate its commercial plane fuel pumps. The models are built using the multiple regression technique discussed above. The simulation is done based on a commercial cross-country flight and an endurance run show in Figure 7-5.

7.2 Throttle Control

As discussed above, throttle control uses a fixed speed pump with a control valve to "throttle" the flow coming out of the pump. Typically pumps are selected to match the peak flow requirement when the valve is fully open and then are choked down for the majority of their operation. These pumps will operate at or to the left of their BEP for their entire life. A common application of such a pump is using a level gauge in a downstream system to vary the position of the control valve. As the level drops below a desired threshold, the valve is opened to allow more flow into the system; also, if the system level is getting too high, the valve will close to reduce flow into the system. Another application is in fuel delivery. In this case the control valve is directly coupled to a throttle that the human operator controls. If more speed or acceleration is desired, the operator will push on the throttle which commands the valve to open either by direct mechanical action or in the case of fly-by-wire, by sending an electrical signal to the valve

mechanism. In this control method, a pump may also be operated at zero capacity by deadheading or by completely turning off the pump, but the latter will require additional control that distracts from the simple and low-cost nature of throttle control.

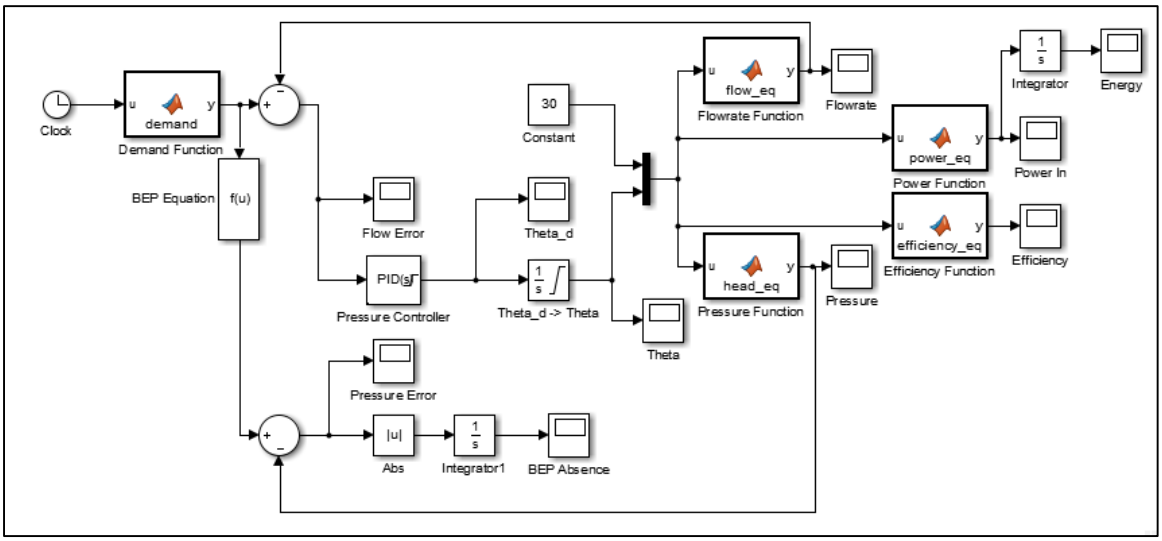

Figure 7-1. Simulink diagram for throttle control.

The Simulink diagram of the control system is shown in Figure 7-1. For this system the voltage input to the pump is fixed at its highest acceptable value, 30 V, and a single PID controller is used to vary the position of the valve. The valve itself is modeled after the gear-driven ball valve used in the physical experiments, but its peak turning speed is increased 100x and its hysteresis is removed. This is not an unreasonable change since the valve is currently working with a 600:1 gear ratio and a very low speed, low torque hobby stepper motor. High performance industrial hardware is easily capable of rotating a valve with high speed and accuracy. The demand input is a series of step changes to the reference input provided in Figure 7-5. There is no static head or elevation head change in this system since the model does not contain that information and the controller does not respond to such disturbances.

Several values are collected during this simulation and recorded to the MATLAB workspace for further analysis; this will be discussed further in the sections below.

7.3 Speed Control

Speed control can be applied very similarly to the above throttle control using level sensors or some other form of demand input. Although speed control promises to save money over time, its application is still quite sparse in established industries like transportation and chemical processing. Variable speed control can be applied to any size system since modern electronics allow for the creation of very small motor drivers and the fact that AC induction motors can become variable speed motors by using a Variable Frequency Drive (VFD).

One important differentiator between speed and throttle control however is that there is typically no valve in a speed control system to offset the additional cost of the more expensive pump, motor, and controller. The cost is also amortized by the reduced energy consumption over the life of the pump, but sometimes capital costs can appear prohibitive when changing over systems.

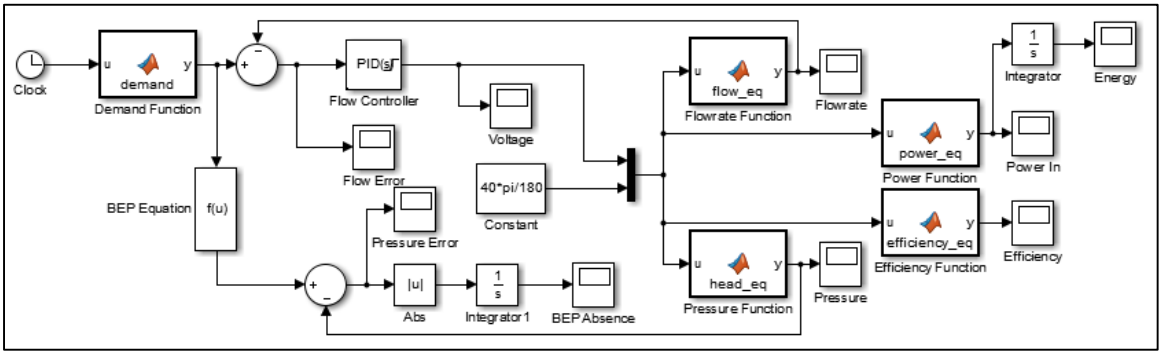

Figure 7-2. Simulink diagram for speed control.

The Simulink diagram for the speed control system is shown in Figure 7-2. This system changes the voltage being applied to the motor to meet the flow requirement generated by the demand function—which is the same as the function shown in the other control systems. Here the position of the valve is shown fixed to simulate a constant K factor for the system losses. The selection of the particular K factor used is subjective since it can vary depending on a particular system setup, but here it is selected such that the pump operates at its BEP for the highest desired flowrate. This means that the pump will always operate at or to the left of the BEP. By lowering K, the pump can be made to always operate to the right of the BEP and at less energy, but with the undesirable increase in risk of cavitation.

This particular control system is popular among researchers for its dramatic decrease in energy consumption over throttle control, but it leaves something to be desired in terms of BEP performance. Dual control takes advantage of both systems and creates a means of dramatically reducing the required energy consumed, similar to speed control, but with the added dexterity of also regulating the operating pressure of the target system.

7.4 Dual Control

Dual control for a centrifugal pump system is the combination of throttle and speed control. Dual control is an iterative improvement on speed control which reintroduces a control valve and allows for system tuning to always track a target objective. Here, the BEP is the target point of desired performance; but in general, any performance criteria can be specified and controlled for by this method: using dual control the operational state of the pump can be moved anywhere in the P-Q region. For example, the pump can be made to operate at varying pressures and constant flowrate or constant pressure and varying flowrate: if there is an engineering advantage to do so.

Dual control gives control over the pump as well as the system to achieve unparalleled performance and functionality.

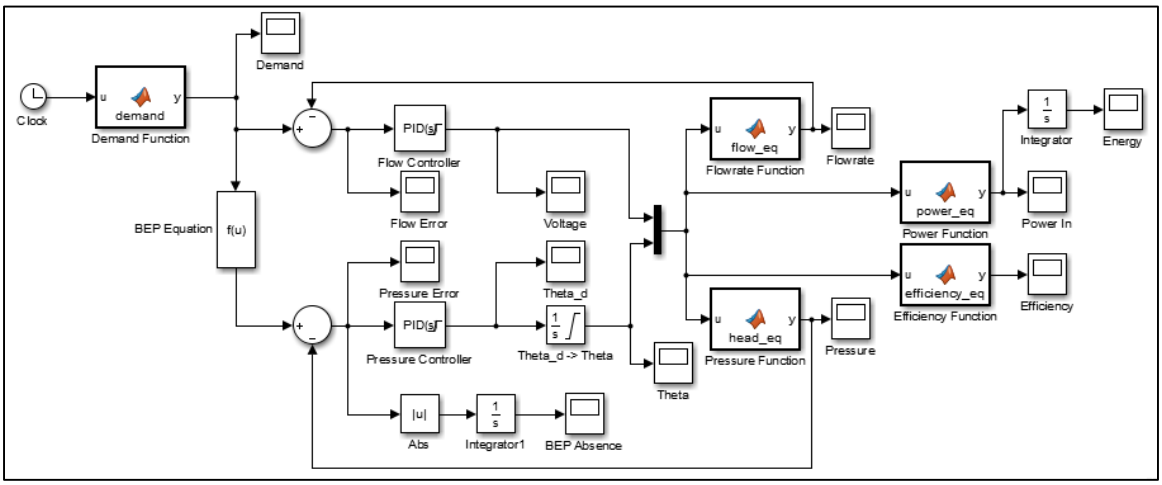

Figure 7-3. Simulink diagram for dual control.

The Simulink diagram for dual control is shown in Figure 7-3. This system contains two PID controllers for regulating the voltage (speed) of the pump and the position of the control valve (K-factor of the system). In this particular model, the reference pressure is driven by the demand flow being passed through the BEP equation to get the pressure that represents the optimal operating point for any given flowrate. However, this is not the only operational mode for this system, the pressure reference can be anything that falls within the P-Q curve for the pump to achieve virtually any performance characteristic.

Dual control in this form is only limited by a factor K_{MIN} which represents the smallest possible value for K in Equation 6-8. On the other end, the value for K can be increased as high as desirable with the valve being fully closed representing $K=+\infty$.

The capabilities of dual control are of an entirely different nature to speed or throttle control alone. In the following analysis, the results when compared with speed control do not appear to be

much different, but that is only driven by the nature of the problem being solved. In reality, dual control allows for the manipulation of a hydraulic system to operate in any way or form as the operator desires. By setting the pressure and flow requirement—so long as they fall within the operational envelope—any state can be achieved.

Figure 7-4 shows the true capabilities of dual control. Under this method flow and pressure are independently tunable (to a degree). In the simulation, the voltage of the pump and the position of the ball valve are limited since the model becomes inaccurate for settings outside of the chosen domain. The tail in each figure is due to numerical limitations since the model needs to first resolve its own initial conditions, but it only takes a matter of milliseconds to do so. The various figures show actual simulation results that are obtained simply by changing the pressure and flowrate demand. Figure 7-4 a) shows the range of operation for the chosen domain; although the range could extend all the way to the left if the valve were allowed to close all of the way. Figure 7-4 b)-f) show different demands that were selected to prove the power of dual control. Flowrate and pressure can be set to any combination within the envelope and the controller will rapidly converge on the proper configuration to meet those settings. The implication of this is that dual control doesn't care about the system being worked on, only the choices of the operator for where to operate; as long as the requirement is within the capabilities of the pump and requires a value for $K \geq K_{MIN}$, the controller will make it happen.

This way of looking at pump operation may appear very unusual, but it is actually the only correct way to view how pumps operate. By only looking at valve or speed effects individually, systems are limited in their capability to respond to complex problems and operational states: like BEP optimization.

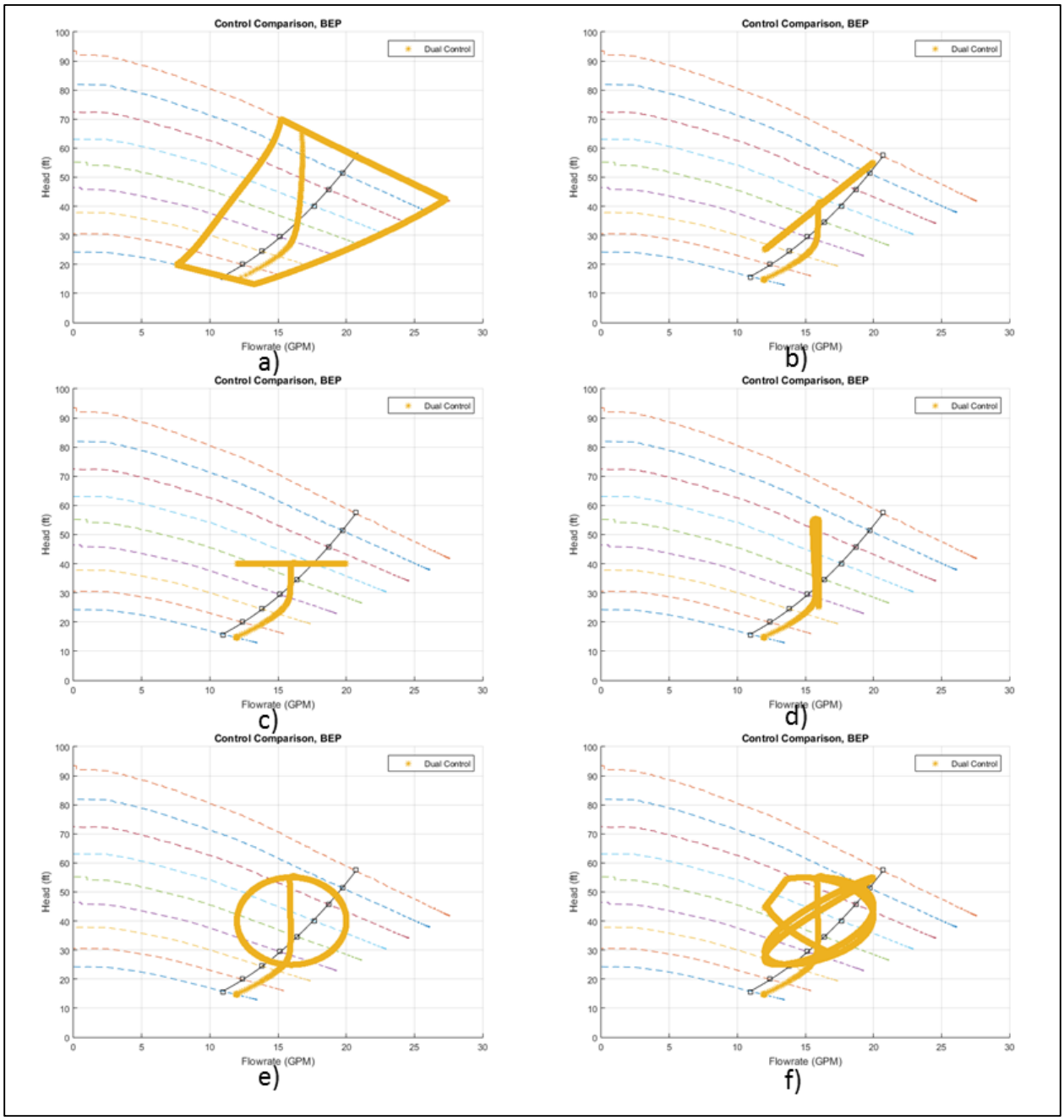

Figure 7-4. Dual control: a) operational envelope within voltage and valve position limits, b) proportional pressure and flow demand, c) fixed pressure, d) fixed flowrate, e) sinusoidally varying demand with time for pressure and flow with equal period and π phase difference, f) quasi-random pressure and flow requirements.

7.5 Performance Comparison

7.5.1. General Performance Characterization

While running simulations of the control systems listed above, several values were recorded to compare performance. The most obvious data to collect is the flowrate and pressure to observe where the pump is operating along the P-Q curve, especially in relation to the BEP. In that same vein, the error values for pressure and flowrate with respect to the reference inputs are also recorded to observe the ability of the system to respond to the range of inputs. For this study, energy usage is also an important factor in determining the performance of the control system, so that is also recorded by integrating over time the electrical power being consumed by the pump; this data is mapped from the physical data similar to the pressure and flow model. Efficiency is recorded, but due to the nature of the pump that is being used, the actual hydraulic efficiency of the pump is unknown, this value only represents the sum of all losses in the motor and pump combination. Control efforts are also recorded and are the voltage being supplied to the pump and the position/velocity of the ball valve.

Equation 7-1
$$\varphi = \int_0^t \left| H_{measured} - H_{ref} \right| dt$$

The last value being recorded in all three models is referenced here as BEP absence, φ, shown in Equation 7-1 where $H_{measured}$ is the instantaneous total head at the outlet of the pump and H_{ref} is the target BEP head. Since one of the most important performance factors being measured here is how well the pump maintains performance at its BEP, there needs to be a way to measure it. All three control systems are designed to control for flowrate and match the demand flow as closely as possible within the applicable range, and all three control systems do this fairly

well as will be seen below. The only difference between the three systems as far as the BEP is concerned, is that each achieves the desired flow at different pressures; for this reason, the metric used here is the vertical distance on the P-Q diagram that the pump is operating away from the BEP at that particular flow. The reduction in reliability is based both on the distance away from the BEP and for how long the pump is operating. Also, operating on opposite sides of the BEP do not negate one another, so the magnitude of the difference is all that is taken. By integrating the absolute value of the pressure error over time, a value hereafter known as BEP absence is obtained and will be used to determine pump performance with respect to the BEP.

BEP absence is a new term, and as a result will take some time to find the most appropriate definition. The way it is defined here is based on the notional system being analyzed. In general discussions regarding BEP, the distance used to determine how far the pump is operating away from the BEP is the horizontal distance on the P-Q diagram (see Figure 2-1). In fact, the reliability when operating to the right of the BEP degrades much faster than when operating to the left since the failure mechanism is much different. However, in this study, during normal operation the pump is only ever operating at or to the left of the TBEP curve, so this asymmetry is mostly ignored. One might also find that the vector which represents the minimum distance to the TBEP curve is the most appropriate value for determining reliability, or perhaps another method still, but these will all need to be investigated in future works.

7.5.2. Demand Function

The demand functions being used to compare the performance of the three control systems are based on data provided by Boeing for cross-country and endurance flights. Figure 7-5 shows the fuel consumption as a function of time for a 4 hour cross-country flight (blue) and a 16 hour

endurance run (red). The large initial spike represents takeoff with the long flat regions being cruise speed, periodic spikes represent occasional increases in power consumption whether that be changes in altitude, speed, or on-board electrical power.

Unfortunately, due to computational constraints, the full multi-hour flight cannot be simulated. The many millions of time steps would take unnecessarily long amounts of time. Therefore, the timescale on each flight is scaled down by 100x to a more reasonable duration for simulation. This will affect time-dependent values such as energy and absence, but they will only change the final result by that same factor of 100, so 1 hp-h of consumed energy would represent 100 hp-h of real energy. Also, since the comparison between all three models is relative and involves very little transience, the results will show the same relationships regardless of time scale.

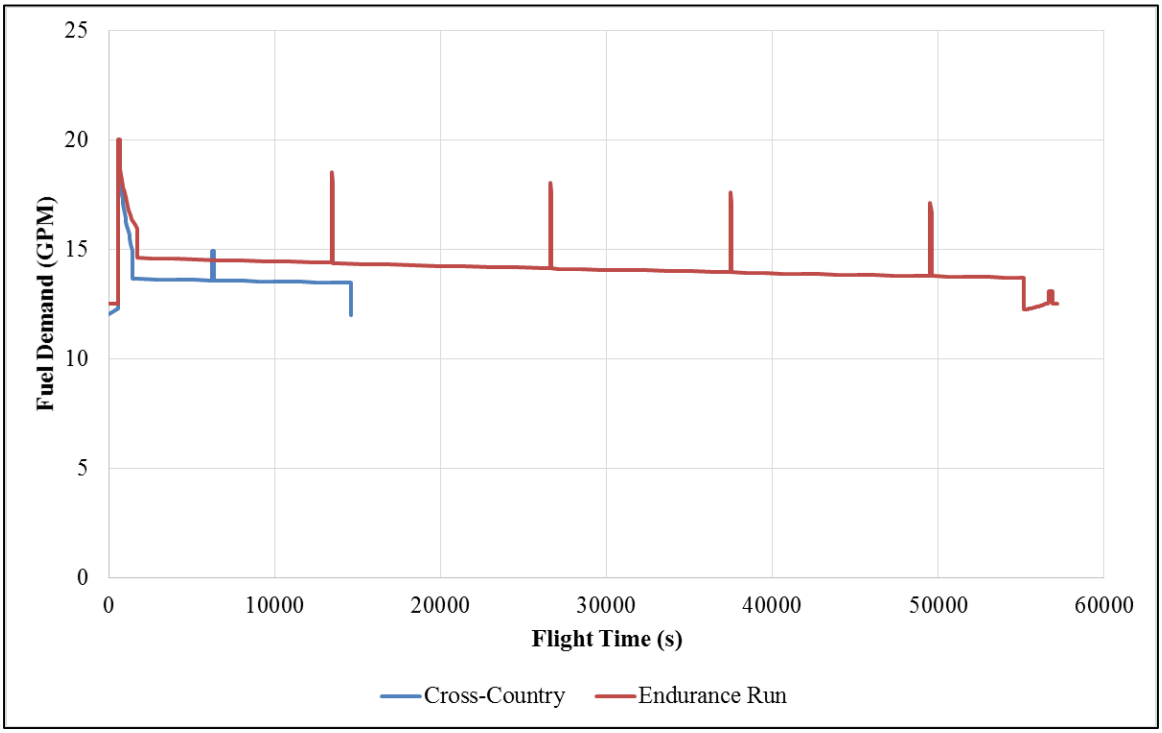

Figure 7-5. Fuel demand during two flight scenarios.

The following analysis is discussed using the values for the cross-country flight. At the end of the discussion, the same data will also be showing using the endurance run data, which only serves to further fortify the characteristics shown in the initial data.

7.5.3. Control Error Performance

The most logical starting point to compare various control methodologies is by seeing how well each method is capable of minimizing error. The control target of all three methods is to minimize flow error for a time-dependent demand function. All three systems use a fairly simple PID controller to achieve this, but each controller is only capable of influencing a specific aspect of the system. Figure 7-6 shows the error response of all three controllers.

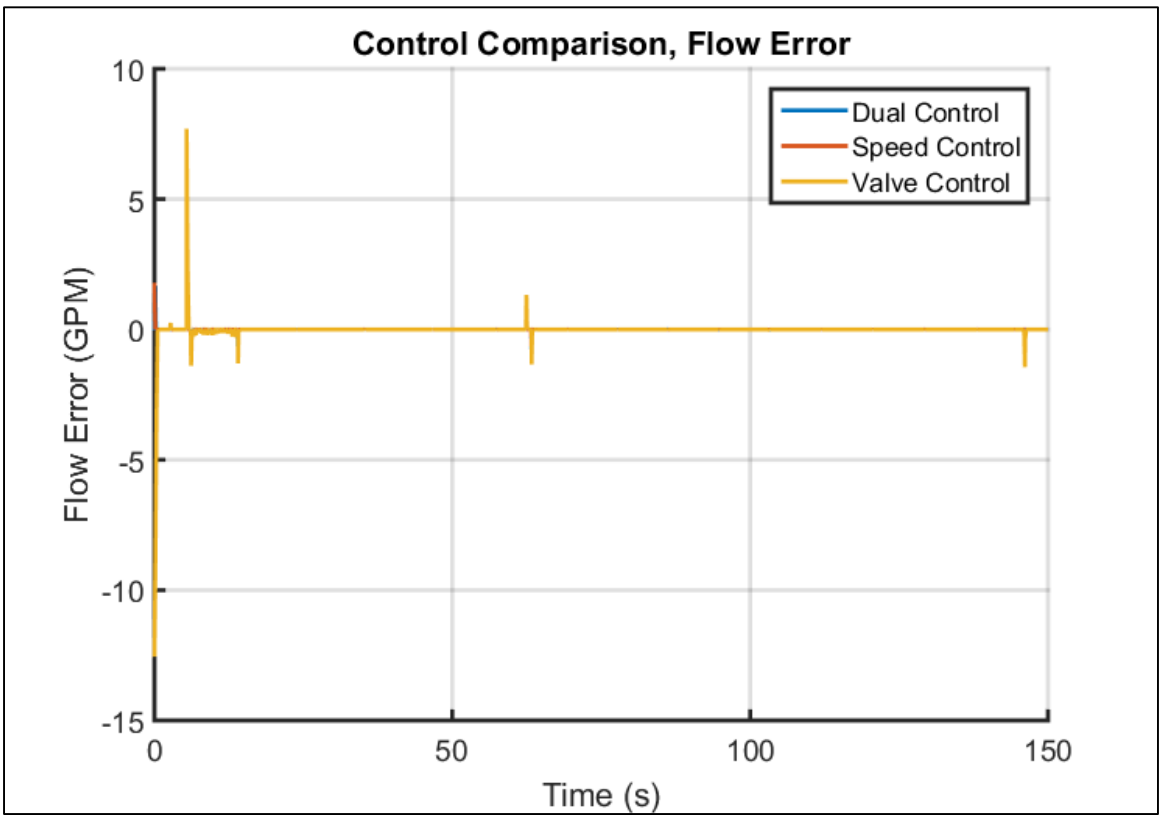

Figure 7-6. Three control systems response, flowrate error.

With the exception of transient spikes that occur at the times of step changes in flow demand, all three control systems have almost zero error for the entire flight. In fact, each system achieves << 1% relative error on the order of milliseconds as shown in Figure 7-7. Although there is some apparent performance differentiation, the time scale of the transient response is still very short even for the slowest system; therefore, saying one system has an advantage over the others at this point would require a very rigorous transient objective for justification.

The important point to be made at this stage is that all three systems are capable of achieving the target flow requirements across the entire objective region. And as a result, each system can be compared equally on the various other performance variables without bias.

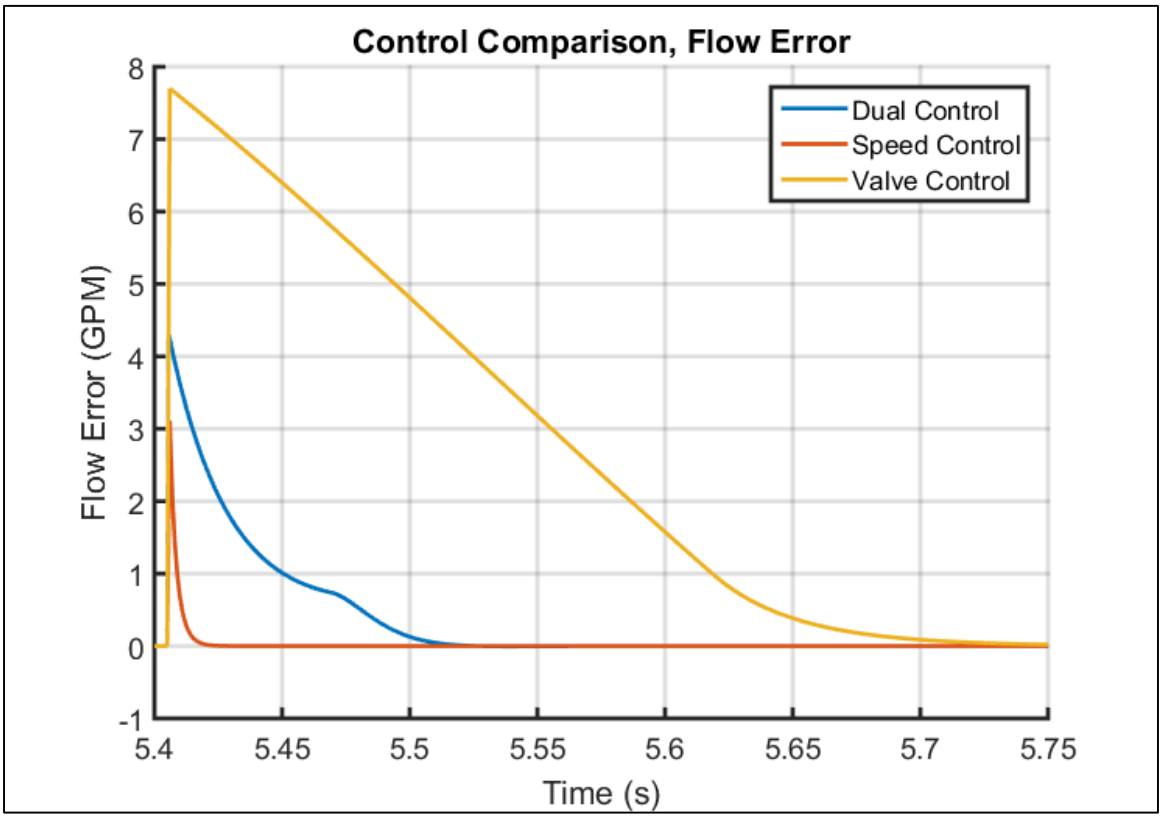

Figure 7-7. Transient error response.

7.5.4. Power/Energy Performance

A common topic of discussion is regarding methods for reducing the energy consumption of pumps. With a fairly large portion of the world energy supply being consumed by various pumps, this presents a fairly low-hanging fruit for making overall improvements. Methods for reducing energy typically pull heavily from the affinity laws and the relationship between pump speed and consumed energy, but there are other methods. Proper process design and pump selection as well as regular maintenance are shown to contribute heavily to energy cost reductions, often more than offsetting the additional cost to implement. However, with any of these methods, the efficiency of the pump is not always considered in order to simplify the problem which is often a mistake.

Figure 7-8 shows the power efficiency of the three control methods. Contrary to what might be expected based on intuition, valve control actually has the highest efficiency across a large range of flowrates; in fact, only at very low rates does speed control barely take over. However, this efficiency is the ratio between the electrical power entering the motor and the hydraulic power leaving the pump. Due to the throttling valve, a very large percentage of the generated power is being dissipated almost immediately without ever contributing to the operation of the downstream system. It is true that, for the pump, operating at the highest point of efficiency presents the highest possible Mean Time Between Failures (or MTBF); however, there is a disproportionate rise in energy usage for an unimpressive increase in life when compared to the other two methods. It is for this reason that efficiency can be ignored in this application to be replaced by direct measurement of power and energy usage. As long as operation is as close as possible to the TBEP curve, reliability can be considered mostly unaffected for any capacity.

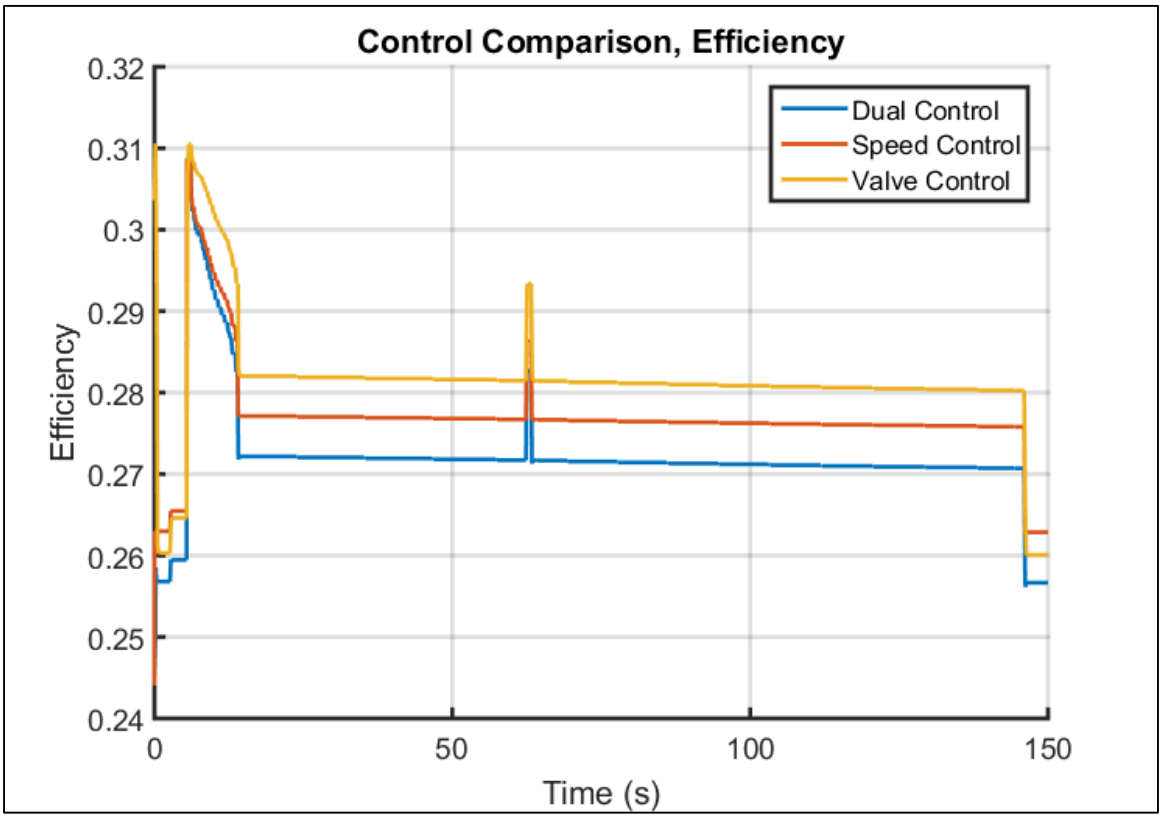

Figure 7-8. Three control systems response, efficiency.

When discussing the power advantages of each system, the absolutely lowest energy consumption will always be the setting that provides the desired flowrate at the lowest pressure drop. This would typically mean throwing out any sort of valve or other throttling device, replacing all piping with large diameter smooth-walled PVC, and eliminating any joints, lengths of pipe, or change in pressure or elevation possible. Unfortunately, this also means that as resistance is removed from the system, that the pump starts to operate in an ever more increasing "free rotation". As the downstream resistance of the system decreases, fluid will move through the pump faster and faster even at lower speeds. As the velocity of the fluid increases and the static pressure drops, the vapor pressure of the fluid will eventually start to drop below zero (often inside the pump where fluid stream velocity is greatest) and cavitation will begin. Cavitation is the formation of bubbles inside a low pressure fluid that collapse dramatically and cause dramatically accelerated

wear on mechanical parts. Cavitation can also be known to cause undesirable mechanical vibration and presents and audible noise much like gravel spinning inside the pump. Low pressure cavitation is known far and wide by hydraulic engineers to be one of the most destructive forms of wear that can occur inside a pump. By operating so far to the right of the BEP, energy consumption can be reduced, but at the expense of dramatically increasing the wear on the pump. For this reason, operation in this state is considered highly undesirable. It is also for this reason that the pressure drop for the speed control system was selected such that the operation is never to the right of the BEP.

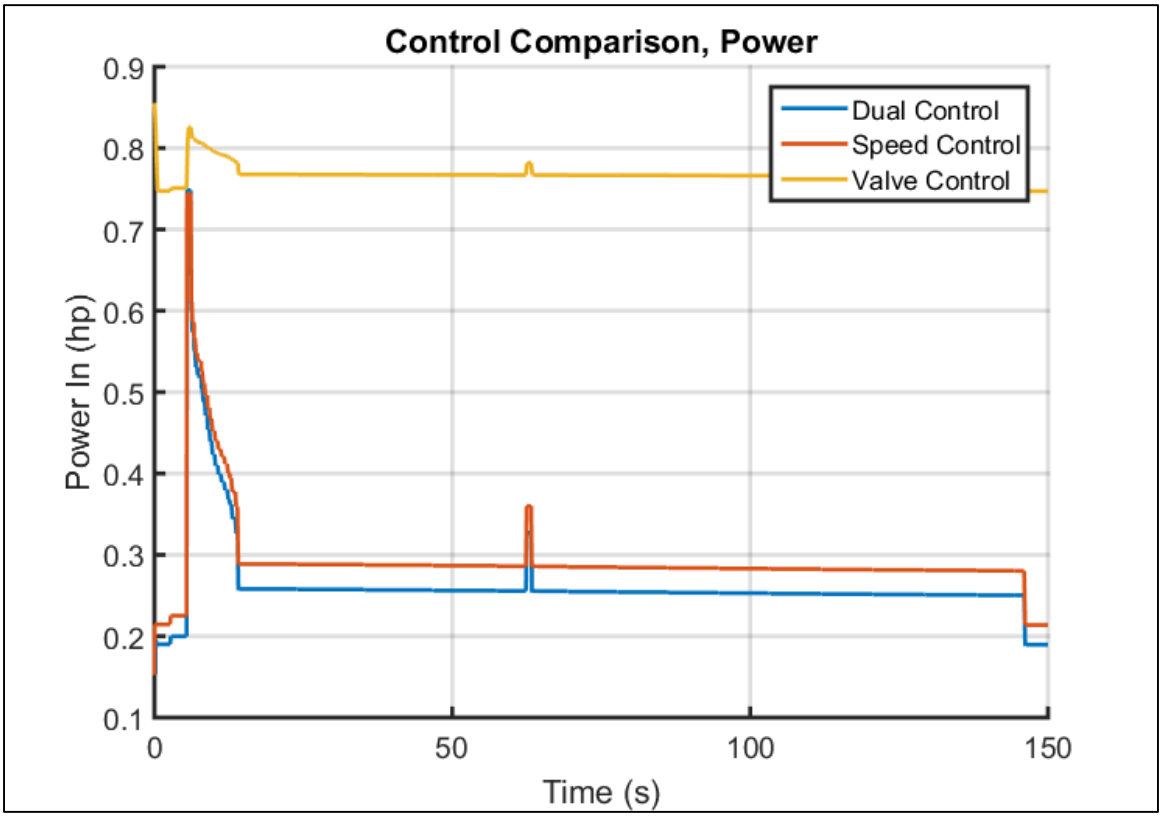

Figure 7-9. Three control systems response, power.

Taking the above facts into consideration, Figure 7-9 and Figure 7-10 show the instantaneous power and total electrical energy consumption throughout the cross-country flight.

Across the board speed control and dual control use considerably less energy than throttle control: the energy savings is on the order of 60-70%. The dual control also manages to just barely edge out speed control at this particular setting even despite the fact that speed control shows higher overall efficiency. The power data is calculated based on experimental data, but is integrated over time to achieve the energy data, therefore Figure 7-10 is the direct time integral of Figure 7-9.

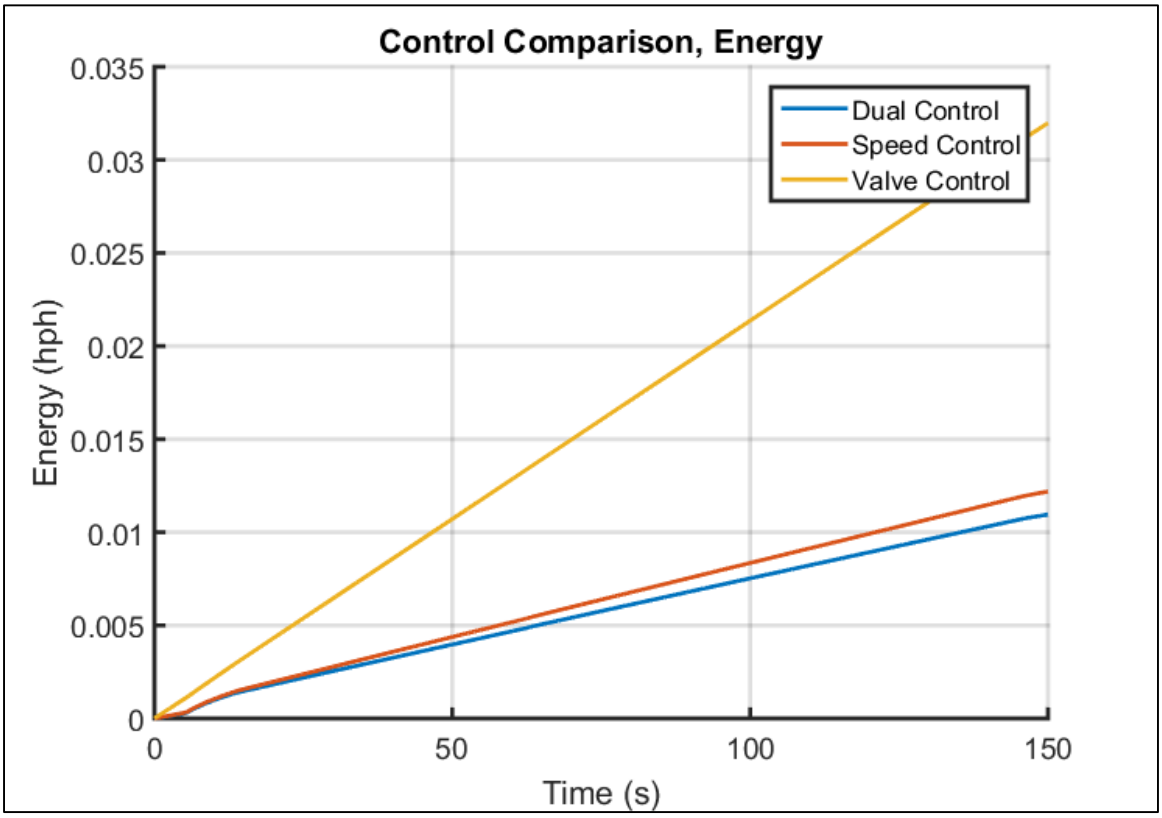

Figure 7-10. Three control systems response, energy.

Regarding aerospace applications in particular, power and energy reduction each affect a specific location where the overall aircraft system can be modified or improved to increase flight time or reduce cost. When looking at power, the peak power consumption drives the size of the generator that will be used to power the pumps; as the peak power goes down, that savings is multiplied by every pump currently in service (there are often serval on each tank operating

redundantly). If this power requirement goes down enough, the size of the on-board electric generators may be reduced which will also reduce the weight of the aircraft overall, and weight is paramount for aerospace applications. In Figure 7-9 the peak power consumption is reduced by approximately 10% which is not insignificant and could lead to the improvements discussed.

When looking at total energy consumption, the energy source becomes the target for improvement. In flight, nearly all of the on-board energy is stored in the form of jet fuel. The less of this energy that is used by the fuel (or other) pumps, the more that can be used for propulsion and flight times can be lengthened proportionally or less fuel can be stored for short flights making the plane weigh less and further contributing to energy reduction. Here (again) speed and dual control both use considerably less energy than throttle control with (again) dual control slightly edging out speed control. The difference in energy usage versus power is that power can peak near the same value for all three control systems, but energy can differ dramatically based on how long those peaks last.

7.5.5. BEP Performance

Perhaps the most difficult performance to quantify is the reliability of the pump when operated under each control scheme. In an ideal situation, several pumps would be tested in various accelerated wear conditions to determine what has an effect on life and how pronounced that effect is. It is clear that operation at the BEP results in the least wear, but how quickly that changes as operation moves to left, or to the right, is not immediately clear. Therefore, the method of quantifying this wear will be the pressure absence of the operational state with respect to the BEP. It is discussed above why this particular method was selected to quantify wear, but it does take

into consideration both distance from the BEP and time which are known to be two important factors in wear and reliability.

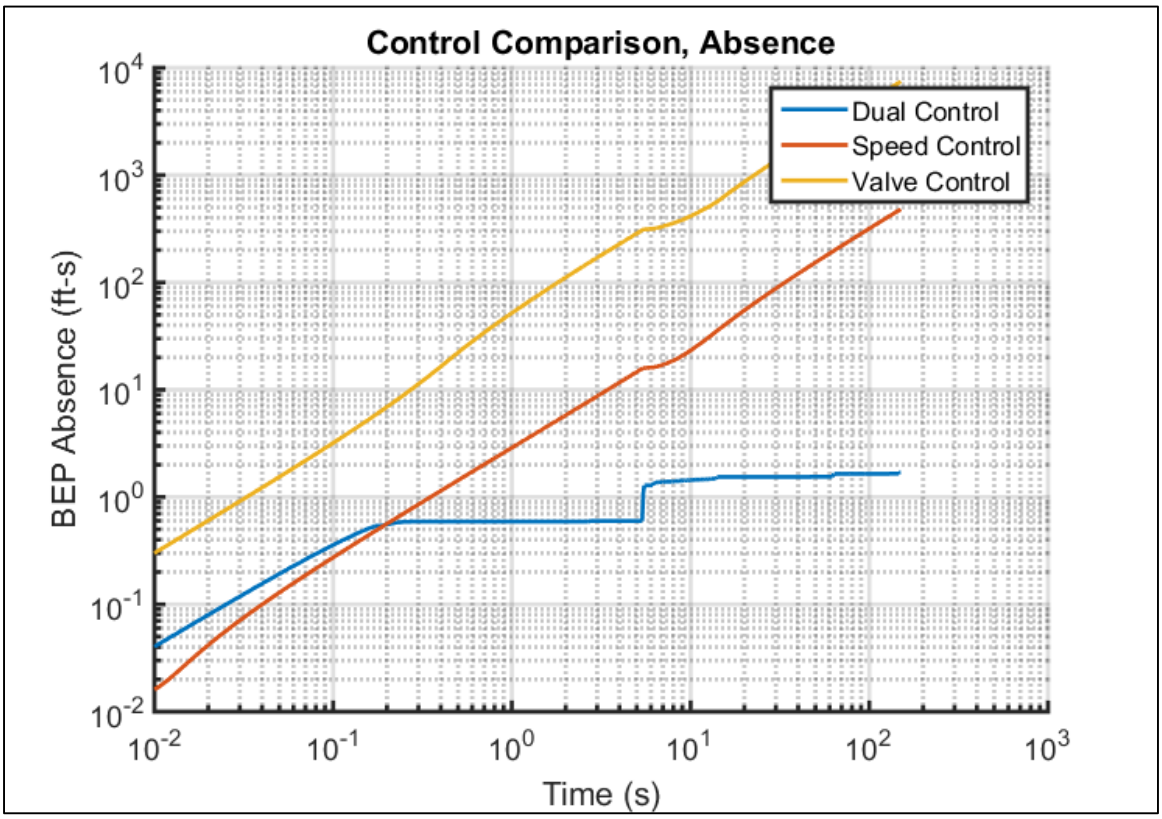

Figure 7-11. Three control systems response, BEP absence.

Figure 7-11 shows the plot of BEP absence for the cross-country flight simulation for all three control systems. The data is shown on a log-log plot since operational time is typically measured on such a scale when discussing lifetime effects and reliability; the y-axis is also logarithmic because the massive difference in scale between the three systems would be almost entirely illegible. Here dual control really starts to differentiate its abilities; which is not unexpected since minimizing distance from the BEP is one of the two objectives of the dual control system when operated in this manner. The figure shows that the effects of time are almost completely negated by the dual control system which means that nominal wear rates will always

apply. Also seen here is that speed control is better for life than valve control. But since there is still a distance between the operating point for most flowrates and the TBEP curve, the effect compounds with time. More work will need to be done to tie this difference to a life change prediction, but for now it is sufficient to understand that dual control will result in the longest expected pump life of all three systems.

7.5.6. Pressure/Flow Curve Results

The results are detailed with respect to the various performance values, but how does each control system look from the perspective of the system. Each controller is only able to control the speed of the pump or the position of the control valve or both, but the system only cares about the pressure and flowrate that results from these changes. Figure 7-12 shows the pressure and flow values for the system as measured directly at the output of the pump for all three controllers.

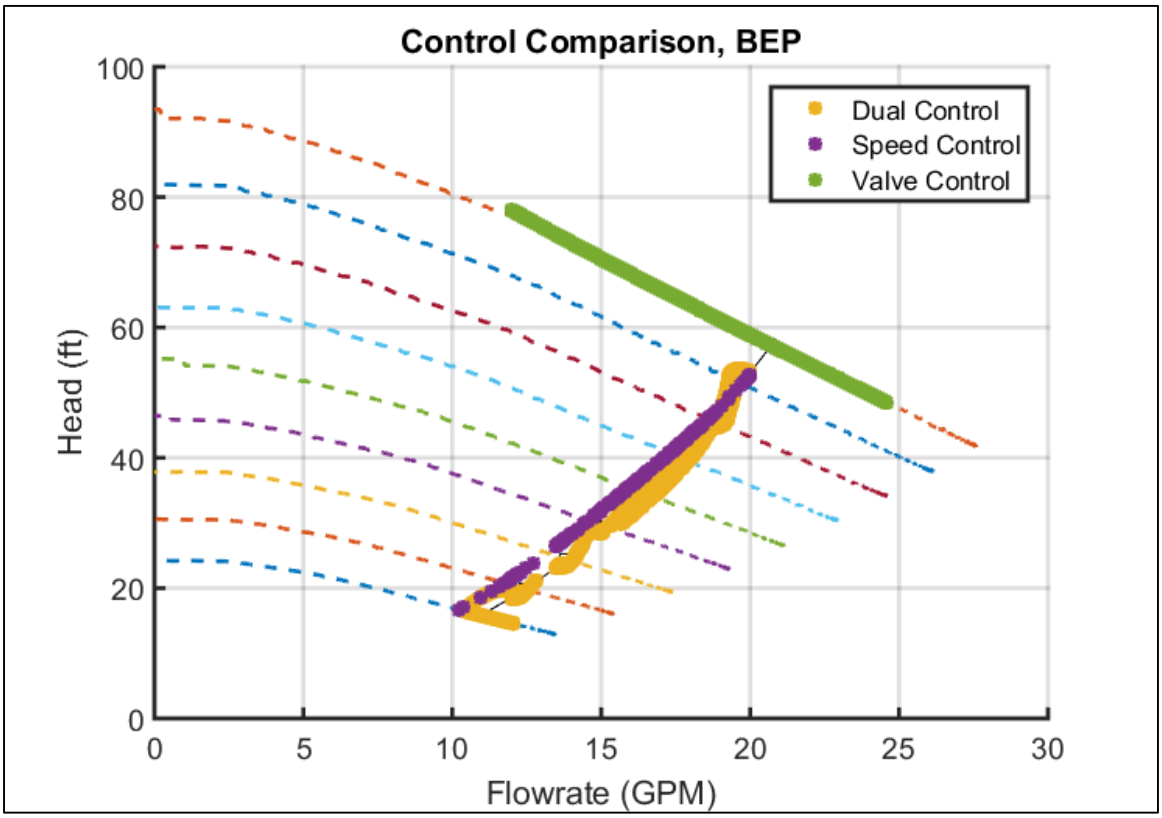

Figure 7-12. Three control systems response, P-Q diagram.

Valve control moves back and forth along a constant speed curve to achieve the desired flowrate, this is obviously expected since the pump is operated at a constant speed (or in this case voltage). Although the pump is shown to go to the right of the BEP, this is only during the transient start-up period where the simulation is converging to the correct state from the initial guess. This is purely a numerical phenomenon and only lasts for an amount of time on the order of milliseconds. The same phenomenon occurs for dual control at the flat region shown on the lowest speed curve. The P-Q diagram makes the difference between valve control and the other two very obvious and helps to explain why the performance results are so dramatically different for it when speed and dual control are much more similar to one another. Throttle control uses higher pressure drop across a valve to decrease flowrate, which expends more energy than the other methods since the hydraulic energy used to pump through a system is represented in this chart by the area below

and to the left of any operating point as shown in Figure 7-13. There is also a small amount of tailing that is shown at the far left extend of the valve control data. This shows the limitation of the model and how it starts to become less accurate as the valve closes due to nonlinear effects.

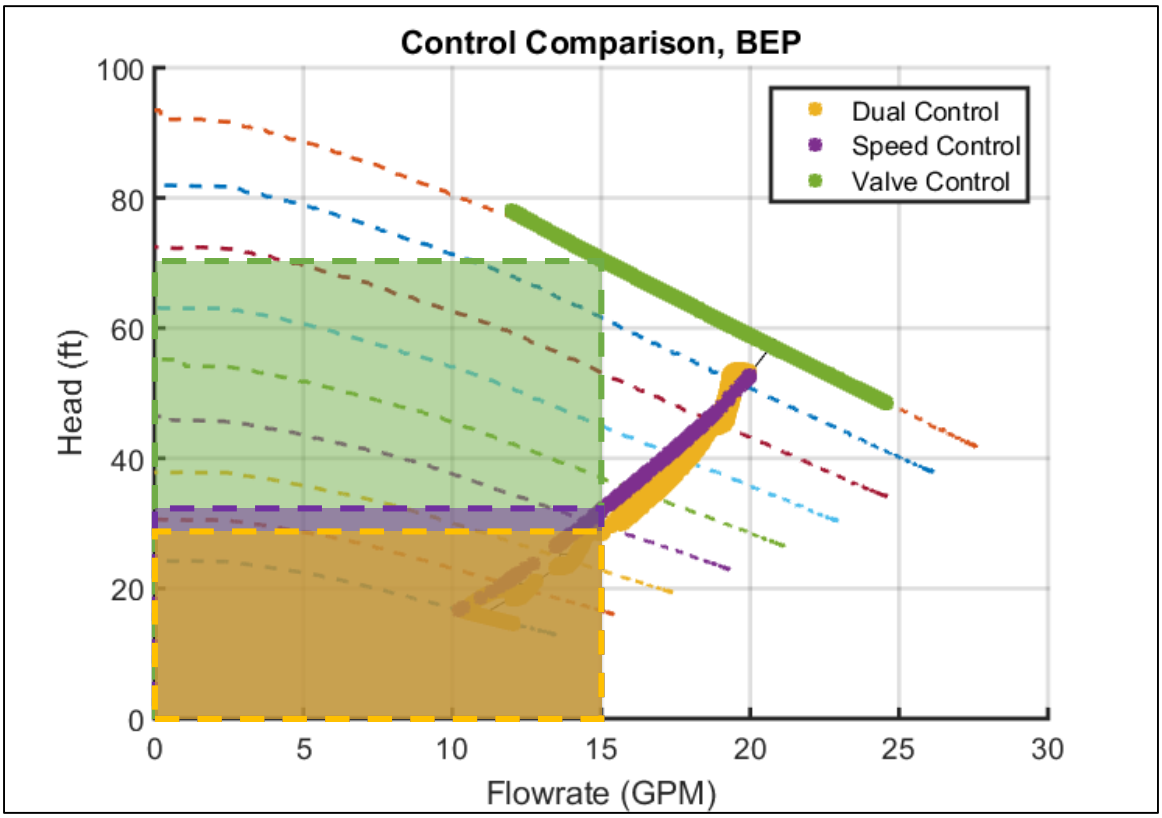

Figure 7-13. Energy consumption from P-Q diagram.

Speed control is a very popular improvement over throttle control, and the performance data here shows why. For most systems with simple flow requirements and periodic changes, basic speed control offers nearly all the same advantages as dual control with slightly less technical difficulty. The primary technical difficulty with speed control is that the pump should be selected such that basic operation is close to the BEP of the pump. Although this is true for fixed speed pumps as well, with variable speed pumping the design engineer must weigh the different expected capacities and durations with the risks of operating to the right of the BEP. A judgement call could

be made to select a pump that operates directly on the TBEP for 80% of the time and a small amount to the right of the TBEP for 10% of the time to reduce overall energy costs, but at the sacrifice of some pump life. In this simulation, the pump was selected to operate at or to the left of the TBEP always. And since the TBEP falls more rapidly than the system curve, this means that the peak expected flowrate will be at the TBEP and the pump will operate more and more to the left of the TBEP as flowrate decreases. Because of the difference in the TBEP and the system curve, this particular pump will not be able to operate along the TBEP with speed control alone, but it is still sufficiently close to gain many of the advantages of doing so.

Dual control is shown in Figure 7-12 as seemingly erratic. This is the result of the fact that pressure and flow are each being corrected simultaneously; also, since the maximum speed of the valve is increased in the simulation, there is also more oscillation during convergence. The point of this oscillation is that the controller is attempting to minimize the distance to the TBEP while also maintaining a specified flowrate. Due to the similar shape to speed control, the power advantages are similar, but for this particular scenario, dual control almost always consumes less energy as shown in Figure 7-13. The primary advantage over speed control is that the system—once it converges—is always directly on the TBEP for any flowrate requirement.

7.5.7. Endurance Run

All of the above analysis was repeated for the endurance run data shown in Figure 7-5. The results are shown below in Figure 7-14. For the most part, the results are similar to the cross-country run, but with the greater duration and number of elevation changes, the absence and energy usage are much greater for the speed and throttle control. Again, the throttle control shows much

worse performance across the board when compared to speed and dual control. And again, dual control surpasses the other two in energy consumption and BEP absence.

The total energy saved between throttle control and dual control, according to the simulation, is approximately 0.07 hp-h (or 64%); however, since the simulation scaled by 100x, the actual energy savings is 7 hp-h. This equates to about 18,000 BTU of energy. In reality, Jet-A fuel contains about this much energy per pound, and a commercial airliner can carry upwards of 40,000 lb of fuel. Although saving a single pound of fuel for such a large quantity can seem woefully insignificant, this pump is not sized for a commercial airliner. More likely the pumps will be at least an order of magnitude larger and several of them will be used in parallel (at least one per engine). This means that the relative savings should be much larger in application. Also, when considering centrifugal pump applications in general, some pumps can operate on the order of thousands of horsepower; these pumps benefit the most from reduced energy consumption.

Also to consider is the cost related to replacing one of these pumps. Due to heavy regulation and reliability requirements, the pump used in this study costs around $30,000. This cost will also scale with size so pumps in commercial planes can be significantly higher. By minimizing BEP absence, the reliability of these pumps will improve, reducing cost while simultaneously improving safety.

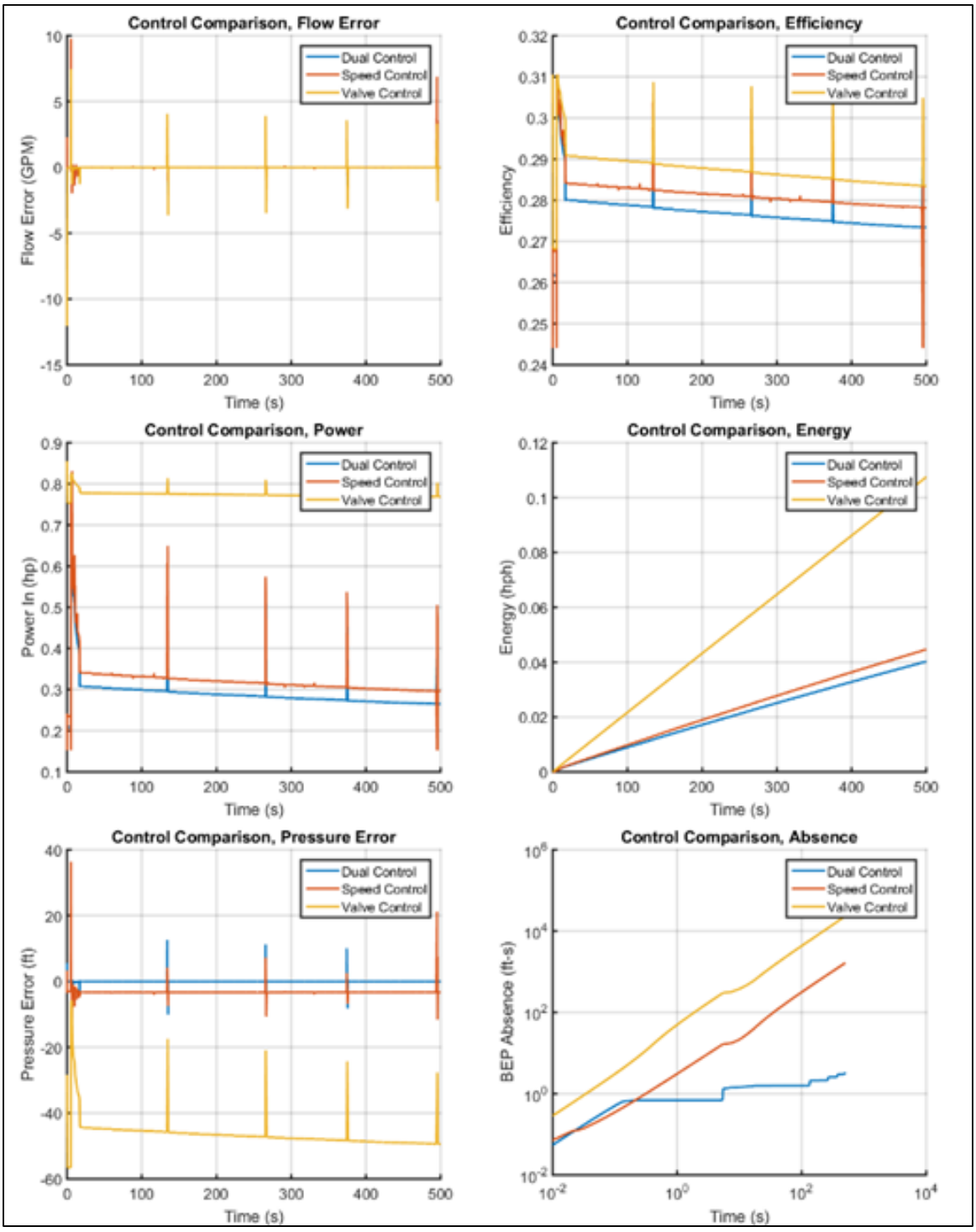

Figure 7-14. Results of endurance run simulation.

8 General Pump Application

So far the topics discussed herein are almost exclusively targeted toward the aerospace industry; however, any application that requires variable capacity flow and currently employs the use of centrifugal pumps can benefit from this type of optimization. An estimated 117 TWh of energy (totaling approximately 10% of all energy consumed by in the secondary and tertiary sectors) is consumed each year exclusively by centrifugal pumps [1, 2]. In the aerospace industry alone upwards of 40% energy savings can be expected from normal operation, which means equally substantial savings may exist anywhere variable capacity flow is implemented. Until pump manufacturers start making this information standard with Variable Speed Pumps (VSPs), the following steps can allow any variable capacity pumping application to use a VSP and benefit from improved lifespan and reduced energy consumption.

Any VSP can be characterized by comparing the input energy to output energy at various pressures and flowrates.

1. No matter how input to the pump is metered (voltage, current, frequency, etc.), the input to the pump should be fixed while allowing the system parameters to change. This can be done by fixing the speed of the pump using a Variable Frequency Drive with an AC motor or by fixing the voltage or current being supplied to a DC motor; in any case, it is crucial that the motor input not be allowed to vary so that its reaction to the downstream system can be monitored.
2. Have a means to measure the pressure and flowrate of the system at a point very near where it can be measured in application. Although flowrate is only affected by leakages, pressure is continuously lost through a system due to viscous friction. By measuring pressure at two

different points, two different static pressures can be seen as the “ideal pressure”; it is important to know the optimum pressure at a location that can be measured in application for this reason. If a measurement point is not known (perhaps this data is collected by the pump manufacturer or distributor), then the static pressure directly at the outlet of the pump should be measured and any system that it is applied to should correct for this difference by predicting any additional major and minor losses.

3. With the input to the pump fixed, the output of the pump should be measured as the system is varied, typically using valves or other flow control devices. During this step it is essential to have a means for measuring input power as well as output power (Equation 4-4). Input power can be electrical power, as in the example above for a coupled pump-motor system, or can also be the brake horsepower (BHP) of a separate motor being used to drive the pump; in either case, both input power and output power combined are used to determine the efficiency of a pump under various operating conditions.
4. Repeat steps 2 and 3 with various fixed inputs to create parallel performance curves. From lowest to highest operating capacity, the pump performance, fully plotted, will show the optimum operating points similar to what is shown in Figure 6-3.
5. Using the peaks of the efficiency curves, a True Best Efficiency Point (TBEP) equation can be made to define the optimum pressure for any flowrate within the operational range of any given pump. Equation in hand, a control system can be developed to operate the pump along the TBEP curve to vastly improve energy efficiency and lifespan.
6. If so desired, the data for any performance characteristic can be recorded for use with the control system. Recall that dual control does not have to be used to any particular end.

Simply knowing the desired operational state of the pump is enough to create a control system to operate the pump at that point.

7. Add a dual control algorithm as described above with reference input based on 5. (or even 6., if desired). Set any operational boundaries desired; these boundaries may be driven by hardware or software limitations.
8. If the operational envelope after bounding is unknown and cannot be determined via simulation, then the system may be operated to its extremes to determine the total operational envelope.

As mentioned above, any application that requires variable capacity flow and does not currently utilize a dual control system stands only to gain by taking advantage of the process described here. Even cost is not much of an issue since currently about 85% of the total cost of a pump is from the energy it consumes; therefore, it is simple to justify the additional investment to improve pump performance since even small decreases in power consumption can lead to large returns over time.

9 CONCLUSIONS

9.1 Contributions

In summary, the work discussed herein incrementally builds upon the current state of technology surrounding centrifugal pumps. Centrifugal pump systems have existed for several decades and their application has penetrated nearly every industrial and commercial sector, making these pumping systems a popular target for incremental improvement. This work builds upon technical concepts, such as Best Efficiency Point (BEP) and modern control techniques, to create a technically superior solution to what is currently being discussed in relevant literature. The following concepts are the primary takeaways from this work and present the areas of continued future development:

- True Best Efficiency Point or Best Efficiency Curve: A new way of describing the relationship between pump operation and efficiency that takes into consideration the speed of the pump in addition to the instantaneous pressure and flowrate.
- System Modelling: An analytical pump model is developed and supported by empirical data. This model is used with numerical software to predict controller performance and to simulate a wide range of control applications.
- Best Efficiency Point Absence: A new method for quantifying the reliability of pump operation. The pressure error of the operating point of the pump is integrated over time to accumulate the effect of pump wear in terms that can be easily compared between control regimes.
- Dual Control: By combining speed control and throttle control, a new method of controlling centrifugal pumping systems is developed. This method of control

allows for operation of the pump with two degrees of freedom along the P-Q diagram. This tool is essential for controlling pumps in a manner that optimizes efficiency across a wide range of pressures and flowrates.

9.2 Detailed Conclusion

Based on an analysis of the published work around centrifugal pumping systems, there exists a gap in control technology. Modern systems rely solely on either valve control or speed control to generate flow based on the demand input. This results in an output that suffers from reduced efficiency, up to 60% or more, when compared to the proposed system which combines the two traditional methods to allow for greater process control.

This new control method, known herein as dual control, is capable of taking the BEP as a reference input and controlling the output to follow a parameter described as the true best efficiency point, or TBEP. The BEP is typically defined for a fixed speed on the pressure-flow diagram for a pump. However, there is a unique BEP for each speed. So when operating at variable speed, a relationship is needed between speed and BEP, this is the TBEP curve.

9.2.1. True Best Efficiency Point (or Best Efficiency Curve)

According to basic pump theory, the BEP of the pump is the point at which a pump operates nearest to its designed capacity. However, when variable speed operation is involved, the definition of BEP becomes more difficult to define. According to the Affinity Laws, the capacity and pressure that is output from a pump scales with the speed or diameter of the impeller. Traditionally, pumps were designed to have their impellers replaced with ones of different diameters to achieve different operational capacities. The manual task of replacing the impeller

requires that the pump be taken offline and disassembled. This processes is made easier by the existence of back pullout pumps, which allow for the changing of impellers with minimal time and effort. However, with the rising availability of Variable Speed Drives (VSDs), these pumps are being phased out in exchange for variable speed versions.

Due to the common practice of replacing impellers, pump manufacturers have been publishing variable diameter P-Q diagrams for some time. However, this practice has not evolved a great deal since the rise in popularity of variable speed pumps and controllers. The TBEP, described herein, is a new way of looking at the BEP as it changes with speed. Instead of looking at individual speeds of operation, the TBEP describes the BEP of the pump as a function of desired capacity. This approach turns the standard up on its head since, traditionally, speed is the control variable instead of flowrate. But looking at variable speed devices as if they are still only capable of operating at discretized speeds only subtracts from the true capabilities of variable speed control. The TBEP is the first step in changing the way that centrifugal pumps should be viewed. They are not simply flow generating mechanisms, but actually energy conversion mechanisms. By looking at pressure and flowrate instead of speed, this starts to bring attention to the true capabilities of centrifugal pumps.

The TBEP of the study pump, shown in Figure 6-4, is the result of efficiency analysis of the study pump across a range of flowrates. The TBEP function takes desired flowrate as an input—since most pumping applications care almost exclusively about flowrate—and returns the pressure at which said pump can operated ideally. This information would be useless in a simple throttle control or speed control system, but in the dual control system discussed herein this simply becomes a new performance metric for the desired operational state.

9.2.2. System Modelling

Along with a new way of looking at the performance metrics of pumps, a new method for describing those metrics must be employed. Traditionally, pumps are characterized in one of a few ways. The P-Q curve is by far the most common for industry and basic research applications as it presents the operational envelope for a pump, but proper selection is left up to the system engineer who must match the pump performance with the expected system pressure drop and desired capacity. Solid modelling tools can be used in conjunction with Computational Fluid Dynamics (CFD) software to approximate performance, but this is only common with research in impeller and volute design where the performance is largely unknown and a physical device is not present for testing. Some researchers start with the P-Q diagram, but then employ the Affinity Laws to try to predict performance at different speeds or with different diameter impellers.

The most difficult method for predicting the performance of a pump is by analytically predicting the performance from real physical characteristics. Some researchers do this by looking at the impeller geometry, but this is very specific and narrow. In this paper, a pump is viewed as a fluid energy source whose parameters vary from pump to pump. In order to create a reliable model, real data needs to be taken from an existing pump and fit according to the model. This fit is achieved using a variation on multiple regression that takes into account the two control variables that are available to predict the performance of the real pump.

The least squares method is first applied to find a relationship between valve position and the various performance outputs. This creates a throttle control model that accurately predicts the performance at a fixed pump voltage (or speed). By increasing the order of this fit, more uncertainties are included in the model making it more accurate for interpolation at the sacrifice

of losing the ability to accurately extrapolate. After this, the coefficients of first set of polynomials are fit using the least squares method again. This time the control variable is the voltage being applied to the pump to get a model of the pump as if it were being operated in speed control. The convolution of these two models creates a model that can be used for dual control to simulate the reaction of a real system when operated using nontraditional reference inputs, such as the TBEP.

9.2.1. Best Efficiency Point Absence

When operating at the TBEP the power and energy requirements of the pump are significantly reduced when compared to throttle control and marginally improved when compared to speed control. However, the true advantage comes in the form of improved life and reliability. A new means of measuring the effect of operational state on life is used, BEP absence, to show the effect of operating away from the BEP and how this is impacted by time. BEP absence is the time integral of the pressure error of the pump output with respect to the BEP pressure. Even if the power consumption is insignificant for a particular application, reliability and life of a pump can sometimes be orders of magnitude more important even in terms of cost.

9.2.2. Dual Control

Using the above system modelling and performance criteria, a novel method for controlling centrifugal pumps is developed, wherein the speed of the pump as well as the pressure drop of the system are controlled simultaneously to achieve any desirable operational state. The new control regime, called dual control, looks not just at the pump, but at the entire system to find the best way to implement control. Throttle control alone looks only to vary the minor losses in a system through the use of a variable orifice (control valve). Speed control only attempts to vary the characteristic

speed of the pump to achieve different capacities. Either of these methods, when used alone, only work on their own part of the engineering problem. Dual control combines the two so that the pump and system can be optimized simultaneously. In this paper, dual control is used to operate the pump along its TBEP curve for any desired flowrate. In reality, this is only a one small capability for dual control. By its nature, dual control can set the head and flowrate of a pump to any desired value within the system operation envelope, which is only limited by the size of the pump and any other artificially imposed restrictions. Figure 7-4 shows the true capabilities of dual control. Pressure and flow are independently controlled by two distinct controllers and the control variables—pump voltage and control valve position—possess virtually zero cross-correlation. This results in a nominally stable and superiorly performing controller. The reference input for this control system can be anything that the operator desires, which makes the application possibilities endless.

9.3 Future Work

Moving forward with the topics discussed herein is essential in the pursuit of improving performance and efficiency for centrifugal pump systems. The following are the best candidates for what should be next in further developing these novel concepts that have been described in this work.

BEP absence is a brand new concept for quantifying the reliability of pump operation. However, the method as it currently exists requires maturing before it can become an industry standard. Right now the BEP absence is defined as the pressure error of the pump integrated over time, but this method was only used as it made the most sense for the control system being developed. Further work needs to be done to best describe the relationship between the operating

point of a pump and its corresponding BEP, and how those effects compound with time. By better understanding these effects on pump life, control systems can be tuned to further improve performance while sacrificing a minimum amount of pump reliability.

As for dual control, although its concept is very straightforward, it can be further improved by combining the concept with modern control techniques as opposed to using classical PID controls. Modern control is a continuously evolving field that has produced many great new tools to the technology surrounding control systems. Further development of dual control can stand to benefit from these modern control methods to improve response time and accuracy as well as lend to improved health monitoring when combined with BEP absence.

All of these ideas seek to improve pump efficiency and reliability and can be used in conjunction with other diagnostic tools as a stepping stone for a subject known as ‘Total Health Monitoring’ of centrifugal pump systems. This allows for operators to be able to evaluate the health of a pump system in real time and make any necessary adjustments to keep systems running effectively and reliably.

10 REFERENCES

Aleksandrov, V. Y. & Klimovskii, K. K. (2012). Assessing the Efficiency of centrifugal pumps. *Russian Engineering Research*, 32, 526-528.

Bachus, L. & Custodio, A. A. (2003). *Know and understand centrifugal pumps*. Oxford: Elsevier.

Bakman, I., Gevorkov, L., & Vodovozov, V. (2014). Predictive control of a variable-speed multi-pump motor drive. *Industrial Electronics*, 1409-1414.

Barringer, P. (2001) *Pump Practices & Life*. Barringer & Associates, Inc.

Beebe, R. S. (2004). *Predictive maintenance of pumps using condition monitoring*. Kidlington, Oxford, UK: Elsevier Advanced Technology.

Bloch, H. P., & Budris, A. R. (2006). *Pump user's handbook: life extension* (2nd Ed.). Lilburn, GA: Fairmont Press.

Blough, J. (2002). A survey of DSP methods for rotating machinery analysis, what is needed, what is available. *Journal of Sound and Vibration*, 707-720.

Borghesani, P., Pennacchi, P., Chatterton, S., & Ricci, R. (2013). The velocity synchronous discrete Fourier transform for order tracking in the field of rotating machinery. *Mechanical Systems and Signal Processing*, 118-133.

Burden, R. L. & Faires, J. D. (2011). *Numerical Analysis* (9th Ed.). Boston, MA: Brooks/Cole.

Cao, S., Zhu, Z., Huang, W., & Ju, H. (2013). Speed estimation based on time-frequency fusion and its application in feature extraction of bearing fault. *Zhendong Yu Chongji/Journal of Vibration and Shock*, 32, 18, 174-178.

Chantasiriwan, S. (2013). Performance of Variable-Speed Centrifugal Pump in Pump System with Static Head. *International Journal of Power and Energy Systems*, 15-21.

Energy Technology Support Unit. (2001). *Study on Improving the Energy Efficiency of Pumps*. Commissioned by the European Commission.

Ertöz, Ö. A. (2003). Pompalarda enerji verimliligi. *Ulusal Tesisat Muhendisligi Kongresi Ve Sergisi*.

Fernandez, K., Pyzdrowski, B., Schiller, D. W., & Smith, M. B. (2002). Understanding the basics of centrifugal pump operation. *Fluids/Solids Handling*, 52-56.

Fischer, K. A. & Leigh, D. J. (1983). Using pumps for flow control. *Instruments & Control Systems*, 56, 3, 45-48.

Ford, R. (2011). Why They Work & When They Don't: Affinity Laws. *ASHRAE Journal*, *53*, 42-43.

Gao, X., McInerny, S. A., & Kavanaugh, S. P. (2001). Efficiencies of an 11.2 kW variable speed motor and drive. *ASHRAE Transactions*, 107, 259-265.

Garibotti, E. (2008). Energy savings and better performances through variable speed drive application in desalination plant brine blowdown pump service. *Desalination*, 220, 496-501.

Gibson, I. H. (1993). Variable-speed drives as flow control elements. *Advances in Instrumentation and Control*, 48, 3, 1939-1948.

Halkijevic, I., Vukovic, Z., & Vouk, D. (2013). Frequency pressure regulation in water supply pumps. *Water Science & Technology: Water Supply*, 13, 4, 896-905.

Hall, J. H. (2010). Process pump control. *Chemical Engineering*, 117, 12, 30-33.

Howard, K. J. (2014). Understand the fundamentals of centrifugal pumps. *Chemical Engineering Progress*, 106, 10, 22-28.

Institute of Systems and Robotics – University of Coimbra. (2000). *Improving the Penetration of Energy-Efficient Motors and Drives*. Commissioned by the European Commission, Directorate-General for Transport and Energy, SAVE II Programme 2000.

Karassik, I. J., Messina, J. P., Cooper, P., & Heald, C. C. (2008). *Pump handbook* (4th ed.). New York: McGraw-Hill.

Kaya, D., Yagmur, E. A., Yigit, K. S., Kilic, F. C., Salih, A. E., & Celik, C. (2008). Energy Efficiency in Pumps. *Energy Conversion and Management*, 49, 1662-1673.

Kim, J. H., Choi, J. H., Husain, A., & Kim, K. Y. (2010). Multi-objective optimization of a centrifugal compressor impeller through evolutionary algorithms. *Proceedings of the Institution of Mechanical Engineers, Part A: Journal of Power and Energy*, 711-721.

Ladouani, A. & Nemdili, A. (2013). Development of new models of performance correction factors of centrifugal pumps as a function of Reynolds number and specific speed. *Forsch Ingenieurwes*, 77, 59-69.

Li, Y., Gu, F., Harris, G., Ball, A., Bennett, N., & Travis, K. (2005). The measurement of instantaneous angular speed. *Mechanical Systems and Signal Processing*, 19, 4, 786-805.

Livoti, W. C., McCandless, S., & Poltorak, R. (2009). Improving pumping system efficiency at coal plants. *Power Engineering*, 113, 3, 46-52.

Manring, N. D. (2005). *Hydraulic Control Sysytems*. Hoboken, NJ: Wiley & Sons, Inc.

Martins, G., & Lima, E. (2008). How to improve reliability in centrifugal pumps systems through the automatic tuneup of pumps within their best operational condition. *Proceedings of the Twenty-Fourth International Pump Users Symposium*, 11-18.

Mele, J., Guzzomi, A., & Pan, J. (2014). Correlation of centrifugal pump vibration to unsteady flow under variable motor speed. *Mechanics & Industry*, 15, 525-534.

Miedima, S. A. (N. D.). Modelling and simulation of the dynamic behaviour of a pump/pipeline system.

Morales, S., Culman, M., Acevedo, C., & Rey, C. (2013). Quality evaluation of energy consumed in flow regulation method by speed variation in centrifugal pumps. *Materials Science and Engineering*, 59.

Morton, W. R. (1975). Economics of AC adjustable speed drives on pumps. *IEEE Transactions on Industry Applications,* IA-11, 282-286.

Munk, E., & Fyfe, K. (n.d.). Computed order tracking applied to vibration analysis of rotating machinery. *Department of Mechanical Engineering, University of Alberta, Edmonton, Alberta,* 57-58.

Munson, B. R., Okiishi, T. H., Young, D. F., & Huebsch, W. W. (2009). *Fundamentals of Fluid Mechanics* (6th ed.). Hoboken, NJ: J. Wiley & Sons.

Nilsson, J. W. & Riedel, S. (2014). *Electric Circuits* (10th Ed.). Upper Saddle River, NJ: Prentice Hall.

Pemberton, M. (2005). Intelligent pumps improve efficiency and reliability. *Pollution Engineering*, 15-17.

Pemberton, M. (2005). Variable speed pumping: myths and legends. *World Pumps*, 22-24.

Rémond, D., Antoni, J., & Randall, R. (2014). Editorial for the special issue on Instantaneous Angular Speed (IAS) processing and angular applications. *Mechanical Systems and Signal Processing*, 45(1), 24-27.

Rivola, A., & Troncossi, M. (2014). Zebra tape identification for the instantaneous angular speed computation and angular resampling of motorbike valve train measurements. *Mechanical Systems and Signal Processing,* 44, 1-2, 5-13.

Smith, C. L. (2008). Watch out with variable speed pumping. *Chemical Processing*.

Taber, G. (2011). Improving Pump Efficiency. *HPAC Engineering*, 42-44.

Tutterow, V. C., Doolin, J. H., & Paul, B. O. (1996). Energy-efficient pumping systems. *Chemical Processing*, 59, 8, 30-37.

Volk, M. W. (1996). *Pump characteristics and applications*. New York: M. Dekker.

Warring, R. H. (1984). *Pumps: selection, systems, and applications* (2nd Ed.). Houston, TX: Gulf Publishing Company.

Wen, Y., Zhang, X. & Wang, P. (2010). The relationship between the maximum efficiency and the flow of centrifugal pumps in parallel operation. *Journal of Pressure Vessel Technology*, 132.

Zhang, Q. H., Xu, Y., Shi, W. D., & Lu W. G. (2012). Research and Development on the Hydraulic Design System of the Guide Vanes of Multistage Centrifugal Pumps. *Applied Mechanics and Materials*, 24-30.

A APPENDIX:

MATLAB CODE

A.1. Figure Generation

```
function [result,varargout] = make_plot(varargin)
for(ii=1:nargin)
end
cal_d_p_m = 5.9994; cal_d_p_a = -0.0385;
cal_m_p_m = 6.0018; cal_m_p_a = -0.0425;
cal_p_p_m = 9.987;  cal_p_p_a = -0.089;
cal_a_p_m = 6.0072; cal_a_p_a = -0.024;
cal_f_m = 6.4076;   cal_f_a = -1.2904;
cal_v_m = 4.981469; cal_v_a = 0;
cal_c_m = 5.9427;   cal_c_a = 0.0432;
cal_i_t_m = 20.35;  cal_i_t_a = -1.249;
cal_o_t_m = 20.401; cal_o_t_a = -1.347;
cal_a_m = 21.635;   cal_a_a = -0.3245;
filename = dir('*.tdf');
count = numel(filename);
for(ii = 1:count)
    clear data;
    data = tdfread(filename(ii).name);
    result(ii).time = data.Time; %s
    result(ii).temp_in = data.Temp_In*cal_i_t_m+cal_i_t_a; %°C
    result(ii).temp_out = data.Temp_Out*cal_o_t_m+cal_o_t_a; %°C
    result(ii).p_d = data.Discharge_Pressure*cal_p_p_m+cal_p_p_a; %PSI
    result(ii).p_i = data.Inlet_Pressure*cal_m_p_m+cal_m_p_a; %PSI
    result(ii).current = data.Current*cal_c_m+cal_c_a; %A
    result(ii).angle = data.Valve_Angle*cal_a_m+cal_a_a; %°
    result(ii).flow = data.Flowrate*cal_f_m+cal_f_a; %GPM
    result(ii).v = data.Voltage*cal_v_m+cal_v_a; %V
    result(ii).power_in = result(ii).v.*result(ii).current/745.7; %hp
    d = 1.188; %in
    A = pi*d^2/4; %in^2
    vel = result(ii).flow*231/A/60; %in/s
    rho = 8.34*0.862/231; %lbm/in^3
    p_dyn = 0.5*rho*vel.^2/(32.2*12); %PSI
    result(ii).p_tot = ((result(ii).p_d-result(ii).p_i)+p_dyn)/rho/12;
%ft
    result(ii).power_hyd =
result(ii).p_tot.*result(ii).flow*rho*231/60/550; %hp
    result(ii).eta_ = result(ii).power_hyd./result(ii).power_in;
    result(ii).polyeta = polyfit(result(ii).flow,result(ii).eta_,2);
    result(ii).deta = polyder(result(ii).polyeta,1);
    fopt(ii) = roots(result(ii).deta);
    eopt(ii) = polyval(result(ii).polyeta,fopt(ii));
```

```
    [~,a] = min((result(ii).flow-fopt(ii)).^2);
    popt(ii) = result(ii).p_tot(a); %ft
    [~,index1] = min(abs(result(ii).angle*pi/180-0.6));
    result(ii).p_mean = mean(result(ii).power_hyd(index1:end));
    result(ii).v_mean = mean(result(ii).v);
    figure(1);hold all;
    plot(result(ii).flow,result(ii).power_in,'--');
    figure(2);hold all;
    plot(result(ii).flow,result(ii).p_tot,'--');
    figure(3);hold all;
    plot(result(ii).flow,result(ii).eta_,'--');
    figure(4);hold all;
    plot(result(ii).angle*pi/180,result(ii).p_tot,'--');
    figure(5);hold all;
    plot(result(ii).angle*pi/180,result(ii).flow,'--');
    figure(6);hold all;
    plot(result(ii).angle*pi/180,result(ii).power_hyd,'--');
end
polypbep = polyfit(fopt,popt,2);
figure; plot(fopt,eopt);
polyebep = polyfit(fopt,eopt,2)
fbep = linspace(min(fopt),max(fopt));
ebep = polyval(polyebep,fbep);
pbep = polyval(polypbep,fbep);
figure(1); grid on; pbaspect([1 0.676 0.676]);
legend('14 V','16 V','18 V','20 V','22 V','24 V','26 V','28 V','30
V');
axis([0 30 0 1]);
plot(fbep,(fbep.*pbep*rho*231/60/550)./ebep,'k-');
xlabel('Flowrate (GPM)'); ylabel('Power (hp)');
figure(2); grid on; pbaspect([1 0.676 0.676]);
legend('14 V','16 V','18 V','20 V','22 V','24 V','26 V','28 V','30
V');
axis([0 30 0 100]);
plot(fbep,pbep,'k-');
plot(fopt,popt,'ks');
xlabel('Flowrate (GPM)'); ylabel('Head (ft)');
figure(3); grid on; pbaspect([1 0.676 0.676]);
legend('14 V','16 V','18 V','20 V','22 V','24 V','26 V','28 V','30
V');
axis([0 30 0 0.4]);
xlabel('Flowrate (GPM)'); ylabel('Efficiency');
figure(4); grid on; pbaspect([1 0.676 0.676]);
legend('14 V','16 V','18 V','20 V','22 V','24 V','26 V','28 V','30
V');
```

```
xlabel('Valve Angle (rad)'); ylabel('Total Head (ft)');
figure(5); grid on; pbaspect([1 0.676 0.676]);
legend('14 V','16 V','18 V','20 V','22 V','24 V','26 V','28 V','30
V');
xlabel('Valve Angle (rad)'); ylabel('Flowrate (GPM)');
figure(6); grid on; pbaspect([1 0.676 0.676]);
legend('14 V','16 V','18 V','20 V','22 V','24 V','26 V','28 V','30
V');
xlabel('Valve Angle (rad)'); ylabel('Hydraulic Power (hp)');
```

A.2. Data Fitting

```
function [varargout] = fit_data(varargin)
%#ok<*AGROW>
%#ok<*NO4LP>
%#ok<*NASGU>

option = zeros(1,4);
n = zeros(4,2);
k = 0;
for(ii = 1:nargin)
    if(k)
        k = k - 1;
        continue;
    end
    switch varargin{ii}
        case 'flow'
            option(1) = true;
            n(1,:) = varargin{ii+1};
            k = 1;
            continue;
        case 'head'
            option(2) = true;
            n(2,:) = varargin{ii+1};
            k = 1;
            continue;
        case 'power'
            option(3) = true;
            n(3,:) = varargin{ii+1};
            k = 1;
            continue;
        case 'eff'
            option(4) = true;
            n(4,:) = varargin{ii+1};
```

```
            k = 1;
            continue;
        otherwise
            continue;
    end
end
cal_d_p_m = 5.9994; cal_d_p_a = -0.0385;
cal_m_p_m = 6.0018; cal_m_p_a = -0.0425;
cal_p_p_m = 9.987;  cal_p_p_a = -0.089;
cal_a_p_m = 6.0072; cal_a_p_a = -0.024;
cal_f_m = 6.4076;   cal_f_a = -1.2904;
cal_v_m = 4.981469; cal_v_a = 0;
cal_c_m = 5.9427;   cal_c_a = 0.0432;
cal_i_t_m = 20.35;  cal_i_t_a = -1.249;
cal_o_t_m = 20.401; cal_o_t_a = -1.347;
cal_a_m = 21.635;   cal_a_a = -0.3245;
filename = dir('*.tdf');
count = numel(filename);
for(ii = 1:count)
    clear data;
    data = tdfread(filename(ii).name);
    result(ii).time = data.Time; %s
    result(ii).temp_in = data.Temp_In*cal_i_t_m+cal_i_t_a; %°C
    result(ii).temp_out = data.Temp_Out*cal_o_t_m+cal_o_t_a; %°C
    result(ii).p_d = data.Discharge_Pressure*cal_p_p_m+cal_p_p_a; %PSI
    result(ii).p_i = data.Inlet_Pressure*cal_m_p_m+cal_m_p_a; %PSI
    result(ii).current = data.Current*cal_c_m+cal_c_a; %A
    result(ii).angle = (data.Valve_Angle*cal_a_m+cal_a_a)*pi/180; %°
    result(ii).flow = data.Flowrate*cal_f_m+cal_f_a; %GPM
    result(ii).v = data.Voltage*cal_v_m+cal_v_a; %V
    result(ii).power_in = result(ii).v.*result(ii).current/745.7; %hp
    d = 1.188; %in
    A = pi*d^2/4; %in^2
    vel = result(ii).flow*231/A/60; %in/s
    rho = 8.34*0.862/231; %lbm/in^3
    p_dyn = 0.5*rho*vel.^2/(32.2*12); %PSI
    result(ii).p_tot = ((result(ii).p_d-result(ii).p_i)+p_dyn)/rho/12;
%ft
    result(ii).power_hyd =
result(ii).p_tot.*result(ii).flow*rho*231/60/550; %hp
    result(ii).eta = result(ii).power_hyd./result(ii).power_in;
    result(ii).polyeta = polyfit(result(ii).flow,result(ii).eta,2);
    result(ii).deta = polyder(result(ii).polyeta,1);
    [~,pos_2] = min((result(ii).angle-30*pi/180).^2);
    [~,pos_1] = min((result(ii).angle-70*pi/180).^2);
```

```
    short(ii).angl = result(ii).angle(pos_1:pos_2)';
    short(1).volt(ii) = str2double(filename(ii).name(1:2));
    short(ii).flow = result(ii).flow(pos_1:pos_2)';
    short(ii).ptot = result(ii).p_tot(pos_1:pos_2)';
    short(ii).powr = result(ii).power_in(pos_1:pos_2)';
    short(ii).eta_ = result(ii).eta(pos_1:pos_2)';
end
angl_fit = linspace(30*pi/180,70*pi/180);
count = 1;
if(option(1))
    polypoly.flow = make_fit(short,3,n(1,:));
    curvefit.flow = fit_curve(polypoly.flow,short(1).volt,angl_fit);
    make_fig([],short,3);
    plot(angl_fit,curvefit.flow,'-');
    xlabel('Valve Position (rad)'); ylabel('Flowrate (GPM)');
    title('Raw Data vs Fit Data');
    varargout{count} = polypoly.flow;
    count = count + 1;
end
if(option(2))
    polypoly.ptot = make_fit(short,4,n(2,:));
    curvefit.ptot = fit_curve(polypoly.ptot,short(1).volt,angl_fit);
    make_fig([],short,4);
    plot(angl_fit,curvefit.ptot,'-');
    xlabel('Valve Position (rad)'); ylabel('Total Head (ft)');
    title('Raw Data vs Fit Data');
    varargout{count} = polypoly.ptot;
    count = count + 1;
end
if(option(3))
    polypoly.powr = make_fit(short,5,n(3,:));
    curvefit.powr = fit_curve(polypoly.powr,short(1).volt,angl_fit);
    make_fig([],short,5);
    plot(angl_fit,curvefit.powr,'-');
    xlabel('Valve Position (rad)'); ylabel('Power Input (hp)');
    title('Raw Data vs Fit Data');
    varargout{count} = polypoly.powr;
    count = count + 1;
end
if(option(4))
    polypoly.eta_ = make_fit(short,6,n(4,:));
    curvefit.eta_ = fit_curve(polypoly.eta_,short(1).volt,angl_fit);
    make_fig([],short,6);
    plot(angl_fit,curvefit.eta_,'-');
    xlabel('Valve Position (rad)'); ylabel('Efficiency');
```

```
    title('Raw Data vs Fit Data');
    varargout{count} = polypoly.eta_;
    count = count + 1;
end
end

function fit_ = make_fit(data,field_,order)
fields_ = fieldnames(data);
for(ii = 1:numel(data))
    y = getfield(data(ii),fields_{1});
    z = getfield(data(ii),fields_{field_});
    poly_(ii,:) = polyfit(y,z,order(1));
end
x = getfield(data(1),fields_{2});
for(ii = 1:order(1)+1)
    fit_(ii,:) = polyfit(x',poly_(:,ii),order(2));
end
end

function z = fit_curve(fit_,x,y)
for(ii = 1:numel(x))
    for(jj = 1:numel(fit_(:,1)))
        p(jj) = polyval(fit_(jj,:),x(ii));
    end
    z(ii,:) = polyval(p,y);
end
end

function [varargout] = make_fig(num_in,data,field_)
if(isempty(num_in))
    fig = figure;
    num_out = fig.Number;
    varargout{1} = num_out;
else
    figure(num_in);
end
hold all; grid on;
fields_ = fieldnames(data);
for(ii = 1:numel(data))
    y = getfield(data(ii),fields_{1});
    z = getfield(data(ii),fields_{field_});
    plot(y,z,'--');
end
end
```

A.3. Simulink Functions

```
function compare_models
%%
q_ref = 14;
p_ref = (0.0831*q_ref^2-0.6465*q_ref+3.4822)*144/53.8;
%%
sim('dynamic_model.slx');

figure(1);

subplot(3,2,1);
plot(flowrate.time,flowrate.signals.values/q_ref,'b-');
title('Output 1: Flowrate');
xlabel('Time (s)')
ylabel('Scaled Output');

subplot(3,2,2);
plot(pressure.time,pressure.signals.values/p_ref,'b-');
title('Output 2: Pressure');
xlabel('Time (s)')
ylabel('Scaled Output');

subplot(3,2,3);
plot(error_flowrate.time,error_flowrate.signals.values/q_ref,'b-');
title('Output 1 Error');
xlabel('Time (s)')
ylabel('Relative Error');

subplot(3,2,4);
plot(error_pressure.time,error_pressure.signals.values/p_ref,'b-');
title('Output 2 Error');
xlabel('Time (s)')
ylabel('Relative Error');

subplot(3,2,5);
plot(voltage.time,voltage.signals.values,'b-');
title('Input 1: Voltage');
xlabel('Time (s)')
ylabel('Control Effort (V)');

subplot(3,2,6);
plot(theta_dot.time,theta_dot.signals.values,'b-');
title('Input 2: Valve Position');
```

```
xlabel('Time (s)')
ylabel('Control Effort (rad/s)');
%%
sim('dynamic_model_linear');

subplot(3,2,1); hold on; grid on;
plot(flowrate.time,flowrate.signals.values/q_ref,'r--');
legend('Full Dynamic','Linearized','Location','SE');
axis([0 10 -0.1 1.1]);

subplot(3,2,2); hold on; grid on;
plot(pressure.time,pressure.signals.values/p_ref,'r--');
legend('Full Dynamic','Linearized','Location','SE');
axis([0 10 -0.1 1.1]);

subplot(3,2,3); hold on; grid on;
plot(error_flowrate.time,error_flowrate.signals.values/q_ref,'r--');
legend('Full Dynamic','Linearized','Location','SE');
axis([0 10 -0.1 1.1]);

subplot(3,2,4); hold on; grid on;
plot(error_pressure.time,error_pressure.signals.values/p_ref,'r--');
legend('Full Dynamic','Linearized','Location','SE');
axis([0 10 -0.1 1.1]);

subplot(3,2,5); hold on; grid on;
plot(voltage.time,voltage.signals.values,'r--');
legend('Full Dynamic','Linearized','Location','SE');
axis([0 10 13 33]);

subplot(3,2,6); hold on; grid on;
plot(theta_dot.time,theta_dot.signals.values,'r--');
legend('Full Dynamic','Linearized','Location','SE');
axis([0 10 -0.015 0.015]);

%%
figure; hold on; grid on;
plot(error_flowrate.time,error_flowrate.signals.values/q_ref,'b-');
xlabel('Time (s)')
ylabel('Relative Error');
plot(error_pressure.time,error_pressure.signals.values/p_ref,'r--');
legend('Flowrate','Pressure','Location','NE');
axis([0 10 0 1]);
```

```
function compare_systems
fprintf('Beginning Simulation...\n');
sim('dynamic_model_dualcontrol');
fprintf('Stage 1 complete. Continuing...\n');
sim('dynamic_model_flowcontrol');
fprintf('Stage 2 complete. Continuing...\n');
sim('dynamic_model_throttlecontrol');
fprintf('Stage 3 complete. Finishing...\n');

figure; hold all; grid on;
plot(power_dual.time,power_dual.signals.values);
plot(power_flow.time,power_flow.signals.values);
plot(power_throttle.time,power_throttle.signals.values);
xlabel('Time (s)'); ylabel('Power In (hp)');
title('Control Comparison, Power');
legend('Dual Control','Speed Control','Valve Control');

figure; hold all; grid on;
plot(efficiency_dual.time,efficiency_dual.signals.values);
plot(efficiency_flow.time,efficiency_flow.signals.values);
plot(efficiency_throttle.time,efficiency_throttle.signals.values);
xlabel('Time (s)'); ylabel('Efficiency');
title('Control Comparison, Efficiency');
legend('Dual Control','Speed Control','Valve Control');

fix_unit = 1/3600;
figure; hold all; grid on;
plot(energy_dual.time,energy_dual.signals.values*fix_unit);
plot(energy_flow.time,energy_flow.signals.values*fix_unit);
plot(energy_throttle.time,energy_throttle.signals.values*fix_unit);
xlabel('Time (s)'); ylabel('Energy (hph)');
title('Control Comparison, Energy');
legend('Dual Control','Speed Control','Valve Control');

figure; hold all; grid on;
loglog(absence_dual.time,absence_dual.signals.values);
loglog(absence_flow.time,absence_flow.signals.values);
loglog(absence_throttle.time,absence_throttle.signals.values);
xlabel('Time (s)'); ylabel('BEP Absence (ft-s)');
title('Control Comparison, Absence');
legend('Dual Control','Speed Control','Valve Control');

figure; hold all; grid on;
plot(error_flowrate_dual.time,error_flowrate_dual.signals.values);
plot(error_flowrate_flow.time,error_flowrate_flow.signals.values);
```

```
plot(error_flowrate_throttle.time,error_flowrate_throttle.signals.valu
es);
xlabel('Time (s)'); ylabel('Flow Error (GPM)');
title('Control Comparison, Flow Error');
legend('Dual Control','Speed Control','Valve Control');

figure; hold all; grid on;
plot(error_pressure_dual.time,error_pressure_dual.signals.values);
plot(error_pressure_flow.time,error_pressure_flow.signals.values);
plot(error_pressure_throttle.time,error_pressure_throttle.signals.valu
es);
xlabel('Time (s)'); ylabel('Pressure Error (ft)');
title('Control Comparison, Pressure Error');
legend('Dual Control','Speed Control','Valve Control');

fig = openfig('BEP.fig');
figure(fig.Number); hold all; grid on;
h1 =
plot(flowrate_dual.signals.values,pressure_dual.signals.values,'*');
h2 =
plot(flowrate_flow.signals.values,pressure_flow.signals.values,'*');
h3 =
plot(flowrate_throttle.signals.values,pressure_throttle.signals.values
,'*');
title('Control Comparison, BEP');
legend([h1,h2,h3],'Dual Control','Speed Control','Valve Control');
end
```

B APPENDIX:

LABVIEW CODE

B.1. DAQ

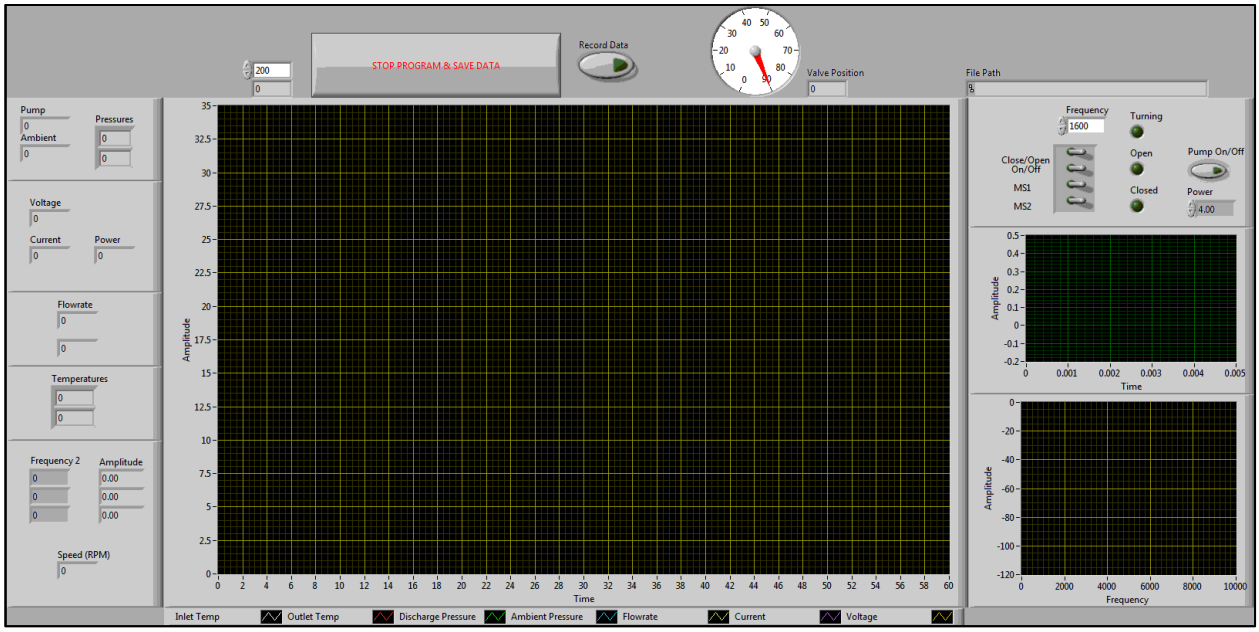

Figure B-1. Front panel of DAQ program.

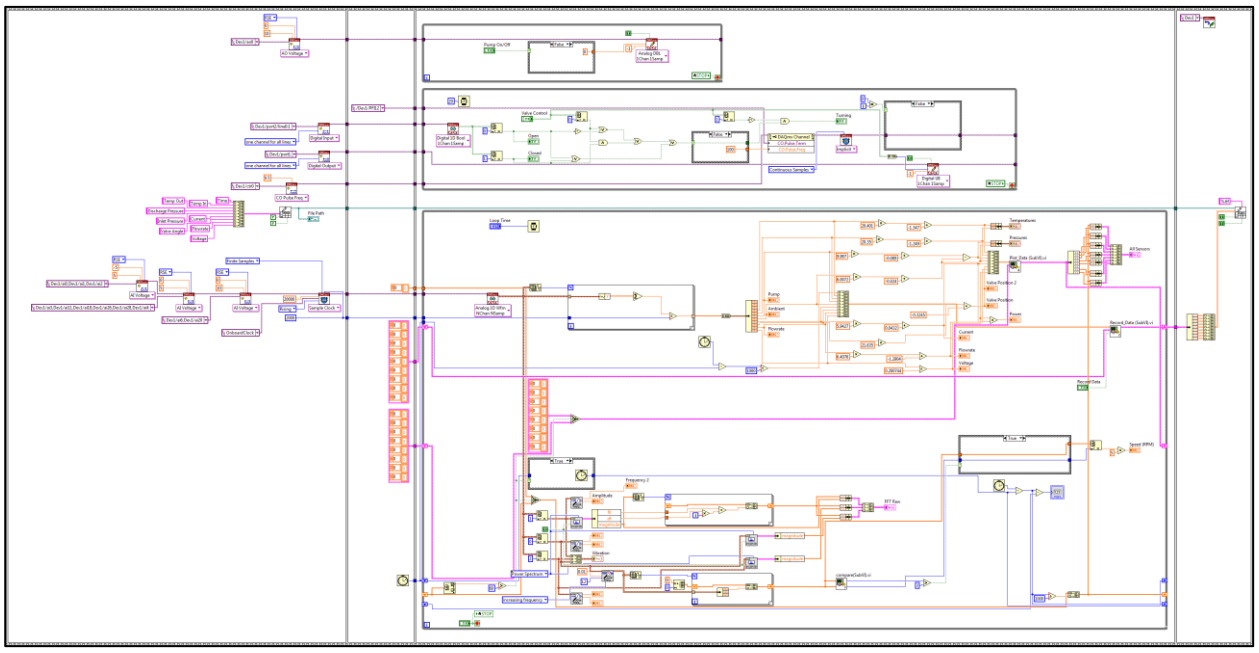

Figure B-2. Block diagram of DAQ program.

B.2. Control System

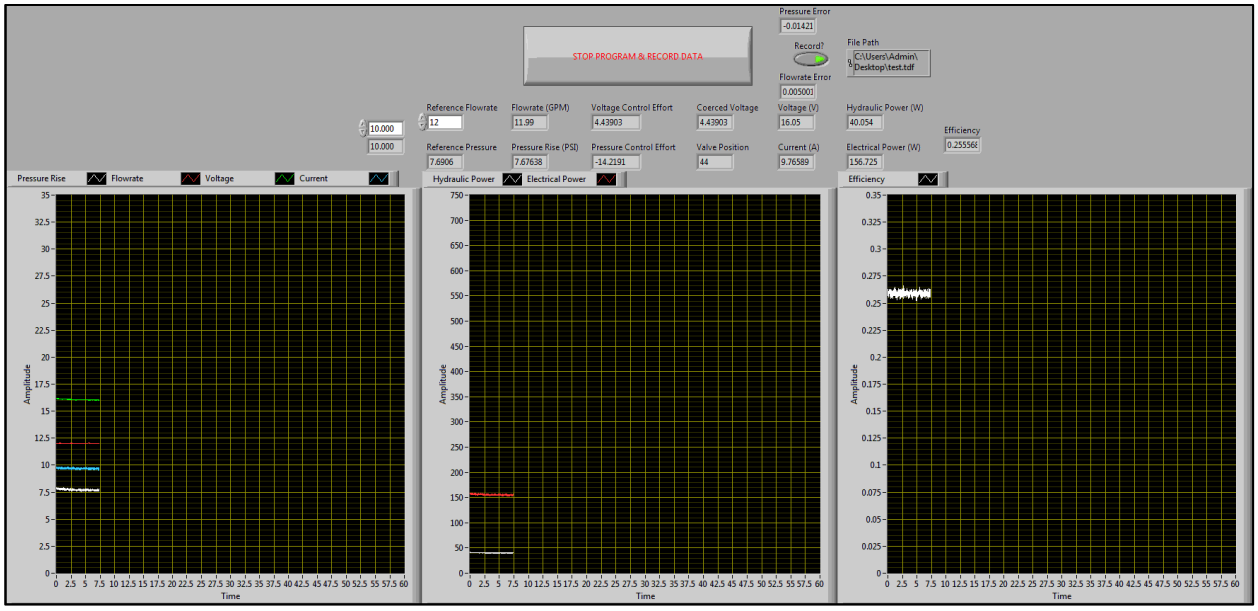

Figure B-3. Front panel of control system.

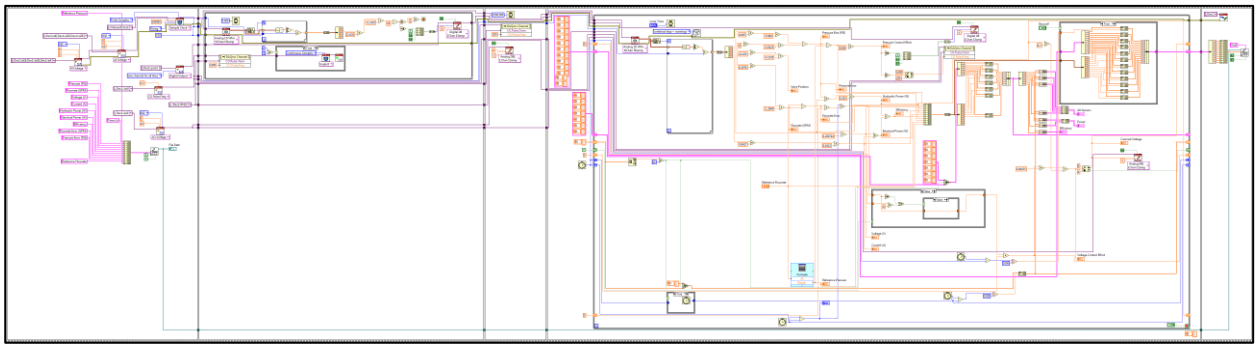

Figure B-4. Block diagram of control system.

Note: Any of the programs in this section may be provided in greater detail upon request.

However, the author shall retain exclusive rights to use and distribution.

C APPENDIX:

SPEED MEASUREMENT TECHNIQUE

C.1. Introduction

When implementing feedback control, one of the most important factors is the ability to accurately measure the objective variable whether it be speed, force, displacement, etc. In the application involving control of variable-speed pumps, the rotational speed of the pump impeller is the objective parameter. Unfortunately, a majority of centrifugal pumps are being operated at a fixed speed so manufacturers are reluctant to increase cost by implementing a speed indicator and instead print the nominal speed on the nameplate. Rotational speed is typically measured by using a device known as a tachometer, of which several designs exist, but these devices usually require physical or visible access to the rotating part being measured. However, in the case of centrifugal pumps, the impulses generated by the impeller and volute coming into close proximity with one another can be measured by a piezoelectric accelerometer. The frequency response of the piezoelectric sensor represents a harmonic of the fundamental frequency of the rotational speed. This process allows for speed measurement of centrifugal pumps where direct access to the rotating components is impractical.

The rotation of the impeller inside of a centrifugal pump generates an impulse every time a vane of the impeller passes the cutwater (tongue) of a volute. This impulse is carried through the pump and motor and can be measured by an externally mounted piezoelectric accelerometer. The fundamental frequency (1^{st} harmonic) of the wave is a whole number multiple of the impeller rotational speed equal to the number of times an impeller passes a cutwater in a single rotation of the impeller.

C.2. Methodology

A pump is fitted with piezoelectric accelerometers along three principle axes to measure the vibration response during operation. A Fast Fourier Transform (FFT) is then used to create a power spectrum of the vibration from which various tones can be extracted. Potential sources for noise are identified and noise filtering such as low-pass, high-pass, stopband, and bandpass filters are implemented through both hardware and software techniques to help in isolating the desired fundamental frequency pertaining to pump speed. Once a tone is extracted, it must be analyzed to determine if it represents the fundamental frequency or another harmonic; once determined, the frequency is scaled by $1/n$ where n is the harmonic being extracted (n = 1 for the fundamental frequency). To analyze the accuracy of this technique, the determined speed is compared to the ground truth by comparing motor voltage and current to a lookup table.

C.3. Specific Aims

The result of the research is a means by which the rotational speed of a centrifugal pump impeller can be measured noninvasively and in the absence of an existing tachometer. Implementation only requires an accelerometer and a microprocessor for sampling, calculating FFT, extracting tones, and displaying calculated speed. The technique has already been validated by qualitative observation of the FFT of the frequency response. Fully automated implementation should provide a high accuracy, low noise measurement of rotational speed with nearly real-time results. Preliminary results show that the Power Spectral Density (PSD) of the vibration response has multiple peaks associated with harmonics of the rotational speed. The 1^{ST} harmonic is 12 times the rotational speed which is the result of 6 impeller blades passing by 4 volutes every rotation; this results in 24 impulses per revolution, but due to the symmetry of the design 2 pulses always

occur simultaneously. The figures below show how the results look and what needs to be extracted for proper analysis. Difficulty lies in determining which peak corresponds to the first harmonic since it is not always the largest amplitude. Also, at some speeds, noise contributors can be on order with rotational vibrations.

C.4. Background

In rotating/oscillating machinery, order tracking is commonly employed to interpret vibration data for the purpose of determining system condition such as wear or fault states (Cao, S., Zhu, Z., Huang, W., & Ju, H., 2013; Munk, E., & Fyfe, K., n.d.; Rémond, D., Antoni, J., & Randall, R., 2014; Rivola, A., & Troncossi, M., 2014). Order tracking involves measuring the vibration of oscillating machinery and then decomposing the vibration data into a spectrum through various techniques such as FFT, Discrete Fourier Transform (DFT), angle domain sampling, Kalman filter, Vold-Kalman, etc. The frequency and amplitude of vibration can be used to determine if a system is damaged or experiencing excessive wear. Typically the vibration spectrum will contain peaks at various multiples of the fundamental frequency, which is defined as the rotating speed of the driving motor. When the measured frequencies are scaled by the fundamental frequencies, they are referred to as orders and shown as frequency-independent in an order plot. Unfortunately, this type of analysis presupposes that the fundamental frequency can be measured for varying speed systems or is simply know for constant speed systems (Blough, J., 2002). Without this information some methods attempt to extract instantaneous speed via instantaneous angular speed methods, but such methods require low noise signals with clearly defined tones to work effectively (Li, Y., Gu, F., Harris, G., Ball, A., Bennett, N., & Travis, K., 2005). Despite the existence of order tracking/analysis tools that have been in development since

the 80s, an effective and reliable method for determining the fundamental frequency of a rotating/oscillating system using only spectral data still needs to be developed.

C.5. Experimental Analysis

Figure C-1 below shows a FFT of the vibration data acquired while running a pump at around 6000 RPM. Eight harmonics (a.k.a. overtones or orders) can be identified, each at a whole number multiple of the apparent fundamental frequency. 'Apparent' is used in this context since it is known from analysis of this system that vibrational energy is primarily generated as a result of an impeller blade passing by a volute cutwater (tongue) which happens 12 times each revolution for this system. Other information about the system such as number and size of bearings or number of DC motor poles is not known and therefore any contributions to the overall vibration cannot be predicted and are considered noise sources. One noise source in particular occurs at about 5.2 kHz and has higher intensity than all but one harmonic frequency including the fundamental frequency. This is one reason that additional filtering is needed beyond peak detection to be able to determine the fundamental frequency.

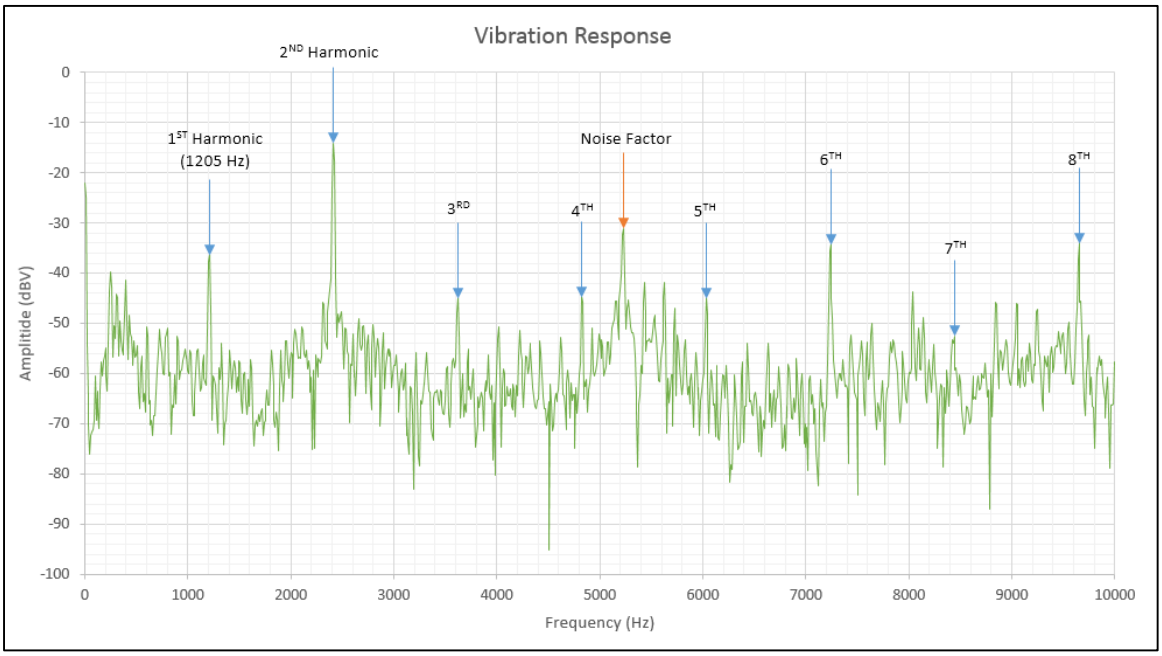

Figure C-1. PSD of pump vibration at ~6000 RPM.

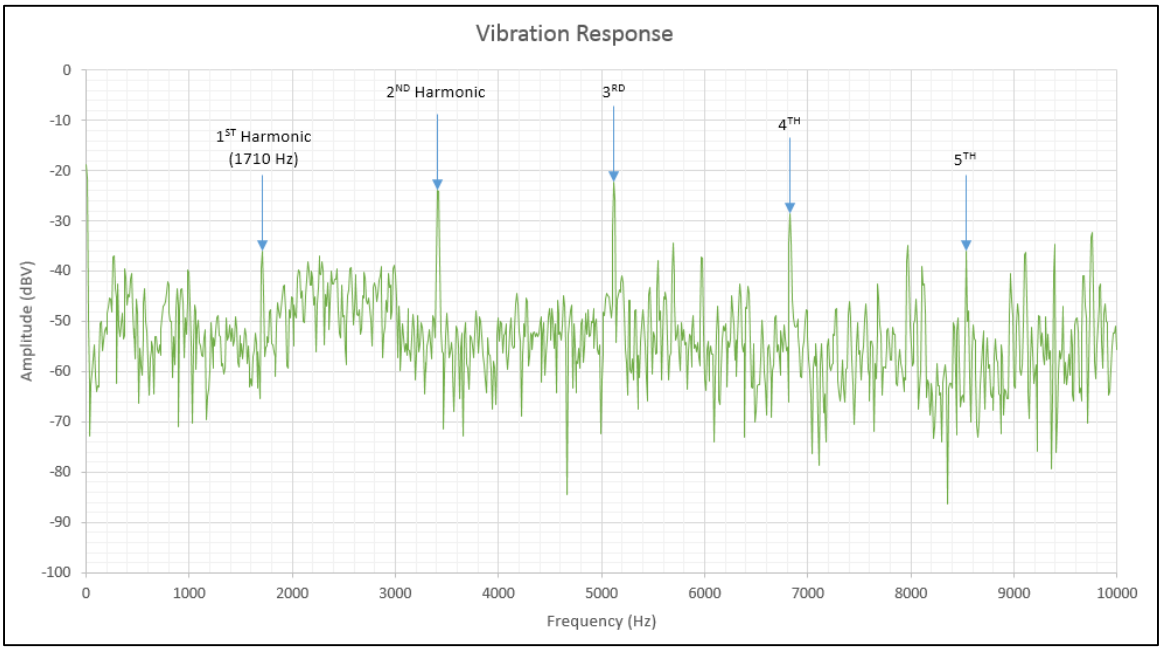

Figure C-2. PSD of pump vibration at ~8500 RPM.

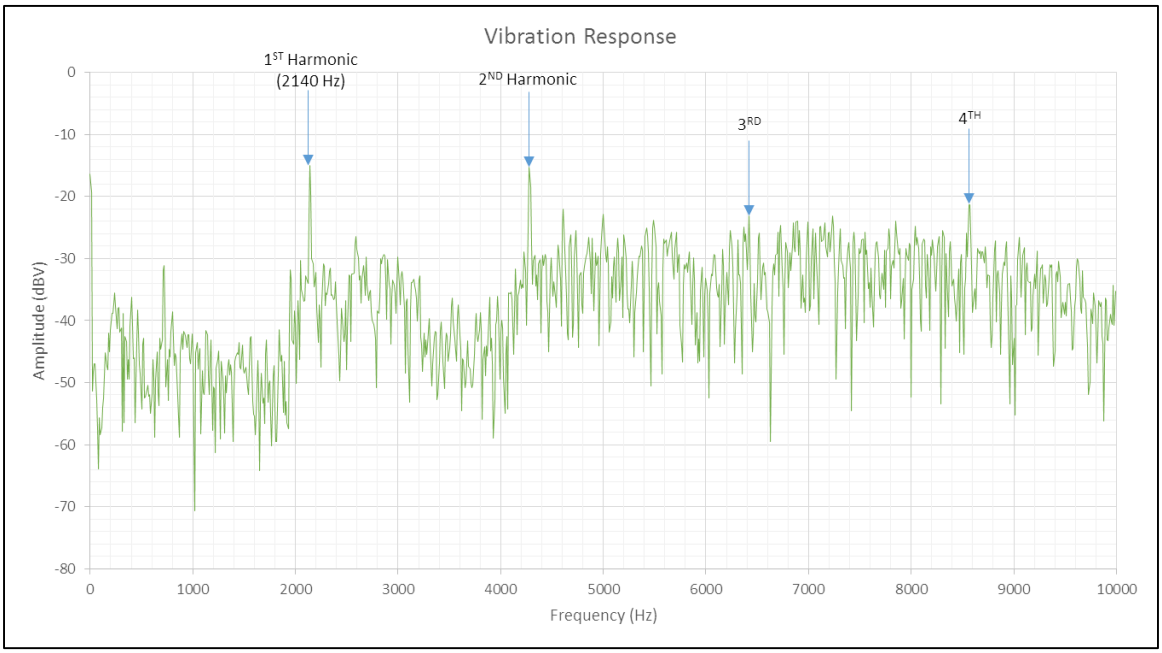

Figure C-3. PSD of pump vibration at ~1100 RPM.

Figure C-2 and Figure C-3 show the FFT of the vibration data at two other fundamental frequencies; in each case, the fundamental frequency can easily be determined through visual observation since some information is known about the expected fundamental frequency (i.e. the operator knows the current pump setting and approximately what the resulting speed should be). However, simply interpolating speed from system settings is only accurate as long as the system continues to operate under the initial conditions where the input/output relationship is originally defined; as the system ages and wears, the pump may not always output the same speed for a given input. Of particular note in Figure C-2 is the fact that the fundamental frequency is of similar order of magnitude to the general random noise values which is visible throughout the entire measured frequency range: the fundamental frequency has a magnitude of approximately -35 dB while noise reaches as high as -32 dB. This combined with the resonant noise found in Figure C-1 are the primary obstacles to overcome when attempting to find the fundamental frequency from spectral data.

C.6. Analytical Approach

The primary tool used in spectral analysis is the FFT. The FFT is a powerful tool that allows for high speed spectral analysis of periodic data (in this case an accelerometer signal) be decomposing the signal into a sum of sines and cosines. Many methods are said to compute the FFT, however this is a misnomer; FFT is actually any algorithm for calculating the DFT which is faster and can sometimes result in better accuracy than directly computing the DFT (Borghesani, P., Pennacchi, P., Chatterton, S., & Ricci, R., 2013).

VITA

Shane Corlman was born October 20, 1989 in West Plains, MO. After graduating from West Plains High School in 2008, Shane enrolled in the Mechanical & Aerospace Engineering program at the University of Missouri–Columbia. Shane graduated in 2011 with a Bachelor of Science in Mechanical Engineering. Shane promptly continued his education by entering the Doctorate program at the University of Missouri to continue work on his research. Shane graduated with a Ph.D. in Mechanical Engineering December 2015.